

# **University of Alberta**

Hyperspectral remote sensing of boreal forest tree diversity at multiple  
scales

by

Evan R. DeLancey

A thesis submitted to the Faculty of Graduate Studies and Research  
in partial fulfillment of the requirements for the degree of

Master of Science

Department of Earth and Atmospheric Sciences

© Evan R. DeLancey  
SPRING 2014  
Edmonton, Alberta

## **Abstract**

This research compared the variability/diversity of spectral information captured with spectrometers at the airborne, field, and leaf level to tree species diversity. Airborne measurements were made over the North Saskatchewan River Valley while field and leaf measurements were done with synthetic tree plots on the roof of the Biological Sciences building, University of Alberta. Measures of optical diversity (spectral variables), such as the standard deviation in vegetation indices, principal components, and slope analysis, showed significant correlation to species diversity indices. The strongest correlations ( $R^2$ : ODI#3 = 0.90, ODI#6 = 0.86) were achieved with linear models using three to five spectral variables, called Optical Diversity Indices (ODIs). Experimental methods found that this correlation was based primarily on variation in leaf optical properties. Additionally, rough canopies increased optical diversity and greater spectral range improved correlations slightly. These findings can help design operational methods for remote assessment of biodiversity based on optical diversity.

## **Acknowledgments**

This research was funded by NSERC Discoverys, Canadian Foundation for Innovation and iCORE/Alberta Innovates funding to John A. Gamon

I wish to thank Li Haitao, Gilberto Pastorello, and David Stonehouse (VeriMap Plus, Calgary, Alberta, Canada) for their work in acquiring and processing the airborne imagery. Without Li and Gilberto's many months of work, Chapter 3 would not have been possible. I would also like to thank Chris Wong for his help in the planting of tree seedlings. Additionally I would like to thank the members of my committee, Dr. David Hik and Dr. Benoit Rivard, for their help and guidance.

Finally, I would like to thank Dr. John Gamon for his continued support and advice in my two plus years studying under him.

## Table of Contents

<b>CHAPTER 1 - INTRODUCTION.....</b>	<b>1</b>
LITERATURE CITED .....	6
<b>CHAPTER 2 - EXPERIMENTAL TESTS OF OPTICAL DIVERSITY.....</b>	<b>14</b>
INTRODUCTION .....	14
METHODS.....	18
<i>Study Design</i> .....	18
<i>Tree plot setup</i> .....	18
<i>Instrumentation</i> .....	20
<i>Spectral measurements – canopy scans</i> .....	21
<i>Spectral measurements – leaf scans</i> .....	21
<i>Biodiversity metrics computed</i> .....	22
<i>Spectral metrics computed</i> .....	22
<i>Additional Analysis</i> .....	25
RESULTS.....	26
<i>ODI Correlation</i> .....	28
<i>Leaf level optical diversity</i> .....	32
<i>Leaf optical diversity versus canopy optical Diversity</i> .....	34
<i>Variable canopy height</i> .....	36
<i>Spectral range</i> .....	38
DISCUSSION .....	39
<i>Spectral variation hypothesis (Canopy)</i> .....	39
<i>Leaf versus Canopy effects on optical diversity</i> .....	40
<i>Canopy height effects</i> .....	43
<i>Spectral range</i> .....	44
CONCLUSIONS.....	45
LITERATURE CITED.....	47
<b>CHAPTER 3 - ASSESSING SPECIES DIVERSITY OF BOREAL FOREST TREES WITH IMAGING SPECTROMETRY.....</b>	<b>53</b>
INTRODUCTION .....	53
METHODS.....	57
<i>Biodiversity Sampling</i> .....	57
<i>Image Processing</i> .....	59
<i>Vegetation &amp; ODI Index Calculation</i> .....	61
RESULTS.....	63
DISCUSSION .....	69
<i>Optical diversity, species diversity correlation</i> .....	69
<i>Factors behind optical diversity – species diversity correlation</i> .....	71
<i>Surrogacy</i> .....	73
<i>Future research needs</i> .....	73
<i>Study Limitations</i> .....	74
CONCLUSION & RECOMMENDATIONS.....	75
LITERATURE CITED.....	77
<b>CHAPTER 4 – SYNTHESIS, CONCLUSIONS, AND FUTURE RESEARCH .....</b>	<b>88</b>
SYNTHESIS OF ROOFTOP AND AIRBORNE DATA.....	88
CONCLUSIONS.....	91
FUTURE RESEARCH .....	92
LITERATURE CITED.....	94

<b>APPENDIX A – INDEX AND PCA CALCULATION FOR ROOFTOP DATA.....</b>	<b>95</b>
INDEX CALCULATION.....	95
PCA ANALYSIS.....	96
<b>APPENDIX B - CALCULATING AN OPTICAL DIVERSITY INDEX (ODI) FROM RAW</b>	
<b>AIRBORNE DATA.....</b>	<b>96</b>
I. GEOREFERENCING.....	96
II. FLAT FIELD CORRECTION (FFC) .....	100
III. OXYGEN BAND CORRECTION .....	100
IV. EMPIRICAL LINE CORRECTION .....	101
V. GEOREFERENCING (ENVI) .....	102
VI. IMAGE SMOOTHING (ENVI).....	103
VII. NDVI, PRI, GREEN/RED INDEX AND MASKING (ENVI).....	103
VIII. PRINCIPAL COMPONENT ANALYSIS ENVI .....	104
IX. OPTICAL DIVERSITY INDEX (ENVI).....	104

## List of Tables

Table 2-1: List of tree species used in study.....	19
Table 2-2: List of vegetation indices .....	24
Table 2-3: List of all canopy level variables and their $R^2$ value when correlated individually against species richness, Simpson Index, log Simpson Index, Shannon Index, and log Shannon Index..	30
Table 2-4: List of ODIs.....	32
Table 2-5: List of all leaf level variables and their $R^2$ value when correlated against species richness, Simpson Index, log Simpson Index, Shannon Index, and log Shannon Index.....	34
Table 3-1: List of all 30x30m plots.....	64
Table 3-2: Optical Diversity Indices (ODIs). .....	66

## List of Figures

Figure 2-1: Diagram of basic rooftop sampling design..	19
Figure 2-2: Five by five tree plot.	20
Figure 2-3: Leaf sampling procedure set up with bifurcated fiber.	21
Figure 2-4: Spectral processing method..	24
Figure 2-5: Canopy level spectra of the 7 tree species used in optical diversity testing.	27
Figure 2-6: Leaf level spectra of the 7 tree species used in optical diversity testing	27
Figure 2-7: Correlation ( $R^2$ value) as a function of wavelength (440-1600nm) for of PCs 1-4 using canopy-scale data.	28
Figure 2-8: The relationship between ODI#1 and the log of Simpson Index.	31
Figure 2-9: The relationship between ODI#2 and the log of Simpson Index.	31
Figure 2-10: The relationship between ODI#3 and the log of Simpson Index.	31
Figure 2-11: Correlation ( $R^2$ value) as a function of wavelength (440-1600nm) for of PCs 1-4 using leaf level data.	33
Figure 2-12: Change in average $R^2$ value between canopy and leaf level scans.	35
Figure 2-13: ODI#3 at the leaf and canopy scale	36
Figure 2-14: Average spectrum (black) with one standard deviation below and above the average (green).	37
Figure 2-15: Average spectrum (black) with one standard deviation below and above the average (green).	37
Figure 2-16: Correlation ( $R^2$ value) as a function of wavelength (440-1600nm) for of PCs 1-4 using uneven canopy data.	37
Figure 2-17: Percent change in the standard deviation of all vegetation indices between a non-uniform canopy and a uniform canopy.	38
Figure 2-18: The change in correlation (species diversity and optical diversity) when the spectral range is changed from 400-1600nm to 400-1000nm.	39
Figure 2-19: The change in correlation (species diversity and optical diversity) when the spectral range is changed from 400-1600nm to 400-800nm.	39
Figure 3-1: 10 River valley plots. In Kinsmen Park/University (top) and Fort Edmonton Park area (bottom)	58

Figure 3-2: Sample spectra of typical forest pixels (Range 400-900nm) with PRI and NDVI wavelengths (equations 3-1 and 3-2) shown with arrows. ....	61
Figure 3-4: The relationship between the standard deviation of NDVI and Shannon Index. ....	67
Figure 3-5: The relationship between the standard deviation of PRI and Shannon Index ....	67
Figure 3-6: The relationship between Optical Diversity Index #5 and Shannon Index ....	67
Figure 3-7: The relationship between Optical Diversity Index #5 and species richness ....	67
Figure 3-8: The relationship between Optical Diversity Index #3 and species richness ....	68
Figure 3-9: Correlation between reflectance value and PC value ( $R^2$ value) as a function of wavelength (400-800nm) for of PCs 1-3.....	68
Figure 4-1: Flow diagram working from original spectral data to an optical diversity index.....	89
Figure 4-2: An ODI (linear combination of NDVI, PC1, and PC2 or PC3 for rooftop) correlated against log of Simpsons Index. ....	90

## **List of Abbreviations**

OD – Optical Diversity

ODI – Optical Diversity Index

SHV – Spectral Variation Hypothesis

VIS - Visible

NIR – Near-Infrared

SWIR – Short Wave-Infrared

SR – Species Richness

SI – Simpson Index

SH – Shannon Index

LSI – log Simpson Index

NDVI – Normalized Difference Vegetation Index

GIC – Gitelson's Chlorophyll Index

SIPI – Structure Independent Pigment Index

PRI – Photochemical Reflectance Index

RWC – Relative Water Content

WBI – Water Band Index

LAI – Leaf Area Index

MLA – Mean Leaf Angle

BRDF – Bidirectional Reflectance Distribution Function

PC – Principal Component

PCA – Principal Component Analysis

RMSE – Root Mean Squared Error

## Chapter 1 - Introduction

Biodiversity is broadly defined as the “full variety of life on Earth” (Takacs, 1996). One of the most common ways to represent biodiversity of a local area is species richness (alpha diversity) (Whittaker 1960, Whittaker 1972). A subset of species richness is functional diversity (linked to genetic diversity) (Scherer-Lorenzen *et al.*, 2005). Functional diversity may be of greater ecological significance than alpha diversity because, by definition, it measures the range and value of species traits that influence ecosystem functioning (Tilman, 2001). Maintaining a high diversity of life is vital for ecosystem function and resilience (Tilman 1996, Naeem 1994, Isbell *et al.* 2011). A number of studies have found that more species promote higher productivity due to certain species being more productive at different times (Yachi & Loreau 1999, Craine 2003, Tilman *et al.* 2006, Zavaleta 2010). A high diversity ecosystem does not always correlate to a highly productive ecosystem because this is more related to the productivity of the dominant species (Millennium Ecosystem Assessment, 2005). A high diversity ecosystem may be more important since many, less dominant, species can act as “insurance” for the ecosystem, adding resilience in the face of disturbance (Millennium Ecosystem Assessment, 2005). From a utilitarian point of view, biodiversity/habitat conservation is vital due to its implications on hydrology, soils, atmospheric composition and food resources (Ghilarov 2000, Millennium Ecosystem Assessment 2005). Increasing temperature, CO<sub>2</sub> levels, pollution, and habitat fragmentation through industrialization are threatening global biodiversity and the essential goods and services it provides (Barnosky *et al.* 2011, Bir *et al.* 2001).

Of particular interest to biodiversity studies is the diversity of vegetation, and tree species in particular. Vegetation is the energy base of most terrestrial food

chains and creates a habitat for many species in the area (Reagan & Vaide, 1996). Thus, the diversity of tree species is often related to the diversity of many other organisms (Pharo & Beattie 2001, Negi & Gadgil 2002, Williams *et al.* 2006), which has been called the surrogacy principle (Gamon, 2008). Because of these reasons, a portion of conservation efforts is typically devoted to maintaining the diversity of forests ecosystems through the creation of nature reserves, and conservation agreements (see Canadian Boreal Forest Agreement). Human development, such as, agriculture in tropical rainforests and resource extraction in the boreal forests are threatening the diversity of these ecosystems (Koh & Wilcove 2008, Dyer *et al.*, 2008, Schindler & Lee, 2010).

Given the importance of vegetation diversity to whole-system diversity, tracking and surveying the diversity of tree species should be a high priority. Traditionally this has been done through the fieldwork of biologists with plot based species counts. These counts can be turned into indices such as the Simpson and Shannon Index to give a numerical representation of biodiversity. Recent advances in remote sensing technology have brought about new methods to sample vegetation diversity. These methods mainly use spectrometers that measure reflected sunlight. The data from this is then analyzed in various ways (explained below) and related to biodiversity. Remote sensing methods provide benefits over fieldwork due to the area that can be covered in a short amount of time and the unbiased nature of remote sensing data.

The remote sensing of biodiversity can be done with airborne instruments, which spectrally distinguish species and map out the number of species in an area (Franklin *et al.* 1994, Gougeon 1995, Jones *et al.* 2010, Féret & Asner 2012, Leutner *et al.* 2012, Clark and Roberts 2012). It can also be done by relating the diversity of

tree species to certain remotely sensed variables (climatic variables, and habitat type) (Fairbanks & McGwire, 2004, Elith *et al.* 2006, Pearson *et al.* 2007, Chaves *et al.*, 2007, Buermann *et al.*, 2008, Saatchi *et al.*, 2008).

A more recent method relates the diversity (or variability) of spectral information to the diversity of vegetation species. This method is referred to as the Spectral Variability Hypothesis (SVH) (Palmer *et al.* 2000, Palmer *et al.* 2002). The SVH states that spectral heterogeneity in space should scale with species diversity (Palmer *et al.* 2000, Palmer *et al.* 2002). The SVH or variations on it have been tested in tundra ecosystems (Gould, 2000), prairie (Palmer *et al.*, 2002), savanna grasslands (Oindo & Skidmore, 2002), Mediterranean scrubland (Zutta 2003, Levin *et al.* 2007), tropical dry forests (Gillespie, 2005), tropical forests (Carlson *et al.*, 2007), wetlands (Rocchini *et al.*, 2007), woodland/marshes (Lucas & Carter, 2008), and highland savanna (Oldeland *et al.*, 2010). The majority of these studies found a correlation between spectral heterogeneity and species diversity but many different methods were used, and causes of the correlations were not fully explored.

Additionally, not all ecosystems have been tested to see if similar relationships exist.

One major ecosystem missed is the boreal forest. The boreal forest's large extent and major role in the carbon cycle (Schlesinger 1997, Magnani *et al.* 2007) make it an important ecosystem to test the SVH. Additionally, human alterations in climate, nutrient cycles, and land use due to industrialization are causing stresses on boreal forest diversity (Schindler 1998, Schindler & Lee 2010). The large seasonality, extent, and lower relative diversity in the boreal forest present new challenges to the remote sensing of biodiversity in such forest.

Along with the incomplete testing across all ecosystems, the SVH also lacks experimental tests and adequate explanations of the driving forces behind the

optical diversity (from now on abbreviated as “OD”)-species diversity correlation. Experimental methods may be able to estimate whether leaf chemical properties or canopy structure is driving spectral variability. This has been debated in the literature. Studies such as Wessman *et al.* (1988), Martin & Abner (1997), Asner *et al.* (2002), and Carlson *et al.* (2007) have found that leaf properties drive vegetation reflectance when canopies are optically thick. Other studies have argued that canopy structure dominates the spectral signal, and leaf chemical properties cannot be detected with canopy level remote sensing (Knyazikhin *et al.*, 2012). These differing results may be a factor of the differing forest types, i.e., dense forests (where leaf properties dominate) versus sparse forests (where canopy structure dominates). Experimental methods may also be able to tell us if additional factors such as tree stand roughness, and nutrient stress are contributing to additional spectral variance.

Finally, experimental tests may also be able to help to standardize the ideal spatial resolution, spectral resolution, and spectral range for use in biodiversity studies. Rocchini *et al.* (2010) argues spectral variability is its highest (i.e. it’s easier to discriminate species) when there are more spectral bands (larger range and more bands within the range) and when pixel size approximates the size of the objects under consideration. On the other hand, greater spectral resolution and range may not be needed if the appropriate, information-dense bands can be identified (Rocchini *et al.*, 2010). Many studies have found that higher spectral resolution rather than higher spatial resolution leads to a better correlation between OD and species diversity (Nagendra *et al.* 2010, Stickler and Southworth 2008). Although, these experiments compared Landsat and IKONOS, both of which do not have high

spectral or spatial resolution in the first place. These issues need to be resolved in order to move towards an operational method of remotely sensed biodiversity.

This study attempts to further the knowledge on the remote sensing of biodiversity with tests in the boreal forest and also experimental analysis of the SVH. Chapter 2 attempts to test the relation of OD to species diversity with a controlled experimental method. Additionally, Chapter 2 explores the relative importance of leaf versus canopy properties on spectral variance, the effect of canopy roughness on spectral variance, and the effect of variable spectral range on the OD-species diversity correlation. These experimental methods can further the understanding of the OD-species diversity relationship and help move towards a standardized method of airborne/satellite biodiversity sampling. The third chapter scales up the tests of the second chapter by surveying optical diversity in boreal forest plots with an airborne imaging spectrometer. With guidance from previous studies (Zutta 2003, Carlson *et al.* 2007, Oldeland *et al.* 2010) various measures of spectral diversity were tested to see if they strongly correlated to tree species diversity as seen in Zutta (2003), and Carlson *et al.* (2007).

## Literature cited

- Asner, G.P., Palace, M., Keller, M., Pereira, R., Silva, J.N.M., & Zweede, J.C. (2002). Estimating Canopy structure in an amazon forest from laser range finder and IKONOS satellite observations. *Biotropica*, 34(4), 483-492.
- Barnosky, A.D., Matzke, N., Tomiya, S., Wogan, G.O.U., Swartz, B. Quental, T.B., Marshall, C., McGuire, J.L., Lindsey, E.L., Maguire, K.C., Mersey, B., & Ferrer, E.A. (2011). Has the Earth's sixth mass extinction already arrived? *Nature*, 471, 51-57.
- Bir, R., S. Kushwah, & V. Kumar. (2001). *Economics of Protected Areas and its Effect on Biodiversity*. APH publishing corporation, New Delhi.
- Buermann, W., Saatchi, S., Smith, T.B., Chaves, B.R., Mila, B., & Graham, C.H. (2008). Predicting species distributions across the Amazonian and Andean regions using remote sensing data. *Journal of Biogeography*, 35(7), 1160-1176.
- Carlson, K.M., Asner, G.P., Hughes, R.F., Ostertag, R., & Martin, R.E. (2007). Hyperspectral remote sensing of canopy biodiversity in Hawaiian lowland rainforest. *Ecosystems*, 10(4), 536-549.
- Chaves, J.A., Smith, T.B., Pollinger, J.P., & LeBuhn, G. (2007). The role of geography and ecology in shaping the phylogeography of the speckled humming bird in Ecuador. *Molecular Phylogenetics and Evolution*, 43, 795-807.
- Clark, M.L., & Roberts, D.A. (2012). Species-level differences in hyperspectral metrics among tropical rainforest trees as determined by a tree based classifier. *Remote Sensing*, 4, 1820-1855.
- Craine, J.M., Reich, P.B., Tilman, D., Elisworth, D., Fargione, J., Knops, J., & Naeem, S. (2003). The role of plant species in biomass production and response to elevated CO<sub>2</sub> and N. *Ecological Letters*, 6, 623-630.

- Dyer, S., Grant, J., Lesack, T., & Weber, M. (2008). *Catching up: Conservation and Biodiversity Offsets in Alberta's Boreal Forest*. Canadian Boreal Initiative, Ottawa, Canada.
- Elith, J., Graham, C.H., Anderson, R.P., Dudik, M., Ferrier, S., Guisan, A., Hijmans, R.J., Huettmann, F., Leathwick, J.R., Lehmann, A., Li, J., Lohmann, L.G., Loizelle, B.A., Manion, G., Moritz, C., Nakamura, M., Nakazawa, Y., Overton, J., Townsend Peterson, A., Phillips, S.J., Richardson, K., Scachetti-Pereira, R., Schapire, R.E., Soberon, J., Williams, S., Wisz, M.S. & Zimmermann, N.E. (2006). Novel methods improve prediction of species' distributions from occurrence data. *Ecography*, 29, 129–51.
- Fairbanks, D.H.K. & McGwire, K.C. (2004). Patterns of floristic richness in vegetation communities of California: regional scale analysis with multi-temporal NDVI. *Global Ecology and Biogeography*, 13, 221–235.
- Franklin, S. E. (1994). Discrimination of subalpine forest species and canopy density using digital CASI, SPOT PLA, and Landsat TM data. *Photogrammetric Engineering and Remote Sensing*, 60, 1233–1241.
- Féret, J.B., & Asner, G.P. (2012). Semi-supervised methods to identify individual crowns of lowland tropical canopy species using imaging spectroscopy and LiDAR. *Remote Sensing*, 4, 2457-2476.
- Gamon, J.A. (2008). Tropical Remote Sensing – Opportunities and Challenges. In: G. Kalacska, & A. Sanchez-Azofeifa. *Hyperspectral Remote Sensing of Tropical and Subtropical Forests* (pp.297-304). Taylor & Francis Group, Boca Raton, FL, USA.
- Ghilarov, A.M., (2000). Ecosystem functioning and intrinsic value of biodiversity. *Oikos*, 90, 408–412.

- Gillespie, T.W. (2005). Predicting woody-plant species richness in tropical dry forests: a case study from South Florida, USA. *Ecological Applications*, 15, 27-37.
- Gougeon, F. A. (1995). Comparison of possible multispectral classification schemes for tree crowns individually delineated on high spatial resolution MEIS images. *Canadian Journal of Remote Sensing*, 21, 1-9.
- Gould, W. (2000). Remote sensing of vegetation, plant species richness, and regional biodiversity hotspots. *Ecological Applications*, 10(6), 1861-1870.
- Isbell, F., Calcango, V., Hector, A., Connolly, J., Harpole, W.S., Reich, P.B., Scherer-Lorenzen, M., Schmid, B., Tilman, D., van Ruijven, J., Weigelt, A., Wilsey, B.J., Zavaleta, E.S., & Loreau, M. (2011). High plant diversity is needed to maintain ecosystem services. *Nature*, 477, 199-202.
- Jones, T.G., Coops, N., & Sharma, T. (2010). Assessing the utility of airborne hyperspectral and LiDAR data for species distribution mapping in the coastal Pacific Northwest, Canada. *Remote Sensing of Environment*, 114, 2841-2852.
- Knyazikhin, Y., Schull, M.A., Stenberg, P., Mottus, M., Rautiainen, Yang, Y., Marshak, A., Carmona, P.L., Kaufmann, R.K., Lewis, P., Disney, M.I., Vanderbilt, V., Davis, A.B., Baret, D., Jacquemoud, S., Lyapustin, A., & Myneni, R. B. (2012). Hyperspectral remote sensing of foliar nitrogen content. *PNAS*, 110(3), 185-192.
- Koh, L.P., & Wilcove, D.S. (2008). Is oil palm agriculture really destroying tropical biodiversity. *Conservation Letters*, 1(2), 60-64.
- Leutner, B.F., Reineking B., Muller, J., Bachmann, M., Beierkuhnlein, C., Dech, S., & Wegmann M. (2012). Modelling forest  $\alpha$ -diversity and floristic composition-

on the added value of LiDAR plus hyperspectral remote sensing. *Remote Sensing*, 4, 2818-2845.

Levin, N. Shmida, A. Levanoni, Q., Tomari, H., & Kark, S. (2007). Predicting mountain plant richness and rarity from space using satellite-derived vegetation indices. *Diversity and Distribution*, 13, 692-703.

Lucas, L.K., & Carter, G.A. (2008). The use of hyperspectral remote sensing to assess vascular plant species richness on Horn Island, Mississippi. *Remote sensing of Environment*, 112, 3908-3915.

Magnani, F., Mencuccini, M., Borghetti, M., Berbigier, P., Berninger, F., Delzon, S., Grelle, A., Hari, P. Jarvis, P.G., Kolari, P., Kowalski, A.S. Lankreijer, H. Law, B.E., Lindroth, A., Loustau, D., Manca, G., Moncrieff, J.B., Rayment, M. Tedeschi, V. Valentini, R., & Grace, J. (2007). The human footprint in the carbon cycle of temperate and boreal forests. *Nature*, 447, 848-850.

Martin, M.E., & Aber, J.D. (1997). High spectral resolution remote sensing of forest canopy lignin, nitrogen, and ecosystem processes. *Ecological Applications*, 7(2), 431-443.

Millenium Ecosystem Assessment. (2005). *Ecosystem and Human Well-being: Biodiversity Synthesis*. World Resources Institute, Washington, DC.

Naeem, S., Thompson, L.J., Lawler, S.P., Lawton, J.H., & Woodfin, R.M. (1994). Declining biodiversity can alter the performance of ecosystems. *Nature*, 368, 734-737.

Nagrenda, H., & Rocchini, D. (2008). High resolution satellite imagery for tropical biodiversity studies: the devil is in the detail. *Biodiversity and Conservation*, 17, 3431-3442.

- Nagrenda, H., Rocchini, D., Ghate, R., Sharma, B., & Pareeth, S. (2010). Assessing plant diversity in a dry tropical forest: comparing the utility of Landsat and IKONOS satellite images. *Remote Sensing*, 2, 478-496.
- Negi, H.R., & Gadgil M. (2002). Cross-taxon surrogacy of biodiversity on the Indian Garhwal Himalaya. *Biological Conservation*, 105(2), 143-155.
- Oindo, B.O., & Skidmore, A.K. (2002). Interannual variability of NDVI and species richness in Kenya. *International Journal of Remote Sensing*. 23, 285-298.
- Oldeland, J., Wesuls, D., Rocchini, D., Schmidt, M., & Jurgens, N. (2010). Does using species abundance data improve estimates of species diversity from remotely sensed spectral heterogeneity? *Ecological Indicators*, 10, 390-396.
- Palmer, M.W., Wohlgemuth, T., Earls, P., Arevalo, J.R., & Thompson, S.D. (2000). Opportunities for long-term ecological research at the tallgrass prairie preserve, Oklahoma. *Proceedings of ILTER regional workshop, Budapest, Hungary, 22-25 June, 1999 (2000)*, 123-128.
- Palmer, M.W., Earls, P.G., Hoagland, B.W., White, P.S., & Wohlgemuth, T. (2002). Quantitative tools for perfecting species lists. *Environmetrics*, 13, 121-137.
- Pearson, R.G., Raxworthy, C.J., Nakamura, M., & Peterson, A. (2007). Predicting species distributions from small numbers of occurrence records: a test case using cryptic geckos in Madagascar. *Journal of Biogeography* 34, 102-117.
- Pharo, E.J. & Beattie, A.J. (2001). Management forest types as a surrogate for vascular plant, bryophyte and lichen diversity. *Australian Journal of Botany*, 49(1), 23-30.
- Reagan, D.P. & Vaide, R.B. (1996). *Food Web of a Tropical Rain Forest*. The University of Chicago press, Chicago, Illinois.
- Rocchini, D., Ricotta, C., & Chiarucci, A. (2007). Using satellite imagery to assess

plant species richness: the role of multispectral systems. *Applied Vegetation Sciences*, 10, 325-331.

Rocchini, D., Balkenhol, N., Carter, G.A., Foody, G.M., Gillespie, T.W., He, K.S., Kark, S., Levin, N., Lucas, K., Luoto, M., Nagendra, H., Oldeland, J., Ricotta, C., Southworth, J., & Neteler, M. (2010). Remotely sensed spectral heterogeneity as a proxy of species diversity: Recent advances and open challenges.

*Ecological Informatics*, 5(5), 318-329.

Saatchi, S., Buerman, W., Mori, S., ter Steege, H., & Smith, T. (2008). Modeling distribution of Amazonian tree species and diversity using remote sensing measurements. *Remote Sensing of the Environment*, 112(5), 2000-2017.

Scherer-Lorenzen, M., Korner, C., & Schulze, E.D. (2005). *Forest Diversity and Function: Temperate and Boreal Systems*. Springer-Verlag Berlin Heidelberg, Germany.

Schindler, D.W. (1998). A dim future for boreal waters and landscapes. *Bioscience*, 48(3), 157-164.

Schindler, D.W., & Lee, P.G. (2010). Comprehensive conservation planning to protect biodiversity and ecosystem services in Canadian boreal regions under a warming climate and increasing exploitation. *Biological Conservation*, 143, 1571-1586.

Schlesinger, W.H. (1991). *Biogeochemistry: An Analysis of Global Change*. Academic Press, San Diego, California, USA.

Stickler, C.M., & Southworth, J. (2008). Application of a multi-scale spatial and spectral analysis to predict primate occurrence and habitat associations in Kinbale National Park, Uganda. *Remote Sensing of Environment*, 112, 2170-2186.

- Takacs, D. (1996). *The Idea of Biodiversity: Philosophies of Paradise*. The Johns Hopkins University Press, Baltimore, MD.
- Tilman, D. (1996). Biodiversity: population versus ecosystem stability. *Ecology*, 77(2), 350-363.
- Tilman, D. (2001). Functional Diversity. In: S.A. Levin. *Encyclopedia of Biodiversity (Vol. 3)* (pp.109-120). Academic Press.
- Tilman, D., Reich, P.B., & Knops, J.M.H. (2006). Biodiversity and ecosystem stability in a decade-long grassland experiment. *Nature*, 441, 629-632.
- Wessman, C.A., Aber, J.D., Peterson, D.L., & Melillo, J.M. (1988). Remote Sensing of canopy chemistry and nitrogen cycling in temperate forest ecosystems. *Nature*, 335, 154-156.
- Whittaker, R. H. (1960). Vegetation of the Siskiyou Mountains, Oregon and California. *Ecological Monographs*, 30, 279-338.
- Whittaker, R.H. (1972). Evolution and measurement of species diversity. *Taxon*, 21, 213-251.
- Williams, G.L., Faith, D., Manne, L., Sechrest, W., & Preston, C. (2006). Complementarity analysis: Mapping the performance of surrogates for biodiversity. *Biological Conservation*, 128, 253-264.
- Yachi, S., & Loreau, M. (1999) Biodiversity and ecosystem productivity in a fluctuating environment: the insurance hypothesis. *Proc. Natl Acad. Sci USA*, 96, 1463-1468.
- Zavaleta, E.S., Pasari, J.R., Hulvey, K.B., & Tilman, G.D. (2010). Sustaining multiple ecosystem functions in grassland communities requires higher biodiversity. *Proc. Natl Acad. Sci USA*, 107, 1443-1446.
- Zutta, B. (2003). Assessing Vegetation Functional Type and Biodiversity in Southern

California Using Spectral Reflectance. *Masters Thesis*. California State University, Los Angeles.

## Chapter 2 - Experimental tests of optical diversity

### Introduction

The concept that optical diversity (OD) relates to species diversity was introduced as the “Spectral Variance Hypothesis” by Palmer *et al.* (2000, 2002). Versions of this have also been tested by Gould (2000), Zutta (2003), Rocchini *et al.* (2004, 2007), Carlson *et al.* (2007) and Oldeland *et al.* (2010). While these studies have all shown correlations between optical diversity and species diversity, they do not always reveal the factors behind the correlations. It is likely that the correlation is a function of reflectance variation at the canopy level and leaf level. The factors affecting the canopy and leaf reflectance are outlined below.

Vegetation reflectance is controlled by physical canopy attributes, leaf optical properties, soil properties, illumination conditions, and view geometry (Ross 1981, Goel 1988, Myneni *et al.* 1989, Jacquemoud *et al.* 1992, Curran *et al.* 1992). With experimental methods, the variation in soil properties, illumination conditions, and view geometry can be minimized, thus clarifying the role of leaf properties and physical canopy structure on the resulting optical signal. According to the Optical Diversity Hypothesis (Ustin & Gamon 2010), these factors can vary between species, but they can also vary in time. This hypothesis states that optical type is a function plant canopy structure, leaf traits (chemistry and physiology), and phenology. While this might explain the drivers of optical diversity, this hypothesis has not been fully tested. A challenging aspect is that species do not always produce unique spectral signatures.

Physical canopy structure causes variable canopy reflectance through the variable orientation of leaves and stems in three-dimensional space (Asner, 1998). This causes differing interactions of photons through multiple scattering on

different surfaces such as leaves, stems, and soil (Asner, 1998). This interaction of photons can be affected by leaf area and leaf angle distribution (Asner, 1998). Erectophile foliar types tend to trap more light in lower levels which results in lower near infra-red (NIR) reflectance than planophile foliar types (Goel 1988, Gitelson *et al.* 2002a). Tree canopy shape can also affect reflectance.

Leaf optical properties are partly controlled by the concentrations of biochemicals and water found in the leaf (Curran *et al.*, 1992). These cause many major absorption features in the VIS-SWIR spectral regions (Curran *et al.*, 1992). The visible region is affected by three pigment types (chlorophylls, carotenoids, and anthocyanins) (Blackburn, 2007). Chlorophylls dominate the absorption of leaf spectra in the blue and red regions (Sims & Gamon, 2002). Carotenoids absorb in the blue region (420-500nm) while anthocyanins absorb in the blue and green wavelengths (Gamon & Surfus 1999, Sims & Gamon 2002, Gitelson *et al.* 2002b, Gitelson & Merzlyak 2004). Water absorption affects several regions in the NIR to SWIR (Peñuelas *et al.* 1997, Curran *et al.* 1992). Other biochemicals, such as cellulose, lignin and nitrogen (largely from proteins) cause absorption features around 2100nm (Kokaly 2001, Kokaly *et al.* 2007, Kokaly *et al.* 2009). Consequently, variation between tree species' leaf optical properties should be controlled by their respective water content, chlorophyll and other pigment absorption, related to photosynthetic capacity (Teillet *et al.* 1997, Gamon *et al.* 1992), and concentration of other chemicals (Curran *et al.*, 1992). According to the functional convergence hypothesis (Field, 1991), canopy structure and leaf properties have also been found to influence each other (Ustin and Gamon 2010, Ollinger 2011). For example, leaf nitrogen content is often associated with higher LAI and photosynthetic capacity, affecting both leaf properties and canopy structure (Field 1991, Ollinger 2011).

Along with variation in individual tree structure, optical properties are affected by the overall structure of the plot in question (i.e. canopy roughness, forest gaps, variation in biomass, and percent cover) (Colwell, 1974). Rough canopy structure along with shadowing can increase the variance of reflectance values across a stand or landscape (Colwell, 1974). As canopy roughness increases, increased multiple scattering also alters reflectance (Jones & Vaughan, 2010).

In forest ecosystems, variation in canopy structure (mainly variation in LAI and leaf angle) is a primary source of variability in optical properties, with secondary effects of leaf optical properties (Asner, 1998). Knyazikhin *et al.* (2012) argued that leaf chemical properties cannot be measured with canopy level remote sensing because variation in physical canopy structure dominates the spectral signal. Other studies have found that leaf properties can become detectable when canopies are optically thick (Wessman *et al.* 1988, Martin & Aber 1997). More recent work has found that, in closed canopy forests, spectral variation is dominated by leaf biochemical properties and less affected by canopy structure (Asner *et al.* 2002, Carlson *et al.* 2007, Clark & Roberts 2012). Consequently, the relative influence of canopy structure vs. leaf properties on optical diversity remains an open question (Townsend *et al.*, 2013).

Considering all these factors, the ideal instrument, to measure spectral variability of vegetation would be a full range spectrometer (400-2500nm) because it can capture the full range of variation in canopy structure and leaf traits. On the other hand, because it is known that many spectral features co-vary, using the full spectral range might be redundant. For example, the nitrogen absorption in the SWIR may not be needed in analysis because nitrogen has also been linked to NIR reflectance (Ollinger *et al.* 2008, Martin *et al.* 2008). Carlson *et al.* (2007) and

Oldeland *et al.* (2010) found full-range spectroscopy to be very helpful in optical diversity studies. Lucas *et al.* (2008) found full range measurements lead to a slight improvement in tree species classification, but the majority of the information was in the VIS-NIR region. To my knowledge no studies have explicitly examined the effect of different spectral ranges on optical diversity.

The main aim of this chapter was to test the OD-species diversity relationship with boreal forest tree species. Additionally I wanted to test the relative effects of leaf properties versus canopy structure on optical diversity, see how varying tree heights affect the variance of spectral indices, and explore how increasing or decreasing spectral range effects the correlation between OD indices and species diversity indices. Given the results seen in previous studies (Zutta (2003), and Carlson *et al.* (2007)), I predicted that optical diversity would correlate with species diversity for synthetic tree plots. The debate over the effect of leaf versus canopy properties on overall reflectance suggests a stronger effect of leaf properties when canopies are optically thick (Wessman *et al.* 1988, Martin & Aber 1997). Other studies have argued that only canopy structure affects reflectance (Knyazikhin *et al.*, 2012). Therefore, I hypothesized that optical diversity is controlled by both leaf traits and canopy structure. From my knowledge of light scattering in rough canopies, I predicted that varying tree height will increase optical diversity. Finally, studies such as Oldeland *et al.* (2010) and Carlson *et al.* (2007) have cited the importance of full spectral range for their results, and, therefore, I predicted that increased spectral range will improve the OD-species diversity correlation.

## **Methods**

### *Study Design*

This set of experiments was conducted to test the OD-species diversity relationship and the factors controlling the relationship, specifically, the effect of: leaf traits and canopy structure, canopy roughness, and spectral range. The general design tested the OD-species diversity relationship while three specific experiments addressed the specific factors behind optical diversity. To accomplish these goals, an experimental design was established where tree seedlings could be arranged into synthetic stands. Using different arrangements of species, low diversity plots were spectrally compared to high diversity plots. This was done at the leaf and canopy scale to investigate the effects of leaf traits and canopy structure on the correlation between OD and species diversity. These plots were also arranged into rough canopies and smooth canopies to investigate the effect of a rough canopy on OD. This data was analyzed at different spectral ranges to investigate if increased spectral range improves correlations between OD and species diversity.

### *Tree plot setup*

Trees were kept in deep tree pots (used to avoid root drying) (TP 49 (10 x 24 cm), Stuewe & Sons, Tangent, Oregon, USA) with a soil mixture of two parts potting soil (Sunshine Mix #4, Sun Gro Horticulture, Agawam, MA, USA), one part topsoil, and 150g/60L of slow release fertilizer (Nutricote 14-14-14, Plant Products Co., Brampton, ON). Trees were watered regularly and treated with liquid fertilizer (Plant Prod Ultimate 20-20-20, Sure-Gro, Brantford, ON) monthly.

Plot setup was done with 1-3 year old seedlings of seven tree species (Table 2-1). Tree species were selected based upon their prevalence in the Edmonton River Valley forest area (study area of Chapter 3). Note that one species (*Larix*

*sibirica*) was an exotic species from the Siberian boreal forest meant to substitute for the local larch (*Larix laricina*), which was not available. The synthetic plots were arranged on a south facing rooftop (sixth floor Biological Sciences building, University of Alberta), in a five by five tree plot (see Figure 2-1 and 2-2). Black tarps were placed around the plot to reduce side lighting, and wind. Pots of grass were placed around the west, north, and east edges of the plot to reduce reflectance from the roof surface.

Table 2-1: List of tree species used in study with their age, and distinguishing traits.

Common Name	Scientific Name	Age (years)	Distinguishing Trait
Green Ash	<i>Fraxinus pennsylvanica</i>	1	Dense canopy
Manitoba Maple	<i>Acer negundo</i>	1	Large leaf area
Schubert Chokecherry	<i>Prunus virginiana</i>	2	Purple colored leaves
Trembling aspen	<i>Populus tremuloides</i>	1	Dark green smaller leaves
White Spruce	<i>Picea glauca</i>	2	Short needle conifer
Lodgepole Pine	<i>Pinus contorta</i>	2	Long needle conifer
Siberian Larch	<i>Larix sibirica</i>	3	Deciduous conifer

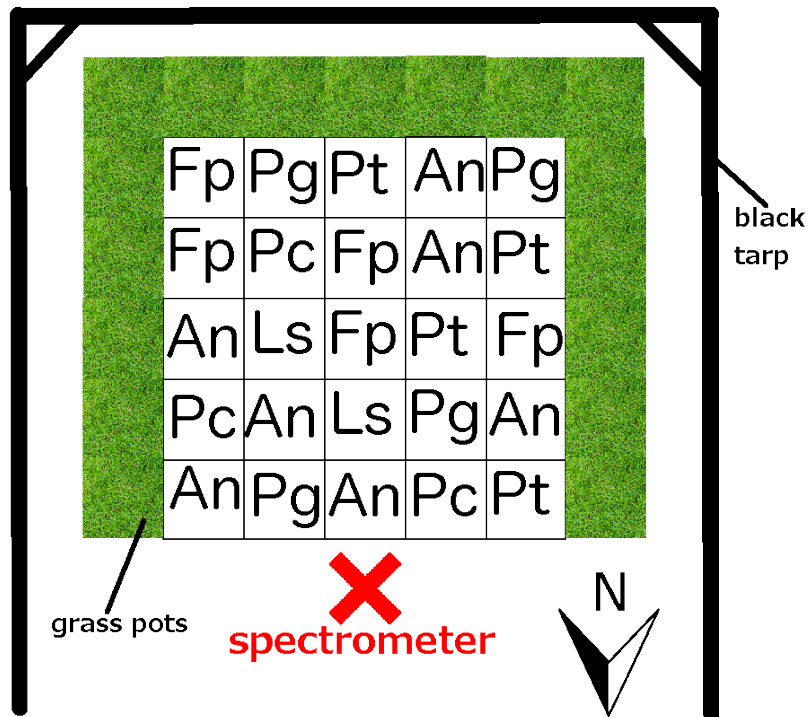


Figure 2-1: Diagram of basic rooftop sampling design. This example shows a species richness 6 plot. Species are labeled by their genus and species initials (*Fraxinus pennsylvanica* = Fp). See Figure 2-2 for representative photo.



Figure 2-2: Five by five tree plot, with a species richness of 5 on the south facing roof to the biological sciences building, University of Alberta. Note black box surrounding plot was not used in August scans, but the black cloth was used on both dates to minimize side lighting and reduce wind.

### *Instrumentation*

All data were collected with a full range (350-2500 nm) spectrometer (PSR series Spectroradiometer, Spectral Evolution, North Andover, MA, USA). The spectral range was reduced to 440-1600nm to allow comparisons with leaf level data. Canopy scans were done by attaching a 4° field of view (FOV) lens to the spectrometer. Leaf scans were done by attaching an optical fiber leaf clip (models UNI410 and UNI501, PP Systems, Haverhill, MA), and halogen light source (Figure 2-3). In the later case, actual sampling spot size was 0.6 mm in diameter, enabling repeatable reflectance measurements on individual leaves, including needle-leaved conifers. Due to light attenuation by the fiber (not specifically designed for the Spectral Evolution instrument), the leaf scans resulted in a useable spectral range of 440-1600nm (limited noise from 440-1000nm, moderate noise from 1000-1600nm). This is due to the detectors changing from a silicon photodiode detector (range 400-

1000nm), to two indium gallium arsenide (InGaAs) detectors (1000-2500nm). The signal to noise ratio was much lower in the InGaAs detectors than the silicon detector.

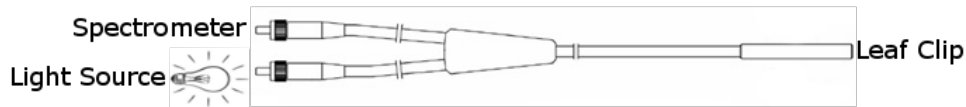


Figure 2-3: Leaf sampling procedure set up with bifurcated fiber.

#### *Spectral measurements – canopy scans*

All data was collected during the spring and summer months of 2013 (May, June, July, August) on the sixth floor roof of the Biological Sciences Building, University of Alberta. Canopy scans (without leaf clip) were only done under clear, to mainly sunny, skies. White scans, using a white panel (Spectralon™, Labsphere, North Sutton, New Hampshire, USA), were done before the first scan and after every 10 scans. The spectrometer was held approximately 180cm off the ground to give a 10cm FOV (size of one pot) and the lens was centered over the trees using a laser. Each tree was scanned once (25 trees resulting in 25 spectra) but each scan was an average of 10 scans for the same location (set during instrument setup). All 25 trees were sampled in a gridded pattern starting in the northwest corner.

#### *Spectral measurements – leaf scans*

Leaf level measurements were done under clear to cloudy weather conditions (clouds did not affect the radiation source, see Figure 2-3). White scans, using a small white reference (Labsphere, North Sutton, NH, USA) were done before the first scan and after every 10 trees (I attempted to use the same spot on the white reference). Using a leaf clip, three leaves were scanned per tree. Again, each

individual leaf scan was an average of 10 scans (set during instrument setup) and all 25 trees were sampled in a gridded pattern. The three leaf scans per tree were then average to get a single scan per tree (25 total scans per plot). These scans were then spectrally smoothed with a 3 band running average (after averaging the three scans). This step helped with the noise from 1000-1600nm, and was needed to compare leaf level slope variables (noisy) to canopy level slope variables (clean).

*Biodiversity metrics computed*

For each plot the species richness, Simpson Index (eq. 2-1), and Shannon Index (eq. 2-2) were computed. The reported Simpson index was actually the reciprocal of Simpson Index (eq. 2-1) because the reciprocal scales positively with diversity (unlike the normal Simpson Index), and because the maximum value is the number of species in the plot (Williams, 1964, Peet, 1974). Additionally, the log of Simpson and Shannon Index were calculated to investigate a possible saturating effect of optical diversity.

$$\text{Reciprocal Simpson Index} = 1 / \sum_{i=1}^S \frac{n_i(n_i-1)}{N(N-1)} \quad (2-1)$$

Where there are S species and  $n_i$  is the number of individuals of the  $i^{\text{th}}$  species and N is the total number of individuals.

$$\text{Shannon Index} = - \sum_{i=1}^S p_i \ln p_i \quad (2-2)$$

$p_i$  is the proportion of individuals from the sample total of species  $i$ .

*Spectral metrics computed*

For each experiment, scans were processed to percent reflectance with processing software (DARWin SP Application Software, Spectral Evolution, North Andover, MA, USA). 25 scans per plot of canopy and leaf scans were processed by first calculating all spectral variables seen in table 2-2 along with the reflectance and

derivative PCA. Principal component analysis (PCA) weightings were calculated from the 25 scans in the highest diversity plot (SR=7). These weightings were then applied to each plot, which resulted in a series of eight PC variables (see Appendix A).

The selection of spectral variables (Table 2-2) was guided by the weighting of each wavelength in the PCA and also their use in prior studies (Zutta 2003, Carlson *et al.* 2007). Based on the PCA, I chose indices from the NIR region (PC1), visible blue and red wavelengths (PC2), and green wavelengths and 1430nm water band region (PC3) (Table 2-2). The 970nm WBI was chosen due to use in Zutta (2003) while slope analyses at 525, 717, and 1150nm were chosen due to use in Carlson *et al.* (2007) and due to their location regarding important chemical and water absorption features. Many spectral variables were used because I wanted to test the relative strengths (correlations) of each type (vegetation indices, PCs, and slope analyses).

Each plot therefore had 25 spectra/scans with 23 associated spectral variables. The 25 scans were then used to compute a standard deviation or range value for the 23 spectral variables. This then resulted in each plot having one standard deviation/range value for each spectral variable (see Figure 2-4 for example with NDVI).

Table 2-2: List of vegetation indices with their abbreviation, formula, and citation

Name	Abbreviation	Formula	Source
<b>Vis/NIR indices</b>			
Gitelson's Chlorophyll Index	GIC	$R_{750}/R_{705}$	Gitelson & Merzlyak, 1997
Normalized difference vegetation index	NDVI	$(R_{800}-R_{680})/(R_{800}+R_{680})$	Sims & Gamon, 2002
Slope at 717nm	Slope717	$(R_{718.6}-R_{717.4})/(718.6-717.4)$	-
Slope at 680nm	Slope680	$(R_{681.7}-R_{680.4})/(681.7-680.4)$	-
Structure independent pigment index	SIPI	$(R_{800}-R_{445})/(R_{800}-R_{680})$	Peñuelas <i>et al.</i> , 1995
Photochemical reflectance index	PRI	$(R_{531}-R_{570})/(R_{531}+R_{570})$	Gamon <i>et al.</i> , 1992
Slope at 550nm	Slope550	$(R_{551.1}-R_{549.7})/(551.1-549.7)$	-
Slope at 525nm	Slope525	$(R_{526.6}-R_{525.1})/(526.6-525.1)$	-
<b>Water indices</b>			
Relative water content	RWC	$R_{1100}/R_{1430}$	Yu <i>et al.</i> , 2000
Water Band Index	WBI	$R_{900}/R_{970}$	Peñuelas <i>et al.</i> , 1997
Slope at 1150	Slope1150	$(R_{1153.4}-R_{1149.5})/(1153.4-1149.5)$	-

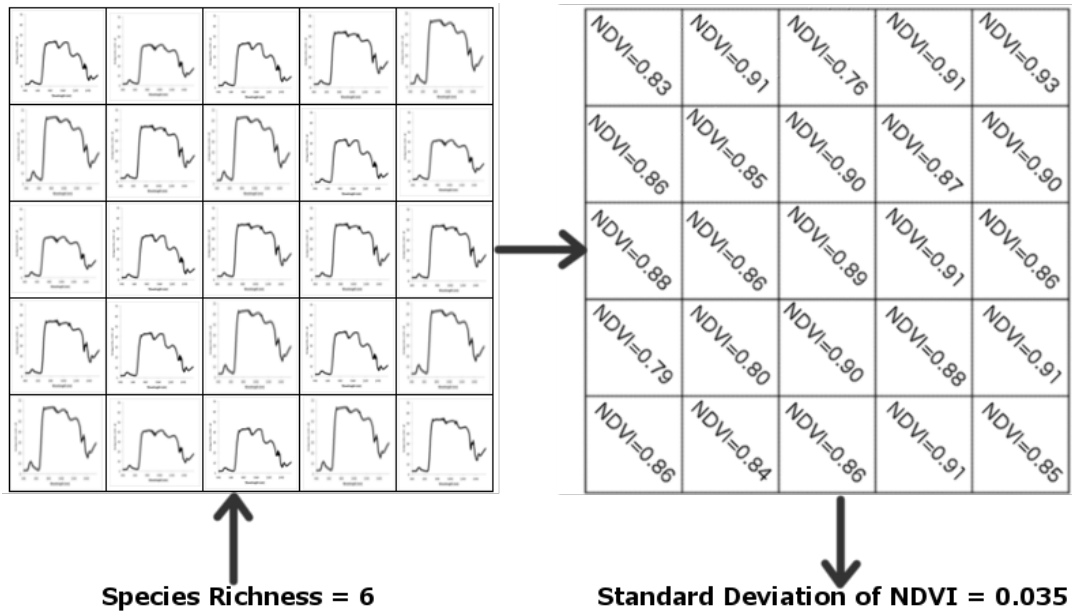


Figure 2-4: Spectral processing method. Start with a five by five tree plot with a species richness of 6. Through the spectral measurement method 25 scans/spectra are acquired. These scans are then converted into a spectral variable (in this case NDVI). Using the 25 values of NDVI, a single standard deviation value is calculated. Therefore in the end the species richness 6 plot has a 0.035 standard deviation of NDVI.

At the leaf and canopy level, each variable was correlated against Simpson Index (SI), log Simpson Index (LSI), Shannon Index (SH), log Shannon index (LSH),

and species richness (SR). With this suite of spectral variables, optical diversity indices (ODIs) were built by using linear models in R statistical software (R: A language and environment for statistical computing, R foundation for statistical computing, Vienna, Austria). Spectral variables (i.e. PC1-4, vegetation indices, and slope variables) were selected based upon their correlation value, p-value, and region in the spectral profile (i.e. 2 variables were not used if measuring the exact same wavelength). ODIs were correlated against all the diversity indices and judged based on their  $R^2$  value, RMSE value, and p-value.

#### *Additional Analysis*

To compare the effect of leaf traits and canopy structure on the OD-species diversity relationship, the correlation (with species diversity) of leaf level spectral variables was compared to the correlation of canopy level spectral variables. This comparison yielded a change in correlation ( $\Delta R^2$ ) between leaf level and the canopy level. This change in correlation was recorded for 18 spectral variables and ODI#3.

The effect of canopy roughness was analyzed by calculating the percent change in standard deviation or range of 18 spectral variables. This was done by taking the standard deviation/range value of rough canopies and subtracting the standard deviation/range value of smooth canopies. The spectral range experiment was done by analyzing canopy level data at three separate ranges (450-1600nm, 450-1000nm, and 450-800nm). At each new range, the correlation (to species diversity) of the PCs and ODI#3 was recalculated. Like the leaf versus canopy experiment, the change in correlation was then recorded for PC 1-4 reflectance and derivative and ODI#3.

## Results

Figures 2-5 and 2-6 show a representative spectral profile for the seven tree species used in this study. Variation between species occurs throughout the whole spectral range but the greatest absolute differences occur in the NIR/SWIR region. The white spruce and lodgepole pine (both conifers) show lower NIR reflectance in both the leaf level (Figure 2-6) and canopy level (Figure 2-5) measurements while the broadleaf trees and Siberian Larch show higher NIR reflectance. Also seen is the increased noise in the leaf level spectra above 1000nm (Figure 2-6) matching the range of the second instrument detector. The maximum noise variation seems to be about 5% reflectance but the general shape of the spectra is still maintained.

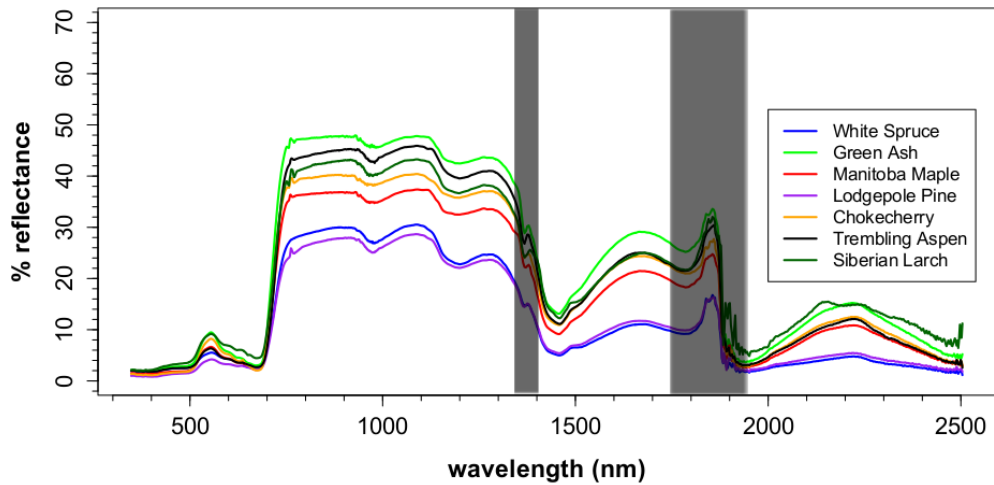


Figure 2-5: Canopy level spectra of the 7 tree species used in optical diversity testing. Spectral range 400-2500nm. Done with even canopy distribution. Spectra not smoothed. Grey regions represent areas of bad data due to water absorption and/or detector transitions.

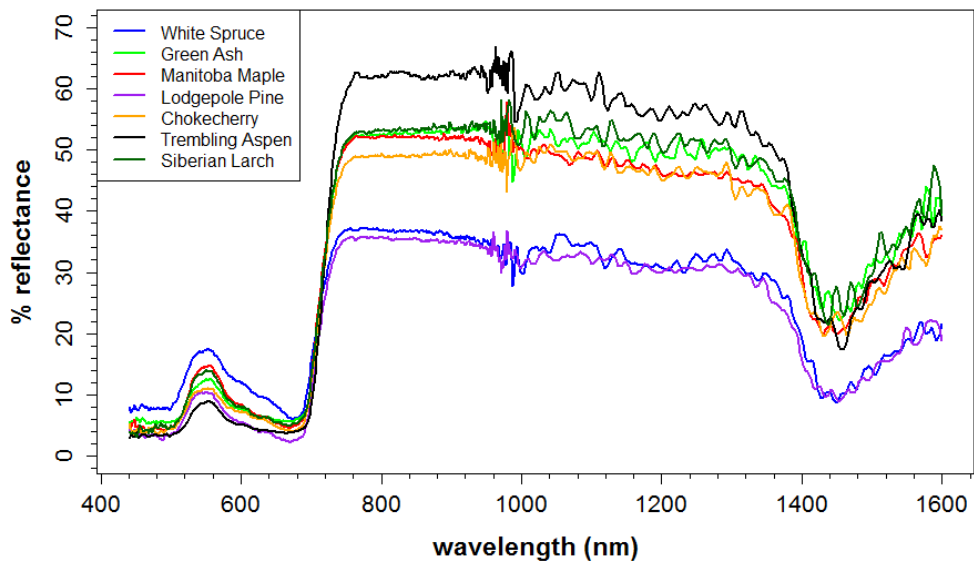


Figure 2-6: Leaf level spectra of the 7 tree species used in optical diversity testing. Spectral range 440-1600nm. Note noise near 1000nm (region of detector change) due to light attenuation by the fiber. Smoothed spectra shown rather than original spectra.

Figure 2-7 relates the PCA weightings to wavelengths, providing insight into the spectral regions with high information content. PC1 appears to be correlated to general brightness and is particularly sensitive to the NIR region and less to the

green (525nm) hump. PC2 is sensitive to the visible spectral range 440nm-700nm, particularly the blue and red regions. PC3 is correlated to the green hump (~525nm) and the water absorption feature at 1400-1600nm. PC4 does not show any strong correlation, but did show a slight double peak near the red edge (the chlorophyll fluorescence region; Gamon *et al.*, 1990). With these spectral regions in mind, I selected vegetation indices that fell in the same regions as indicated by the PC bands.

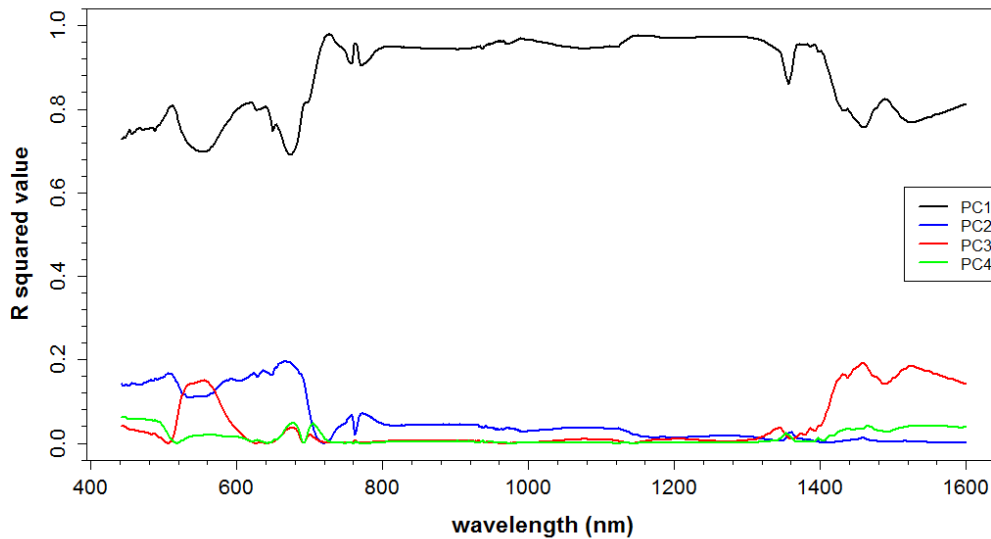


Figure 2-7: Correlation ( $R^2$  value) as a function of wavelength (440-1600nm) for of PCs 1-4 using canopy-scale data.

### *ODI Correlation*

In total, 23 spectral variables were used to analyze the correlation between OD and species diversity at the canopy level (Table 2-3). These variables included several vegetation indices, slope variables, and products of PCA, as described in Methods. Of all the biodiversity indices, log Simpson Index showed the best correlation with spectral variables while species richness showed the worst

correlation. 13 of the 23 indices showed a significant ( $p < 0.05$ ) correlation with log Simpson Index and 8 variables showed a significance of  $p < 0.01$ . Taking the log of an index did not improve results with the Shannon index as the average correlation was higher for the linear version. The highest correlated variables to species diversity appear to be common vegetation indices (SIPI, NDVI, and WBI) and slope variables. These accounted for seven out of the eight most correlated variables. The principal component method resulted in five moderately correlated variables, with the five showing significant ( $p < 0.05$ ) correlations with log Simpson Index. Using the range in slope rather than the standard deviation in slope provided better correlations with biodiversity indices, with a 0.098 average increase in correlation.

Table 2-3: List of all canopy level variables and their R<sup>2</sup> value when correlated individually against species richness, Simpson Index, log Simpson Index, Shannon Index, and log Shannon Index. Variables listed in order from highest average R<sup>2</sup> value to lowest R<sup>2</sup> value. From smooth canopy reflectance spectra. P-value for each correlation listed in parentheses.

	<b>Species richness (SR)</b>	<b>Simpson Index (SI)</b>	<b>Log Simpson Index (LSI)</b>	<b>Shannon Index (SH)</b>	<b>Log Shannon Index (LSI)</b>	<b>Average R<sup>2</sup> value</b>
<b>SIPI<sub>sd</sub></b>	0.482 (0.005)	0.722 (0.0001)	0.651 (0.0004)	0.600 (0.0011)	0.437 (0.01)	0.578 (0.003)
<b>NDVI<sub>sd</sub></b>	0.472 (0.006)	0.494 (0.005)	0.587 (0.001)	0.598 (0.001)	0.577 (0.001)	0.546 (0.003)
<b>525slope<sub>range</sub></b>	0.436 (0.01)	0.610 (0.0009)	0.609 (0.0009)	0.574 (0.001)	0.461 (0.007)	0.538 (0.004)
<b>717slope<sub>range</sub></b>	0.388 (0.02)	0.534 (0.002)	0.595 (0.001)	0.561 (0.002)	0.553 (0.002)	0.526 (0.005)
<b>WBI<sub>sd</sub></b>	0.559 (0.002)	0.532 (0.003)	0.508 (0.004)	0.519 (0.0036)	0.397 (0.015)	0.503 (0.006)
<b>PC1slope<sub>sd</sub></b>	0.358 (0.02)	0.545 (0.002)	0.558 (0.002)	0.513 (0.004)	0.429 (0.01)	0.480 (0.009)
<b>717slope<sub>sd</sub></b>	0.331 (0.03)	0.464 (0.007)	0.471 (0.006)	0.439 (0.009)	0.378 (0.02)	0.416 (0.01)
<b>525slope<sub>sd</sub></b>	0.274 (0.05)	0.479 (0.006)	0.481 (0.006)	0.433 (0.01)	0.334 (0.03)	0.400 (0.02)
<b>PC1<sub>sd</sub></b>	0.317 (0.03)	0.445 (0.009)	0.429 (0.01)	0.399 (0.01)	0.350 (0.02)	0.388 (0.02)
<b>PC3slope<sub>sd</sub></b>	0.277 (0.05)	0.385 (0.02)	0.430 (0.01)	0.403 (0.01)	0.372 (0.02)	0.373 (0.02)
<b>PC3<sub>sd</sub></b>	0.276 (0.05)	0.328 (0.03)	0.414 (0.01)	0.403 (0.01)	0.407 (0.01)	0.366 (0.03)
<b>680slope<sub>sd</sub></b>	0.327 (0.03)	0.287 (0.04)	0.354 (0.02)	0.376 (0.02)	0.345 (0.03)	0.338 (0.03)
<b>PC4<sub>sd</sub></b>	0.169 (0.14)	0.252 (0.07)	0.343 (0.03)	0.324 (0.03)	0.369 (0.02)	0.291 (0.06)
<b>RWC<sub>sd</sub></b>	0.295 (0.04)	0.139 (0.2)	0.181 (0.1)	0.222 (0.09)	0.197 (0.1)	0.207 (0.1)
<b>PRI<sub>sd</sub></b>	0.224 (0.2)	0.170 (0.1)	0.149 (0.1)	0.165 (0.1)	0.0811 (0.2)	0.158 (0.2)
<b>1150slope<sub>range</sub></b>	0.138 (0.1)	0.187 (0.1)	0.185 (0.1)	0.175 (0.1)	0.102 (0.2)	0.157 (0.2)
<b>PC2<sub>sd</sub></b>	0.0639 (0.4)	0.0996 (0.3)	0.186 (0.1)	0.181 (0.1)	0.224 (0.1)	0.155 (0.2)
<b>550slope<sub>sd</sub></b>	0.077 (0.3)	0.102 (0.3)	0.159 (0.2)	0.155 (0.2)	0.203 (0.1)	0.139 (0.2)
<b>PC2slope<sub>sd</sub></b>	0.167 (0.1)	0.115 (0.2)	0.0922 (0.3)	0.100 (0.3)	0.0472 (0.5)	0.104 (0.3)
<b>1150slope<sub>sd</sub></b>	0.0645 (0.4)	0.127 (0.2)	0.106 (0.3)	0.0901 (0.3)	0.0405 (0.5)	0.0859 (0.3)
<b>PC4slope<sub>sd</sub></b>	0.166 (0.1)	0.0689 (0.4)	0.0650 (0.4)	0.0857 (0.3)	0.0314 (0.5)	0.0834 (0.3)
<b>GIC</b>	0.00165 (0.9)	0.0395 (0.5)	0.0603 (0.4)	0.0374 (0.5)	0.04957 (0.5)	0.0375 (0.5)
<b>average</b>	0.266	0.324	0.346	0.334	0.291	

All ODIs showed the highest correlation with the log of Simpson Index.

Based on Zutta (2003), ODI#1 (Figure 2-8) used a combination of NDVI<sub>sd</sub>, PRI<sub>sd</sub>, and

WBI<sub>sd</sub> which resulted in a R<sup>2</sup> of 0.71. ODI#2 (Figure 2-9) showed a slightly higher

correlation at  $R^2$  of 0.75. The most highly correlated ODI in this chapter was ODI#3 (Figure 2-10). This was a combination of  $NDVI_{sd}$ ,  $WBI_{sd}$ ,  $SIPI_{sd}$ ,  $PC3_{sd}$ , and  $525slope_{range}$  and it resulted in a  $R^2$  value of 0.90. All ODIs listed above showed a significant correlation ( $p < 0.01$ ) to log Simpsons Index.

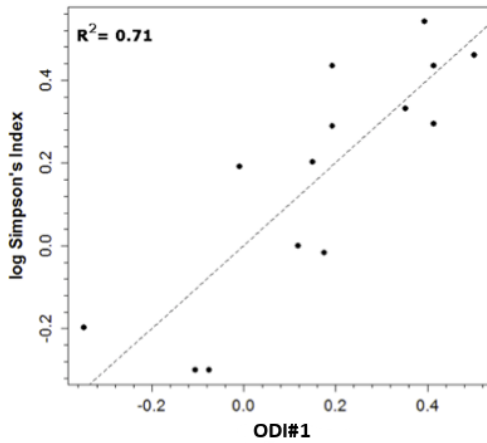


Figure 2-8: The relationship between ODI#1 (a linear combination of  $NDVI_{sd}$ ,  $WBI_{sd}$ , and  $PRI_{sd}$ ) and the log of Simpson Index for 14, 5x5 tree plots of varying diversity.

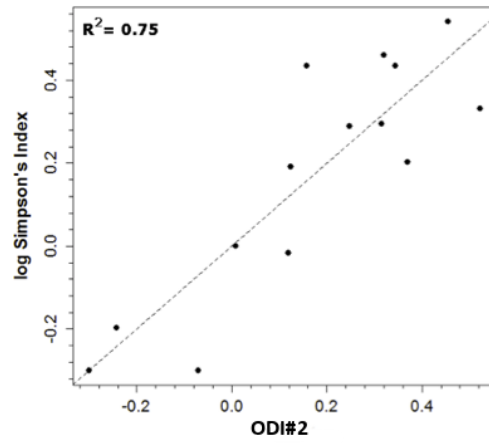


Figure 2-9: The relationship between ODI#2 (a linear combination of  $NDVI_{sd}$ ,  $PC1_{sd}$ , and  $PC3_{sd}$ ) and the log of Simpson Index for 14, 5x5 tree plots of varying diversity.

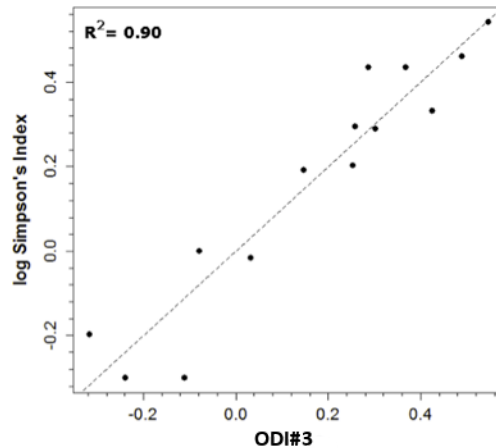


Figure 2.10: The relationship between ODI#3 (a linear combination of  $NDVI_{sd}$ ,  $PC3_{sd}$ ,  $525slope_{range}$ ,  $WBI_{sd}$ , and  $SIPI_{sd}$ ) and the log of Simpson Index for 14, 5x5 tree plots of varying diversity.

Table 2-4: List of ODIs with: diversity index correlated against, spectral variables used in equation, and R<sup>2</sup>, p-value, and RMSE of correlation. Actual equations with coefficients are shown below. Bold equations represent the ODIs shown above.

ODI	Diversity Index	Spectral variables	R <sup>2</sup>	p-value	RMSE
<b>1</b>	<b>Log Simpson</b>	<b>NDVI<sub>sd</sub> + WBI<sub>sd</sub> + PRI<sub>sd</sub></b>	<b>0.71</b>	<b>0.0050</b>	<b>0.15</b>
<b>2</b>	<b>Log Simpson</b>	<b>NDVI<sub>sd</sub> + PC1<sub>sd</sub> + PC3<sub>sd</sub></b>	<b>0.75</b>	<b>0.0020</b>	<b>0.13</b>
<b>3</b>	<b>Log Simpson</b>	<b>NDVI<sub>sd</sub> + PC3<sub>sd</sub> + 525slope<sub>range</sub> + WBI<sub>sd</sub> + SIPI<sub>sd</sub></b>	<b>0.90</b>	<b>0.0006</b>	<b>0.087</b>
slope	Log Simpson	524slope <sub>range</sub> + 717slope <sub>range</sub> - 1150slope <sub>range</sub>	0.76	0.001	0.13
PCA	Log Simpson	PC1slope <sub>sd</sub> + PC1 <sub>sd</sub> - PC3slope <sub>sd</sub> + PC3	0.59	0.06	0.17

$$\text{ODI\#1} = 21.4\text{NDVI}_{sd} + 8.844\text{WBI}_{sd} + 16.302\text{PRI}_{sd} - 1.23 \quad (2-3)$$

$$\text{ODI\#2} = 25.3\text{NDVI}_{sd} + 0.00122\text{PC1}_{sd} + 0.00954\text{PC3}_{sd} - 1.17 \quad (2-4)$$

$$\text{ODI\#3} = 13.9\text{NDVI}_{sd} + 0.00543\text{PC3}_{sd} + 1.09(525\text{slope}_{range}) + 2.73\text{WBI}_{sd} + 28.1\text{SIPI}_{sd} - 1.142 \quad (2-5)$$

$$\text{ODI}_{slope} = 2.468(524\text{slope}_{range}) + 0.4425(717\text{slope}_{range}) - 0.1352(1150\text{slope}_{range}) - 0.936 \quad (2-6)$$

$$\text{ODI}_{PCA} = 4.225\text{PC1slope}_{sd} + 0.0026\text{PC1}_{sd} - 0.084\text{PC3slope}_{sd} + 0.00151\text{PC3} - 1.02 \quad (2-7)$$

### *Leaf level optical diversity*

Figure 2-11 shows how leaf level PCA weightings are correlated to wavelength. PC1 is related to NIR brightness and less to the VIS region. PC2 is related to the VIS region, and the red region in particular. PC3 is related to the green region (~550nm) while having a smaller relation to the red edge region. PC4 is sensitive to the water absorption from 1400-1600nm. In general, leaf level weightings seem to be responsive to small-scale features rather than general region brightness

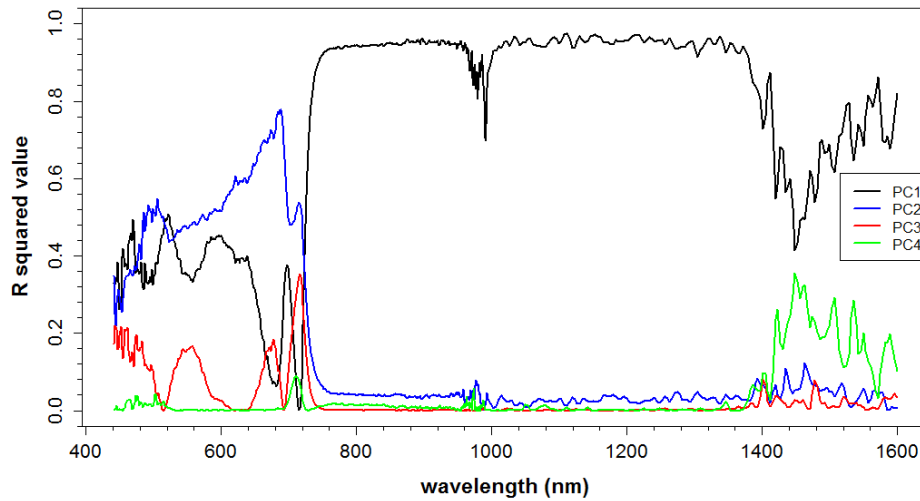


Figure 2-11: Correlation ( $R^2$  value) as a function of wavelength (440-1600nm) for of PCs 1-4 using leaf level data.

Table 2-5 shows the correlation between 18 spectral variables and species diversity indices at the leaf level ( $PC_{\text{derivative}}$  1-4 not used due to noise past 1000nm). Log Simpson Index showed the highest correlation to leaf level optical variables while species richness showed the lowest correlation. 9 out of the 18 variables showed a significant ( $p\text{-value} < 0.05$ ) correlation with log Simpson Index and 8 showed a significance of  $p < 0.01$ . Slope analysis in the green slope and NIR slope regions had four out of the six highest correlated spectral variables. The range in 717nm slope showed the highest correlation to any biodiversity index at a  $R^2$  value of 0.851 (to log SI).

Table 2-5: List of all leaf level variables and their R<sup>2</sup> value when correlated against species richness, Simpson Index, log Simpson Index, Shannon Index, and log Shannon Index. Variables listed in order from highest average R<sup>2</sup> value to lowest R<sup>2</sup> value. P-values are shown in parentheses.

	<b>SR</b>	<b>SI</b>	<b>Log SI</b>	<b>SH</b>	<b>Log SH</b>	<b>Average R<sup>2</sup></b>
<b>717slope<sub>range</sub></b>	0.625 (0.0007)	0.754 (5E-5)	0.851 (2E-6)	0.833 (5E-6)	0.783 (2E-5)	0.743 (0.0002)
<b>717slope<sub>sd</sub></b>	0.750 (6E-5)	0.585 (0.001)	0.436 (0.01)	0.571 (0.007)	0.591 (0.003)	0.590 (0.004)
<b>GIC<sub>sd</sub></b>	0.402 (0.01)	0.602 (0.001)	0.704 (0.0002)	0.658 (0.0004)	0.635 (0.0006)	0.569 (0.005)
<b>NDVI<sub>sd</sub></b>	0.404 (0.01)	0.467 (0.007)	0.589 (0.001)	0.585 (0.001)	0.66 (0.0003)	0.486 (0.007)
<b>525slope<sub>sd</sub></b>	0.612 (0.0009)	0.484 (0.005)	0.345 (0.03)	0.364 (0.02)	0.174 (0.13)	0.480 (0.01)
<b>525slope<sub>range</sub></b>	0.303 (0.04)	0.499 (0.005)	0.617 (0.0008)	0.467 (0.002)	0.264 (0.04)	0.473 (0.02)
<b>PC1<sub>sd</sub></b>	0.244 (0.07)	0.433 (0.01)	0.549 (0.002)	0.505 (0.004)	0.518 (0.003)	0.409 (0.02)
<b>PC2<sub>sd</sub></b>	0.281 (0.05)	0.431 (0.01)	0.495 (0.005)	0.464 (0.007)	0.489 (0.005)	0.403 (0.02)
<b>SIPI<sub>sd</sub></b>	0.300 (0.04)	0.329 (0.031)	0.405 (0.01)	0.407 (0.01)	0.458 (0.008)	0.345 (0.3)
<b>PC4<sub>sd</sub></b>	0.103 (0.3)	0.234 (0.08)	0.252 (0.06)	0.220 (0.09)	0.244 (0.07)	0.196 (0.1)
<b>RWC<sub>sd</sub></b>	0.115 (0.2)	0.103 (0.2)	0.24 (0.07)	0.265 (0.06)	0.415 (0.01)	0.155 (0.2)
<b>PC3<sub>sd</sub></b>	0.159 (0.2)	0.0645 (0.4)	0.128 (0.2)	0.161 (0.2)	0.159 (0.2)	0.117 (0.2)
<b>1150slope<sub>sd</sub></b>	0.098 (0.3)	0.083 (0.3)	0.098 (0.3)	0.104 (0.3)	0.0866 (0.3)	0.093 (0.3)
<b>WBI<sub>sd</sub></b>	0.0546 (0.4)	0.0654 (0.4)	0.106 (0.3)	0.106 (0.3)	0.157 (0.2)	0.0755 (0.3)
<b>680slope<sub>sd</sub></b>	0.0041 (0.8)	0.0664 (0.4)	0.1173 (0.2)	0.0924 (0.3)	0.147 (0.2)	0.0626 (0.4)
<b>PRI<sub>sd</sub></b>	0.0497 (0.4)	0.0544 (0.4)	0.0828 (0.3)	0.0846 (0.3)	0.0635 (0.4)	0.0623 (0.4)
<b>550slope<sub>sd</sub></b>	0.0322 (0.53)	0.0989 (0.3)	0.0405 (0.5)	0.0270 (0.6)	0.00945 (0.7)	0.057 (0.4)
<b>1150slope<sub>range</sub></b>	0.0000 (0.9)	0.0049 (0.8)	0.0004 (0.9)	0.00029 (0.9)	0.000145 (0.9)	0.0018 (0.9)
<b>average</b>	0.252	0.297	0.337	0.328	0.325	

### *Leaf optical diversity versus canopy optical Diversity*

Figure 2-12 summarizes the change in correlation value from canopy to leaf level scans. 11 out of the 18 spectral variables showed higher correlation in canopy measurements. Common vegetation indices (SIPI, NDVI, WBI, PRI) all showed better correlation in canopy scans. Slope analysis in the green and red slope regions (525nm and 717nm) show higher correlation at the leaf level. Variables such as GIC and PC2 showed a much higher correlation in leaf level scans due to the fact that

there was nearly no correlation at the canopy scale. Figure 2-13 shows ODI#3 correlated against log Simpson Index at the leaf and canopy scale. The canopy level ODI results in a  $R^2$  of 0.90 while the leaf level ODI results in an  $R^2$  of 0.80.

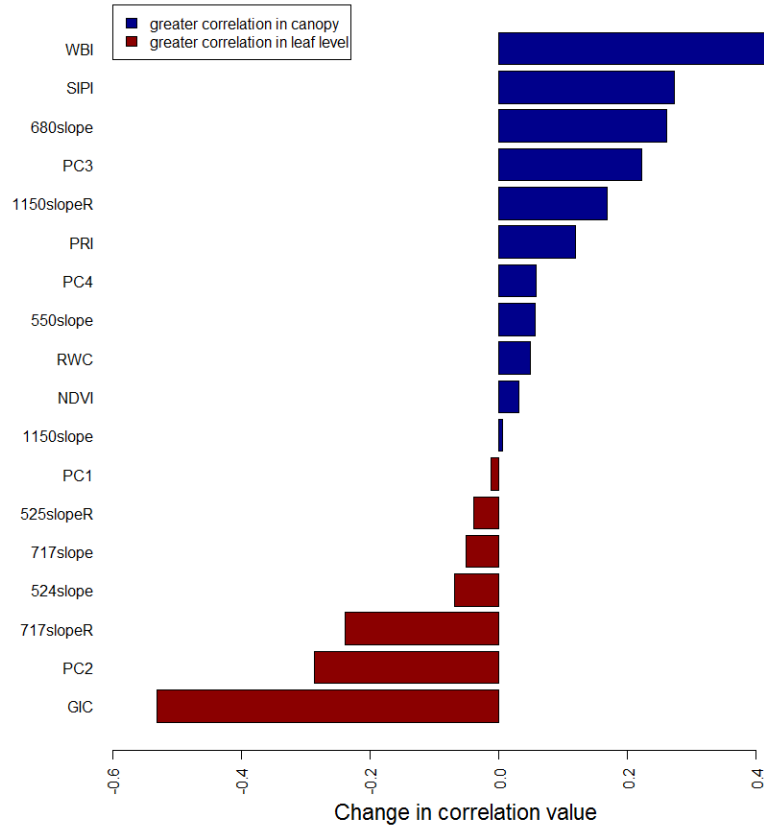


Figure 2-12: Change in average  $R^2$  value between canopy and leaf level scans for all vegetation index seen in Tables 2-3 and 2-5.

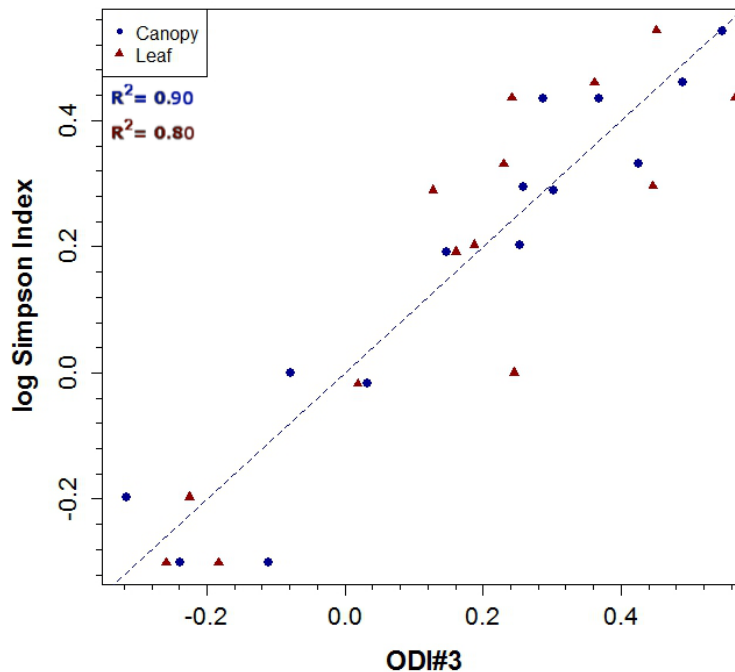


Figure 2-13: ODI#3 at the leaf and canopy scale. Red points represent leaf level data while blue points represent canopy level data.

### *Variable canopy height*

Figures 2-14 and 2-15 demonstrate that spectral variance increases when canopy height is uneven. The uniform height canopy shows a low standard deviation around the average, from 40-60% reflectance in the NIR. The variable height canopy shows a high standard deviation around the average, from 20-60% reflectance in the NIR. Figure 2-16 shows the weighting of the principal component bands with uneven canopies. In general, it seems to be very similar to the even canopy PCA weightings. It does appear to be less sensitive to small absorbance features (i.e. the humps in the VIS region of Figure 2-7). The only major difference between Figure 2-7 and Figure 2-16 is the lack of the green region in PC3. Figure 2-17 shows 15 out of the 18 spectral variables show higher variation in uneven

canopy scans. The only variables with higher variance in uniform canopy scans were three slope variables.

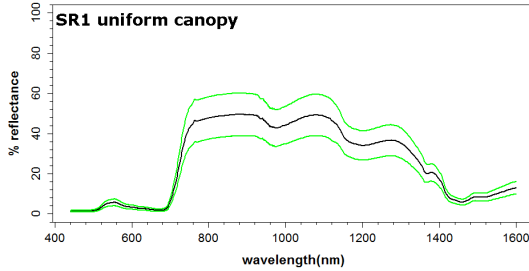


Figure 2-14: Average spectrum (black) with one standard deviation below and above the average (green) for a SR=1 plot with a uniform canopy.

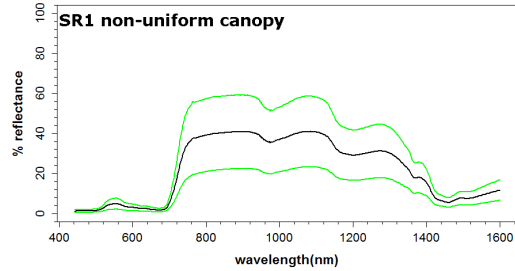


Figure 2-15: Average spectrum (black) with one standard deviation below and above the average (green) for a SR=1 plot with a non-uniform canopy.

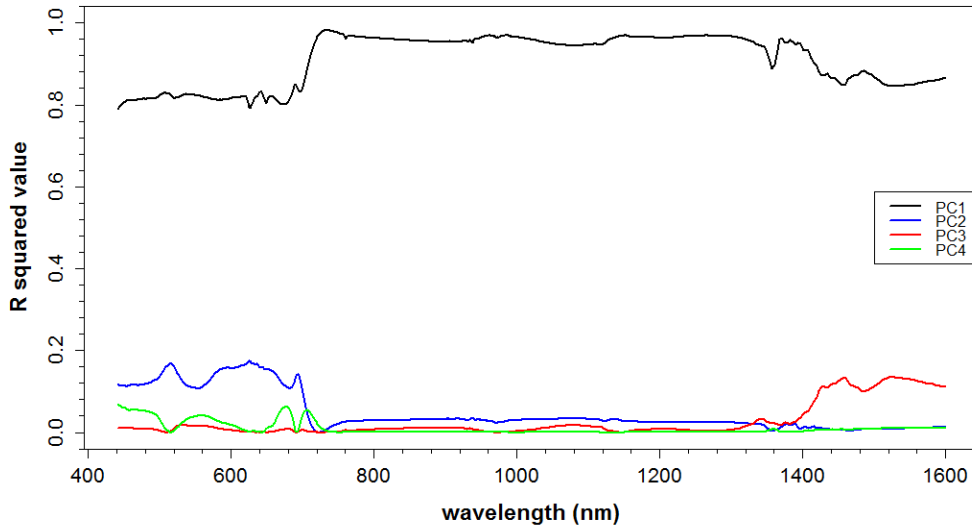


Figure 2-16: Correlation ( $R^2$  value) as a function of wavelength (440-1600nm) for of PCs 1-4 using uneven canopy data.

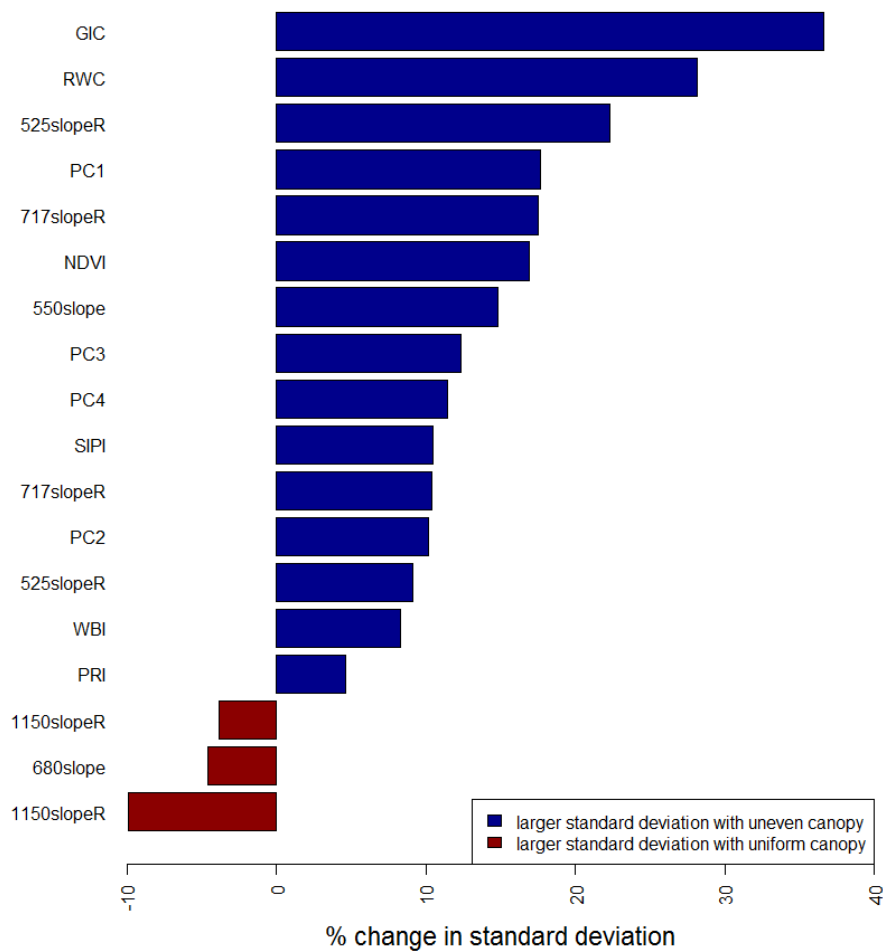


Figure 2-17: Percent change in the standard deviation of all vegetation indices between a non-uniform canopy and a uniform canopy. Greater deviation in non-uniform canopy shown in blue and greater deviation in uniform canopy shown in red.

*Spectral range*

Reducing the spectral range to the range of silicon photodiode spectrometers (400-1000nm) did not show any major change in the correlation of PC variables (Figure 2-18). The change in R<sup>2</sup> value for ODI#3 between the two ranges is mainly due to the loss of the 1400-1600nm water band used in PC3. The only loss of information when decreasing spectral range from 400-1600nm to 400-1000nm is limited to RWC, 1150slope, and one part of PC3. When reducing the range to 400-800nm, PCs 1 and 3 were seen to have a moderate drop in correlation

(about 0.2) while PC2 increased its  $R^2$  value by 0.3 (Figure 2-19). There was little change in the  $PC_{\text{derivative}}$  variables, except for  $PC4_{\text{derivative}}$ , which increased in correlation by 0.369 when moving to 400-800nm range. ODI#3 dropped correlation by 0.14 when using the 800nm range mainly due to the loss of WBI in the linear equation. Note that that these results were only analyzed up to 1600nm and therefore we cannot analyze the change in correlation for a true “full range” detector (range 400-2500nm).

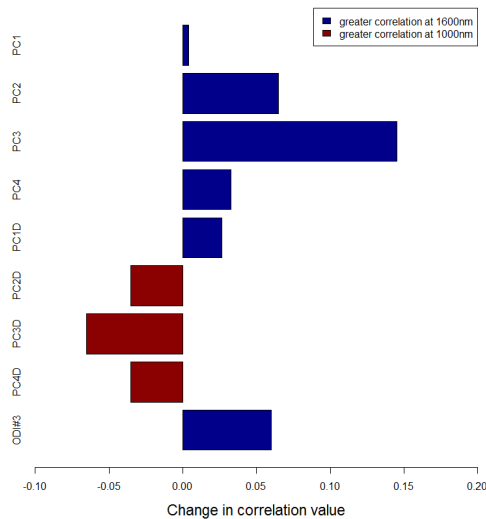


Figure 2-18: The change in correlation (species diversity and optical diversity) when the spectral range is changed from 400-1600nm to 400-1000nm. Blue indicates higher correlation using the 400-1600nm range while red indicates higher correlation using the 400-1000nm range.

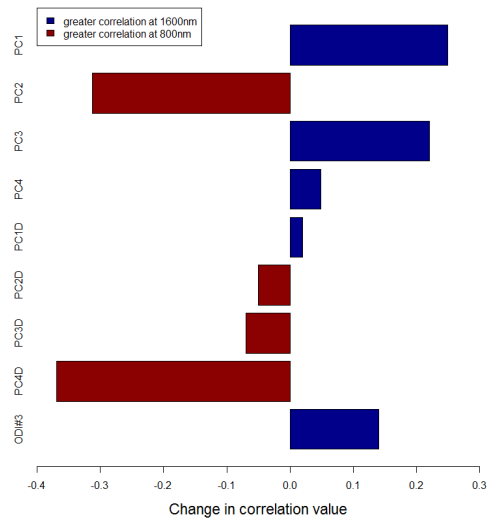


Figure 2-19: The change in correlation (species diversity and optical diversity) when the spectral range is changed from 400-1600nm to 400-800nm. Blue indicates higher correlation using the 400-1600nm range while red indicates higher correlation using the 400-800nm range.

## Discussion

### *Spectral variation hypothesis (Canopy)*

This research shows that the majority of vegetation indices, slope variables, and principal component variables tested show a significant correlation to biodiversity variables. The highest correlated of these spectral variables were vegetation indices and slope variables. This indicates that absorption features used

to measure vegetation function may be useful for optical diversity studies. Additionally, most of these variables had the highest correlation with log Simpson Index. This may indicate that there is a saturating effect associated with optical diversity although the OD relationship with Shannon Index does not show this saturating effect. Therefore, the shape of the relationship between OD and biodiversity indices may depend on the biodiversity index used.

This experiment supports the SVH and, with the suite of variables used, it shows the SVH methods can be assessed many ways. These methods include: the standard deviation of principal components of reflectance spectra (Rocchini *et al.* 2004 and Oldeland *et al.* 2010), the standard deviation of principal components of derivative spectra, the standard deviation or range in slope of absorbance features (similar to Carlson *et al.*, 2007), and the standard deviation of vegetation indices (Zutta, 2003). All these methods yielded at least two spectral variables that showed significant correlation ( $p < 0.05$ ) with biodiversity variables. The most promising method may be to combine these various approaches as seen in ODI#3. This used the highest correlated variables from each method (combined in a linear model) and yielded a total correlation of  $R^2$  0.90 with log Simpson Index.

#### *Leaf versus Canopy effects on optical diversity*

My hypothesis on the effects of leaf versus canopy structure states that part of optical diversity should be affected by leaf traits and part should be affected by canopy structure. Vegetation reflectance is influenced by optical leaf level properties, leaf area, leaf orientation, supporting structure orientation, background reflectance, viewing geometry, and solar geometry (Colwell, 1974). Because the experimental design minimized the variation in background reflectance, viewing geometry, and solar geometry, variation in canopy reflectance should primarily be a

function of variation in leaf properties and canopy structure while variation in leaf reflectance will be a function of leaf properties. If my hypothesis is correct, correlation between optical diversity and species diversity should be higher at the canopy level since canopy reflectance is a function of leaf reflectance plus other structural canopy level variables. The conclusions about this hypothesis are outlined below.

Slope variables at 525 and 717nm appear to refute my hypothesis of a greater correlation with diversity at the canopy scale (Figure 2-12). This is because the correlation between the spectral variables and species diversity is reduced when moving from leaf level to canopy level data indicating a negative effect of canopy structure on the OD-species diversity correlation. These regions represent promising areas for biodiversity detection since they are correlated to species diversity at both the leaf and canopy scale (Carlson *et al.*, 2007). Because the correlation is less at the canopy scale, the effect of varying canopy structure is limiting the ability of these indices to detect optical diversity. The other three spectral variables with lower correlation at canopy scale are likely not suitable indices for biodiversity monitoring since they have little correlation at the canopy scale (except PC1, which has virtually no change in correlation)

In the case of the other 11 spectral variables, there is an increase in correlation at the canopy scale (Figure 2-12). These variables support my hypothesis that optical diversity is a combination of leaf and canopy structure traits because canopy level data increases the ability to detect variation in optical diversity. Leaf scans likely have the ability to distinguish between physiologically different species such as white spruce and trembling aspen. However, when there are seven species, leaf-level scans likely cannot differentiate between spectrally

similar species (e.g. Manitoba maple and three green ash). Canopy scans can more effectively differentiate these due to the additional influence of contrasting canopy structure (e.g. LAI and mean leaf angle (MLA)) (Asner, 1998), which can be estimated through NDVI, SIPI, PC1, and WBI.

Under the conditions of this study, it appears that the majority of the correlation between OD and species is controlled by variation in leaf properties. Figure 2-13 shows leaf level correlation ( $R^2 = 0.80$ ) is very similar to canopy level correlation ( $R^2 = 0.90$ ) (using ODI#3). The variation in leaf level traits or their expression via canopy structure, seen in the 0.80 correlation, is likely a major constituent of the 0.90 correlation seen at the canopy level (hypothetically, a combination of leaf traits and canopy structure). Note that this conclusion may not apply to more complex and less optically thick canopies as seen in the next chapter. The percentage of canopy versus leaf variation also depends on which optical variables are used in the ODI equation. For example, if more slope variables are used, it is likely the role of leaf traits will increase even more.

These findings are consistent with the findings of other studies from other biomes. Carlson *et al.* (2007) found that the variation in leaf level properties could be seen from canopy imagery by calculating the variation in the slope of chemical and water absorbance features. This chapter also showed that the slope of absorbance features was useful for estimating the variation in leaf properties (although varying canopy structure does slightly limit that ability). The majority of my spectral variables and ODIs showed that optical diversity is controlled by both leaf properties (to a larger degree) and canopy structure (lesser degree). Early work by Asner (1998) initially showed variability of vegetation reflectance was primarily related to canopy structure. As more ecosystems were explored, it was found that

as canopies became optically thick, the role of variation in leaf properties became more important (Asner *et al.* 2002, Carlson *et al.* 2007, Clark & Roberts, 2012). This conclusion agrees with this study since the canopies of this experiment were densely packed and my correlations were primarily attributed to leaf properties.

#### *Canopy height effects*

Figure 2-17 clearly shows that uneven canopy structure leads to an increase in OD when compared to the same plot with an even canopy structure. This is likely due to increased shading and increased multiple scattering in the uneven canopies (Chen *et al.*, 1999). This directly affects optical variables such as PC 1-4 since these variables are subject to brightness changes (particularly PC1). Brightness changes will also increase variation in slope and ratio based variables since it has been found that shaded trees will have higher NIR/RED ratios than sunlit trees (Chen *et al.*, 1999) due to higher multiple scattering in the NIR compared to the RED region. Similarly, Danson (1995) found the position in the canopy (i.e., shaded or not shaded) caused substantially different spectral signatures of species. These results give insight into which optical variables are useful for measuring plot level canopy structure (i.e., canopy roughness). Based on Figure 2-17 and the weightings in Figure 2-7, the standard deviation in PC1 is best suited for measuring plot level canopy structure, due to its ability to detect variation in sun exposure, canopy gaps, and general brightness (although more weighted towards NIR brightness).

These results showed that plot level canopy structure (canopy roughness) plays a large role in optical diversity. Fortunately, increased canopy roughness tends to correlate to increased species diversity because different species grow at varying rates (Denslow, 1987). Therefore, variation in tree height (plot level structure), along with physiology, plant structure, and phenology, could be an

additional factor in determining optical diversity. Consequently, optical diversity may be related to functional diversity rather than species diversity per se. Optical diversity may also be a factor of spatial heterogeneity (Rocchini, 2007), which is then secondarily related to functional/species diversity. Experimental tests of the surrogacy hypothesis (Gamon, 2008) would be needed to resolve these issues. Optical diversity is likely capturing significant functional differences in plot level structure (spatial heterogeneity), physiology, plant structure, and phenology.

### *Spectral range*

Changing spectral range was shown to have an effect on the ability of spectral diversity to detect species diversity. When reducing the range from 400-1600nm to 400-1000nm PC3 was the only spectral variable significantly affected while the correlation in ODI#3 was reduced by 0.06 mainly due to the loss of 1400-1600nm in PC3. Two spectral variables were lost with this change (RWC and 1150slope) but these variables were not highly correlated to species diversity.

Reducing the spectral range even further, to 400-800nm, caused the wavelength weightings to change in the PCA. Thus, correlations between PC 1 and 3 and species diversity were reduced while the correlation with PC2 was increased. This change in PC3 plus the loss of WBI in the linear equation resulted in decreased the correlation of ODI#3 by 0.16. In general, increased spectral range does increase the ability to detect optical diversity by increasing the number of spectral regions that can be used to discriminate plant species (Oldeland *et al.* 2010, Palmer *et al.* 2002). Conversely, it appears much of the information needed, in the 400-1600nm range, may be in the VIS and NIR regions as seen with the analysis at 400-800nm and 400-1000nm. Although it should be noted that I did not analyze the full range (400-2500nm) and this region may be an area important for distinguishing some

species and thus increasing optical diversity. Lucas *et al.* (2008) found similar results to this study in that most tree species could be identified with VIS-NIR data and adding SWIR data slightly improved the classification. This may not be the case for all optical diversity studies and may vary between ecosystem types.

Other studies on the remote sensing of biodiversity (Carlson *et al.* 2007, Oldeland *et al.* 2010, Lucas & Carter 2008) have used full range spectrometers (400-2500nm) in their analysis. Carlson *et al.* (2007) cites the need for the water absorption feature at 1201nm and the nitrogen absorption feature at 1523nm as a reason for using full range while Oldeland *et al.* (2010) states covering all spectral regions is a key factor when relating OD to species diversity. It is not yet known if the cost of additional spectral range is worth the improved results. Additional range should improve correlation, but the degree to which it improves the correlation may depend on the ecosystem in question. Future studies could hopefully extend the range to 400-2500nm (not done in this research) and test the effect of incrementally reducing the spectral range.

## **Conclusions**

This study shows that the variance in spectral variables is correlated to species diversity. More than half the spectral variables used showed a significant correlation with species diversity. When used in a linear model, these ODIs correlate very strongly to species diversity ( $R^2 > 0.7$ ). The results on leaf versus canopy effects showed that these ODIs are primarily controlled by variation in leaf properties. It is likely that as canopies become more complex, the importance of canopy structure in detecting diversity will increase. The tree height experiment showed that increased canopy roughness increases the variance in spectral indices while the spectral range

test showed that increasing the spectral range (to 1600nm) does slightly improve correlations between OD and species diversity although tests to the full range (400-2500nm) were not analyzed.

## Literature Cited

- Asner, G.P. (1998). Biophysical and Biochemical Sources of variability in canopy reflectance. *Remote Sensing of Environment* 64, 234-253.
- Asner, G.P., Palace, M., Keller, M., Pereira, R., Silva, J.N.M., & Zweede, J.C. (2002). Estimating Canopy structure in an amazon forest from laser range finder and IKONOS satellite observations. *Biotropica*, 34(4), 483-492.
- Blackburn, G.A. (2007). Hyperspectral remote sensing of plant pigments. *Journal of Experimental Biology*, 58(4), 855-867.
- Carlson, K.M., Asner, G.P., Hughes, R.F., Ostertag, R., & Martin, R.E. (2007). Hyperspectral remote sensing of canopy biodiversity in Hawaiian lowland rainforest. *Ecosystems*, 10(4), 536-549.
- Chen, J.M., Leblanc, S.G., Miller, J.R., Freemantle, J., Loechel, S.E., Walthall, C.L., Innanen, K.A., & White, H.P. (1999). Compact Airborne Spectrographic Imager (CASI) used for mapping biophysical parameters of boreal forests. *Journal of Geophysical Research*, 104, 27945-27958.
- Clark, M.L. & Roberts, D.A. (2012). Species-level differences in hyperspectral metrics among tropical rainforest trees as determined by a tree based classifier. *Remote Sensing*, 4, 1820-1855.
- Colwell, J.E. (1974). Vegetation Canopy Reflectance. *Remote Sensing of Environment*, 3, 175-183.
- Curran, P.J., Dungan, J.L., Macler, B.A., Plummer, S.E., & Peterson, D.L. (1992). Reflectance spectroscopy of fresh whole leaves for the estimation of chemical concentration. *Remote Sensing of Environment*, 39, 153-166.
- Danson, F. M. (1995). Developments in the remote sensing of forest canopy structure. In F. M. Danson, & S. E. Plummer (Eds.), *Advances in Environmental*

- Remote Sensing* (pp. 53–69). Wiley, Chichester, UK.
- Denslow, J.S. (1987). Tropical rainforest gaps and tree species diversity. *Annual Review in Ecological Systematics*, 18, 431-451.
- Field, C.B. (1991). Ecological scaling of carbon gain to stress and resources availability. In: H.A. Mooney, W.E. Winner, & E.J. Pell. *Response of Plants to Multiple Stresses* (pp. 35-65). Academic Press, London.
- Gamon, J.A., Field, C.B., Bilger, W., Bjorkman, O., Fredeen, A.L., & Peñuelas, J. (1990). Remote Sensing of the xanthophyll cycle and chlorophyll fluorescence in sunflower leaves and canopies. *Oecologia*, 85, 1-7.
- Gamon, J.A., Peñuelas, J., & Field, C.B. (1992) A narrow-waveband spectral index that tracks diurnal changes in photosynthetic efficiency. *Remote Sensing of Environment*. 41, 35-44.
- Gamon, J.A., & Surfus, J.S. (1999). Assessing leaf pigment content and activity with a reflectometer. *New Phytologist*. 143, 105-117.
- Gamon, J.A. (2008). Tropical Remote Sensing – Opportunities and Challenges. In: G. Kalacska, & A. Sanchez-Azofeifa. *Hyperspectral Remote Sensing of Tropical and Subtropical Forests* (pp.297-304). Taylor & Francis Group, Boca Raton, FL, USA.
- Gitelson, A.A., Kaufman, Y.J., Stark, R., & Rundquist, D. (2002a). Novel algorithms for remote estimation of vegetation fraction. *Remote Sensing of Environment*, 80, 76-87.
- Gitelson, A.A., Zur, Y. Chivkunova, O.B., & Merzlyak, M.N. (2002b). Assessing carotenoid content in plant leaves with reflectance spectroscopy. *Photochemistry and Photobiology*. 75, 272-281.
- Gitelson, A.A., & Merzlyak, M.N. (2004) Non-destructive assessment of chlorophyll,

- carotenoids and anthocyanin content in higher plant leaves: principals and algorithms. In: S. Stamatiadis, J.M. Lynch, & J.S. Shepers. *eds Remote Sensing For Agriculture and the Environment* (pp. 78-94). Ella, Greece.
- Goel, N.S. (1988). Models of vegetation canopy reflectance and their use in estimation of biophysical parameters from reflectance data. *Remote Sensing Reviews, 4*, 1-212.
- Jacquemound, S., Baret, F., & Hanocq, J.F. (1992). Modeling spectral and bidirectional soil reflectance. *Remote Sensing of Environment, 41*, 123-132.
- Jones, H.G., & Vaughan, R.A. (2010). *Remote Sensing of Vegetation*. Oxford University Press, Oxford, UK.
- Knyazikhin, Y., Schull, M.A., Stenberg, P., Mottus, M., Rautiainen, Yang, Y., Marshak, A., Carmona, P.L., Kaufmann, R.K., Lewis, P., Disney, M.I., Vanderbilt, V., Davis, A.B., Baret, D., Jacquemound, S., Lyapustin, A., & Myneni, R. B. (2012). Hyperspectral remote sensing of foliar nitrogen content. *PNAS, 110(3)*, 185-192.
- Kokaly, R. F. (2001). Investigating a physical basis for spectroscopic estimates of leaf nitrogen concentration. *Remote Sensing of Environment, 75*, 153-161.
- Kokaly, R.F., Rockwell, B.W., Haire, S.L., & King, T.V.V. (2007). Characterization of post-fire surface cover, soils, and burn severity at the Cerro Grande Fire, New Mexico using hyperspectral and multispectral remote sensing. *Remote Sensing of Environment, 106*, 305-325.
- Kokaly, R.F., Asner, G.P., Ollinger, S.V., Martin, M.E., & Wessman, C.A. (2009). Characterizing canopy biochemistry from imaging spectroscopy and its application to ecosystem studies. *Remote Sensing of Environment, 113*, 578-591.

- Liu, Q., & Huete, A. (1995). A feedback based modification of the NDVI to minimize canopy background and atmospheric noise. *IEEE trans Geosci Remote Sensing*, 33, 457-465.
- Lucas, K. L., & Carter, G.A. (2008). The use of hyperspectral remote sensing to assess vascular plant species richness on Horn Island, Mississippi. *Remote Sensing of Environment*, 112, 3908–3915.
- Lucas, R., Bunting, P., Paterson M., Chisholm, L. (2008). Classification of Australian forest communities using aerial photography CASI and HyMap data. *Remote Sensing of Environment*, 112, 2088-2103.
- Martin, M.E., & Aber, J.D. (1997). High spectral resolution remote sensing of forest canopy lignin, nitrogen, and ecosystem processes. *Ecological Applications*, 7, 431-443.
- Martin, M.E., & Abner, J.D. (1997). High spectral resolution remote sensing of forest canopy lignin, nitrogen, and ecosystem processes. *Ecological Applications*, 7(2), 431-443.
- Martin, M.E., Plourde, L.C., Ollinger, S.V., Smith, M.L., & McNeil, B.E. (2008). A generalizable method for remote sensing of canopy nitrogen across a wide range of forest ecosystems. *Remote Sensing of Environment*, 112, 3511–3519.
- Myneni, R.B., Ross, J., & Asrar, G. (1989). A review on the theory of photon transport in leaf canopies. *Agriculture and Forest Meteorology*, 45, 1-153.
- Oldeland, J., Wesuls, D., Rocchini, D., Schmidt, M., & Jurgens, N. (2010). Does using species abundance data improve estimates of species diversity from remotely sensed spectral heterogeneity? *Ecological Indicators*. 10, 390-396.
- Ollinger, S.V., Richardson, A.D., Martin, M.E., Hollinger, D.Y., Frohking, S.E., Reich, P.B., Plourde, L.C., Katul, G.G., Munger, J.W., Oren, R. et al. (2008). Canopy nitrogen,

- carbon assimilation, and albedo in temperate and boreal forests: functional relations and potential climate feedbacks. *PNAS*, *105*, 19335–19340.
- Ollinger, S.V. (2011). Sources of variability in canopy reflectance and the convergent properties of plants. *New Phytologist*, *2*, 375-394.
- Palmer, M.W., Wohlgemuth, T., Earls, P., Arevalo, J.R., & Thompson, S.D. (2000). Opportunities for long-term ecological research at the tallgrass prairie preserve, Oklahoma. *Proceedings of ILTER regional workshop, Budapest, Hungary, 22-25 June, 1999 (2000)*, 123-128.
- Palmer, M.W., Earls, P.G., Hoagland, B.W., White, P.S., & Wohlgemuth, T. (2002). Quantitative tools for perfecting species lists. *Environmetrics*, *13*, 121-137.
- Peñuelas, J., Filella, I., Elvira, S., & Inclin, R. (1995). Reflectance assessment of summer ozone fumigated Mediterranean white pine seedlings. *Environmental and Experimental Botany*, *35(3)*, 299-307.
- Peñuelas, J., Pinol, J., Ogaya, R., & Filella, I. (1997). Estimation of plant water concentration by the reflectance Water Index WI (R900/R970). *International Journal of Remote Sensing*, *18(13)*, 2869-2875.
- Rocchini, D., Chiarucci, A., & Loiselle, S.A. (2004). Testing the spectral variation hypothesis by using satellite multispectral images. *Acta Oecologica*, *26*, 117-120.
- Rocchini, D. (2007). Effects of spatial and spectral resolution in estimating ecosystem  $\alpha$ -diversity by satellite imagery. *Remote Sensing of Environment*, *111(4)*, 423-434.
- Rocchini, D., Ricotta, C., & Chiarucci, A. (2007). Using satellite imagery to assess plant species richness: the role of multispectral systems. *Applied Vegetation Sciences*, *10*, 325-331.

- Ross, J.K. (1981). *Radiation Regime and Architecture of Plant Stands*. Kluwer Boston, Hingham, M.A.
- Sims, D.A., & Gamon, J.A. (2002). Relationships between leaf pigment content and spectral reflectance across a wide range of species, leaf structures and developmental stages. *Remote Sensing of Environment*, *81*, 337-354.
- Teillet, P.M., Staenz, K., & Williams D.J. (1997). Effects of spectral, spatial and radiometric characteristics on remote sensing vegetation indices of forested regions. *Remote Sensing of Environment*, *61*, 139-149.
- Townsend, P.A., Serbin, S., Kruger, E.L., & Gamon, J.A. (2013). Disentangling the contribution of biological and physical properties of leaves and canopies in imaging spectroscopy data. *PNAS*, *110*(12), 1074.
- Ustin, S.L., & Gamon, J.A. (2010). Remote sensing of plant functional types. *New Phytologist*, *186*, 795-816.
- Wessman, C.A., Aber, J.D., Peterson, D.L., & Melillo, J.M. (1988). Remote Sensing of canopy chemistry and nitrogen cycling in temperate forest ecosystems. *Nature*, *335*, 154-156.
- Yu, G.R., Miwa, T., Nakayama, K., Matsuoka, N., & Kon, H. (2000). A proposal for universal formulas for estimating leaf water status of herbaceous and woody plants based on spectral reflectance properties. *Plants and Soil*, *227*, 47-58.
- Zutta, B. (2003). Assessing Vegetation Functional Type and Biodiversity in Southern California Using Spectral Reflectance. *Masters Thesis*. California State University, Los Angeles.

## **Chapter 3 - Assessing species diversity of boreal forest trees with imaging spectrometry**

### **Introduction**

Chapter 2 has shown that optical diversity does correlate to species diversity in a controlled experimental setting. This chapter focuses on scaling up this method to work on an airborne platform over real world forest canopies. This scaling up of airborne biodiversity assessment is important because traditional, plot based sampling methods of biodiversity are often not spatially extensive or frequent enough to meet either modern management or conservation needs. Traditional measures of biodiversity, such as species richness, Shannon Index (Shannon, 1948), and Simpson Index (Simpson, 1949), are common metrics of biodiversity but every index has its weaknesses and criticisms (Goodman 1975, Peet 1974), and may not be practical on a large scale. Measuring the status of biodiversity with remotely sensed data offers an alternative way to gather this information over large areas (Turner *et al.*, 2003).

Many airborne and satellite methods can be used to remotely sense biodiversity. One path is to indirectly relate biodiversity to spectral variables and other remotely sensed variables (i.e. climatic) (Fairbanks and McGwire, 2004, Elith *et al.* 2006, Pearson *et al.* 2007, Chaves *et al.*, 2007, Buermann *et al.*, 2008, Saatchi *et al.*, 2008). One of the more common approaches has been to map species, and species assemblages using classification methods. With the development of airborne LiDAR and imaging spectrometers having high spectral range and high spatial resolution, classification of tree canopies has been advancing quickly. Recent studies have shown promising results by differentiating species based upon their unique spectra effected by varying leaf area index, leaf angle and chemical

composition (Jones *et al.* 2010, Féret & Asner 2012, Colgan *et al.* 2012, Leutner *et al.* 2012, Clark and Roberts 2012). The classification technique seems to be one of the most promising methods because it provides a direct identification of species. On the other hand, this method still often requires ground based reference data to properly classify tree species and classification also becomes more difficult with mixed pixels (Rocchini *et al.*, 2013). Consequently, this method may not be readily applicable to large areas.

Another approach to remotely sense biodiversity is to relate the variation in spectral information content (spectral diversity) to species diversity. While this method is not a direct measure of species identity, like classification mapping, it can provide a “first filter” estimate for patterns of biodiversity (Rocchini *et al.*, 2010). This concept was proposed by Palmer *et al.* (2000, 2002) as the Spectral Variance Hypothesis, which states that spectral heterogeneity in space should scale with species diversity. Many variations of this theme have been successfully explored including the ODIs seen in Chapter 2. Several studies have correlated the standard deviation of a single spectral variable to species diversity (Chapter 2, Gould 2000, Oindo and Skidmore 2002, Gillespie 2005, Lassau *et al.* 2005, Levin *et al.* 2007). Similarly, Zutta (2003) showed that variation in a combination of indices (NDVI, PRI, and WBI) correlated with species richness for shrub-dominated Mediterranean ecosystems. Lucas and Carter (2008) also used the variation in various indices to predict species richness in a wetland ecosystem. In this case, correlations between index variation and species diversity did not hold across all sites. Other studies have used the distance from a spectral centroid relating to species diversity (Rocchini *et al.* 2007, Oldeland 2010). Carlson *et al.* (2007) showed that the range in slope of spectral absorption features strongly correlates to tree species richness.

Additionally, Chapter 2 showed strong correlations ( $R^2 = 0.90$ ) between optical diversity indices and species diversity for controlled experimental plots.

Some of the studies above, have seen the use of vegetation indices for biodiversity monitoring and Chapter 2 has shown that the standard deviation of vegetation indices show some of strongest correlations to species diversity ( $NDVI_{sd}$   $R^2 = 0.58$ ,  $WBI_{sd}$   $R^2 = 0.51$ ). The normalized differential vegetation index (NDVI) (Rouse *et al.*, 1973) is derived from red and NIR radiance or reflectance (Teillet *et al.*, 1997). Depending on the application, it can be used to approximate photosynthetic activity, green canopy structure, and green biomass (Teillet *et al.*, 1997). The photochemical reflectance index (PRI) uses two wavelengths in the green region to monitor changing photosynthetic light-use efficiency related to the xanthophyll cycle pigment conversion (Gamon *et al.* 1992, Peñuelas *et al.* 1995) or seasonally shifting pigment pool sizes (Sims & Gamon 2002, Styliniski *et al.* 2002, Filella *et al.* 2004 & 2009, Garrity *et al.* 2011). The water band index (WBI) uses the water absorption feature in the NIR region to indicate the water content in the fine tissues of the canopy (Peñuelas *et al.*, 1993, Sims & Gamon 2003). These spectral regions are all areas of high information content (Thenkabail *et al.*, 2004) and provide simple summaries of this information. Because different plant species and functional types vary in their structural and physiological properties (Ustin & Gamon, 2010), these indices can also add information useful in interpreting functional diversity.

Despite these recent successes, this research lacks a unified theory explaining how optical diversity detects biodiversity. Chapter 2 did help clarify this by predicting that the OD-species diversity relationship was largely driven by variation in leaf traits, although I also concluded that real world canopies may not

follow this trend due to complex canopy structure and variations in canopy openness. From past studies, using airborne methods, it is known that spectral variance at the canopy level is mainly caused by variation in canopy structure, including leaf area and mean leaf angle, although as canopies become more optically thick and LAI increases the role of canopy chemistry is increased (Asner, 1998). It is also not known if the methods that work in one ecosystem will also work in another (mainly due to large phenology in temperate ecosystems); most emphasis has been on tropical ecosystems, with less emphasis on northern latitudes. Additionally, there is no universally accepted method of biodiversity sampling in the field, with multiple metrics and sampling methods in use (Peet, 1974). Until these issues are resolved, large scale remote sensing of biodiversity will be problematic.

To my knowledge, remote sensing methods of assessing diversity have not been widely tested in the boreal biome, a region of relatively low diversity compared to the tropics. Parviainen *et al.* (2009) tested remote sensing methods in the boreal forest of Europe but these correlations were limited to relating maximum NDVI to species richness. The prospect for rapidly increasing human disturbance combined with climate change threatens to further alter boreal diversity (Dyer *et al.*, 2008, Schindler & Lee 2010), making boreal biodiversity assessment an emerging priority. Using remote sensing methods to do this is particularly important since the boreal forest covers such a large area. The relatively low diversity and large phenological changes in boreal forests distinguish them from tropical forests, where most current efforts have been focused.

With improving instrumentation, the trend with the remote sensing of biodiversity appears to be moving to high quality spectral data covering a full spectral range (400-2500nm) (Carlson *et al.* 2007, Oldeland *et al.* 2010). Carlson *et*

*al.* (2007) used low noise, high spectral range data and took advantage of this by using slope analysis over the full spectral range (400-2500nm). However, the cost of the high-end instruments are beyond the means of most individual investigators or research programs, and their availability is limited to a few well-funded programs – i.e., APEX (Itten *et al.*, 2008), NEON (Kampe *et al.*, 2010), and the Carnegie Airborne Observatory (Asner *et al.*, 2007) – limiting more widespread testing of the optical diversity. On the other hand, a number of new, inexpensive silicon photodiode-based instruments are also emerging that provide a more limited spectral range and lower signal-to-noise, but at about two orders of magnitude lower cost.

This study applied airborne imaging spectrometry to examine biodiversity in the mixedwood boreal ecosystem of Edmonton, Alberta, Canada. My hypothesis was that variation in optical signatures (indices or spectral reflectance) detectable by imaging spectrometry would scale with species diversity, as hypothesized in the Spectral Variation Hypothesis (Palmer *et al.* 2000). The main goal was to see if the relationships between OD and species diversity, found in chapter 2, would scale up to airborne data with real world forest canopies. A secondary goal was to see how well an inexpensive, silicon photodiode imaging spectrometer could capture variations in boreal forest biodiversity.

## **Methods**

### *Biodiversity Sampling*

This study covered forested regions along the North Saskatchewan River Valley of Edmonton, Alberta. This is a city park system with typical mixedwood boreal tree species such as *Populus tremuloides* (Trembling Aspen), *Betula papyrifera* (White Birch), *Pinus banksiana* (Jack Pine), *Picea glauca* (White Spruce),

*Pinus contorta* (Lodgepole Pine), *Fraxinus pennsylvanica* (Green Ash), *Acer negundo* (Manitoba Maple) (City of Edmonton, 1992). Since this park is situated within an urban area, non-native species are also found (City of Edmonton, 1992). Consequently, the river valley can have higher plant species diversity than many other mixedwood boreal habitats.

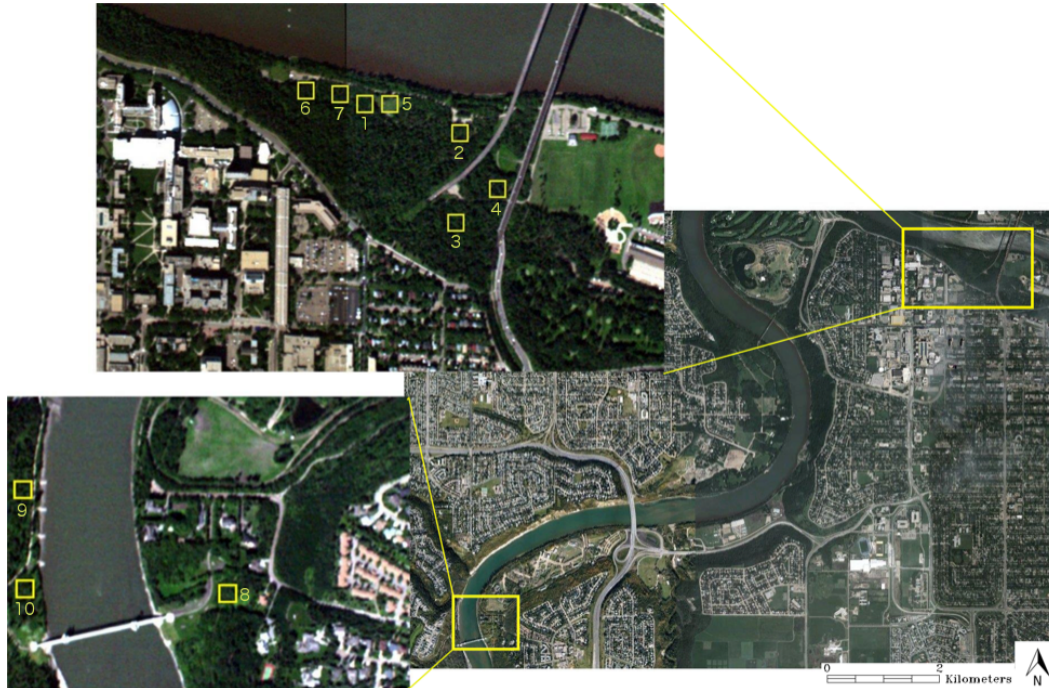


Figure 3-1: 10 River valley plots. In Kinsmen Park/University (top) and Fort Edmonton Park area (bottom). Yellow squares are the 30 x 30m sampling areas (Courtesy Google Earth, 2013).

Field sampling was done during the summer of 2012 (1 year after the remote sensing data was acquired). This may affect the analysis but changes to forest composition take place over a much larger time period (Bergeron & Dubuc, 1989) and therefore any changes are likely very small. The two sampling locations were Kinsman Park/University area (53°31'42.93"N 113°30'51.44"W) and Fort Edmonton Park area (53°29'44.65"N 113°35'15.55"W) (Figure 3-1). To survey for diversity, areas of continuous forest cover within the flight path were identified

from the imagery. Additionally, one area of mown lawn was chosen as a low diversity site. While it is known that lawns are often a mixture of several species of grasses, this site was treated as a single-species monoculture because individual species were not easily identifiable in this mown field. It was included as a base (low point) for the correlation since forest plots with a species richness of one are very rare. From this area, several sampling plots were chosen based upon accessibility, continuous canopy cover, and relatively level terrain. For each plot, four corners were marked with flagging tape (to form a 30x30m, or 900m<sup>2</sup> plot) and each corner had its GPS coordinates recorded. This size of plot was chosen because previous studies (Carlson *et al.*, 2007 and Oldeland *et al.*, 2010) have shown, on average, this size range yields better results. Because the GPS error was approximately 5m, a centroid was generated for each plot, and plots were then located in the imagery based on the assumption of a 30x30m square plot around each centroid. Based upon image inspection, the actual error appears to be 1-2 meters. Within each plot, each species visible in the upper canopy (no understory species) was recorded. For the forest plots, this method emphasized taller plants, typically over two meters in height, and did not include the understory vegetation, or other non-tree species. Consequently, the field biodiversity measurements emphasized dominant trees, and not the total biological diversity of each site.

### *Image Processing*

(See Appendix B for detailed methods)

All project imagery was acquired on August, 8<sup>th</sup>, 2011 using an imaging spectrometer (MicroHyperspec, Headwall, Fitchburg, MA, USA) with a nominal spectral range of 400-1000 nm. The instrument was flown on a fixed-wing aircraft

(Cessna 310) from a height of approximately 1341 m and a speed of 62 meters per second, yielding a resolution (pixel size) of approximately 1m on the ground.

To process the raw radiance data into spectral reflectance, several steps were taken. First, a flat field correction was done to remove patterns inherent in the detector array (Roberts *et al.*, 1986). Next the images were georectified to remove geometric distortions and the images were georeferenced so plots could be found in the image. An initial spectral calibration was applied using a factory calibration from the vendor (Headwall, Fitchburg, MA, USA). A final spectral adjustment was then added using the 760nm oxygen band as a reference point (Richards, 2013). The images were then corrected to reflectance with an empirical linear correction (Roberts *et al.*, 1985) that used 9 x 9 m white, grey and black reference tarps (Odyssey, J.Ennis Fabrics LTD., Edmonton, AB, Canada) placed in the flight path on the ground as references. For this correction, the spectral reflectance of these tarps was determined with a dual-channel spectrometer (UniSpec DC, Amesbury Massachusetts, USA) that was cross-calibrated using a white reference standard (Spectralon™, Labsphere, North Sutton, New Hampshire, USA). To reduce the size of the data and avoid noisy spectral regions, the spectral dimension of the images was reduced to 400-900nm (the bands with acceptable signal-to-noise) (See Figure 3-2). To reduce the remaining noise, an ENVI spatial smoothing filter was applied, with a 3x3 filter size and a multiplicative noise model of 0.25 (see Lee, 1980 for details). Finally a mask was applied which eliminated any pixels with NDVI values below 0.3 (non-vegetated) to avoid any edge effects of nearby paths.

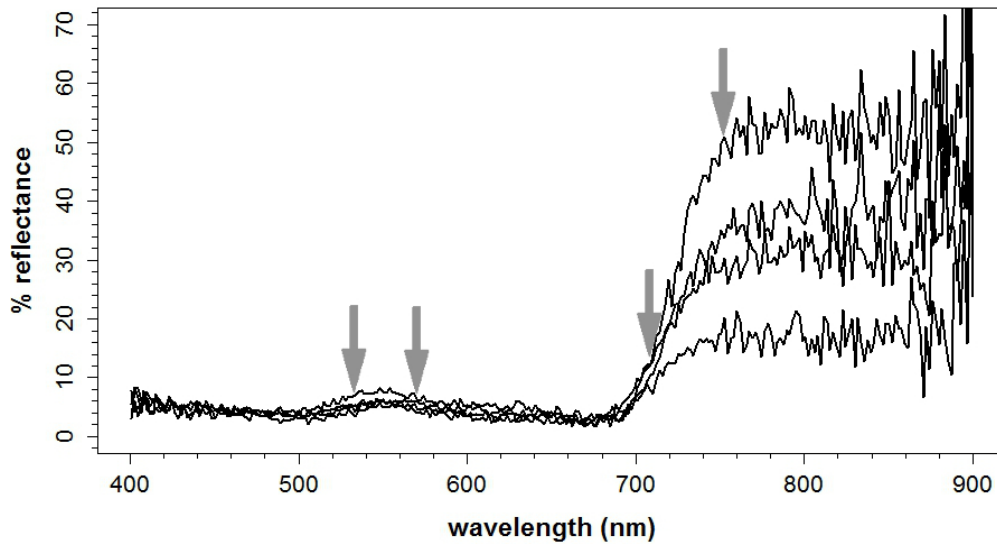


Figure 3-2: Sample spectra of typical forest pixels (Range 400-900nm) with PRI and NDVI wavelengths (equations 3-1 and 3-2) shown with arrows. Pixel spectra taken from forest North of the University of Alberta Campus (See Figure 3-1). Note the increased noise towards 900. Spectra have been smoothed as described in the methods.

#### *Vegetation & ODI Index Calculation*

A modified NDVI was calculated from reflectance images using equation 3-1 (Gitelson and Merzlyak, 1997) in image processing software (ENVI, Exelis Visual Information Solutions, McLean, VA, USA). This version was used rather than more common red and NIR NDVI wavelengths (Rouse *et al.*, 1974) because of the increasing noise towards 900nm (Figure 3-2), and because of the demonstrated sensitivity of these wavelengths to chlorophyll content (Gitelson & Merzlyak, 1997). PRI was calculated from equation 3-2 (Gamon *et al.*, 1993), providing an indicator of chlorophyll:carotenoid ratios (Sims & Gamon 2002, Stylinski *et al.* 2002, Filella *et al.* 2009, Garrity *et al.* 2011).

$$NDVI = (R_{750} - R_{705}) / (R_{750} + R_{705}) \quad (3-1)$$

$$PRI = (R_{531} - R_{570}) / (R_{531} + R_{570}) \quad (3-2)$$

For each plot, the standard deviation of NDVI, and PRI were calculated in ENVI. NDVI and PRI were calculated for every pixel and then the standard deviation (of the plot) was calculated by using the 900 pixels per plot. These standard deviation values were then compared to species richness, reciprocal Simpson Index (eq. 3-3), and Shannon Index (eq. 3-4).

$$\text{Reciprocal Simpson Index} = 1 / \sum_{i=1}^S \frac{n_i(n_i-1)}{N(N-1)} \quad (3-3)$$

Where there are S species and  $n_i$  is the number of individuals of the  $i^{\text{th}}$  species and N is the total number of individuals.

$$\text{Shannon Index} = - \sum_{i=1}^S p_i \ln p_i \quad (3-4)$$

$p_i$  is the proportion of individuals from the sample total of species  $i$ .

Using statistical software (R: A language and environment for statistical computing, R Foundation for Statistical Computing, Vienna, Austria), the variables of standard deviation of NDVI ( $NDVI_{sd}$ ), and standard deviation of PRI ( $PRI_{sd}$ ), were combined in a linear model and correlated against Species Richness (SR), Simpson Index (SI), and Shannon Index (SH) (ODI#4). ODI numbers are continued from the previous chapter. The models were evaluated based upon their  $R^2$  value, RMSE and p-value.

As an alternate method to the index-based approach, an ODI based upon a principal components analysis was also used. To calculate the principal components, the largest, most diverse, continuous forested area in the study area (top photo of Figure 3-1) was used to calculate the weighting for each wavelength in ENVI. These weightings were then applied to each of the 10 plots and principal components (PCs) 1-10 were calculated for each plot. The standard deviation of PCs 1-3 were

then calculated by using the 900 pixel values of PCs 1-3 from each plot to get a single standard deviation value for each plot. Similar to the previous index method, the variables  $PC1_{sd}$ , and  $PC2_{sd}$  were put into a linear model (ODI#5) and judged by  $R^2$ , RMSE and p-value. As a final method, the principal component method was combined with the index method in a linear model and, assessed by  $R^2$ , RMSE and p-value (ODI#6).

## Results

The ten river valley plots had species richness values varying from 1-13 (Table 3-1). Simpson Index values ranged from 0.5-8.5 while Shannon Index ranged from 0-3.23 (Table 3-1). Most plots contained typical mixed wood boreal ecosystem species such as *Populus tremuloides*, *Picea glauca*, *Betula papyrifera*, and *Pinus banksiana* but since this is an urban environment many plots, especially the higher diversity locations, contained many atypical boreal tree species. The most representative plot for a mixedwood boreal is likely plot ten, as four out of the six species are typical boreal species.

Table 3-1: List of all 30x30m plots used with their biodiversity values, species, and centroid latitude and longitude.

<b>Plot</b>	<b>SR</b>	<b>SI</b>	<b>SH</b>	<b>Species</b>	<b>Centroid location</b>
1	6	3.214	1.908	<i>Populus tremuloides</i> , <i>Populus trichocarpa</i> , <i>Acer negundo</i> , <i>Tilia Americana</i> , <i>Quercus rubra</i> , <i>Prunus pensylvanica</i>	53°31'45.45"N, 113°31'4.97"W
2	5	2.348	1.382	<i>Populus tremuloides</i> , <i>Populus trichocarpa</i> , <i>Acer negundo</i> , <i>Ulmus Americana</i> , <i>Picea glauca</i>	53°31'43.64"N, 113°30'52.67"W
3	8	5.411	2.599	<i>Populus tremuloides</i> , <i>Populus trichocarpa</i> , <i>Acer negundo</i> , <i>Betula papyrifera</i> , <i>Betula occidentails</i> , <i>Picea glauca</i> , <i>Cornus stolonifera</i> , <i>Acer pensylvanicum</i>	53°31'39.33"N, 113°30'46.04"W
4	5	3.96	2.018	<i>Populus trichocarpa</i> , <i>Acer negundo</i> , <i>Picea glauca</i> , <i>Sorbus Americana</i> , <i>Prunus pensylvanica</i>	53°31'37.58"N, 113°30'54.92"W
5	1	0.5	0	mowed Unidentified grass species	53°31'45.25"N, 113°31'2.03"W
6	12	6.761	3.029	<i>Populus trichocarpa</i> , <i>Acer negundo</i> , <i>Sorbus Americana</i> , <i>Picea glauca</i> , <i>Tilia Americana</i> , <i>Populus tremuloides</i> , <i>Betula occidentails</i> , <i>Sorbus albus</i> , <i>Prunus pensylvanica</i> , <i>Crataegus douglasii</i> , <i>Prunus virginiana</i> , <i>Fraxinus pennsylvanica</i> ,	53°31'46.78"N, 113°31'11.81"W
7	13	8.511	3.23	<i>Populus trichocarpa</i> , <i>Sorbus Americana</i> , <i>Picea glauca</i> , <i>Tilia Americana</i> , <i>Populus tremuloides</i> , <i>Betula papyifera</i> , <i>Populus balsamifera</i> , <i>Fraxinus pennsylvanica</i> , <i>Crataegus douglasii</i> , <i>Cornus sericea</i> , <i>Prunus pensylvanica</i> , <i>Ulmus Americana</i> , <i>Caragana arborescens</i>	53°31'46.68"N, 113°31'10.40"W
8	3	1.595	0.981	<i>Populus tremuloides</i> , <i>Sorbus aucuparia</i> , <i>Acer negundo</i> ,	53°29'45.38"N, 113°35'12.86"W
9	8	5.04	2.479	<i>Populus trichocarpa</i> , <i>Abies balsamea</i> , <i>Populus balsamifera</i> , <i>Pinus banksiana</i> , <i>Populus tremuloides</i> , <i>Fraxinus pennsylvanica</i> , <i>Crataegus douglasii</i> , <i>Betula occidentails</i> ,	53°29'52.46"N, 113°35'34.13"W
10	6	4.625	2.264	<i>Populus tremuloides</i> , <i>Populus trichocarpa</i> , <i>Pinus banksiana</i> , <i>Prunus pensylvanica</i> , <i>Betula papyifera</i> , <i>Acer pensylvanicum</i>	53°29'45.70"N, 113°35'33.76"W

The ability of optical diversity to depict species diversity can be visualized in Figure 3-3, showing the spatial patterns of NDVI and PC1 for two plots of different species diversity. In the NDVI images, the SR3 plot has a relatively uniform NDVI pattern, while the SR 6 plot shows much more spatial variation. PC1 of the species richness 6 plot also clearly shows more spatial variation than the SR 3 plot, with a more speckled pattern in the SR 6 plot.

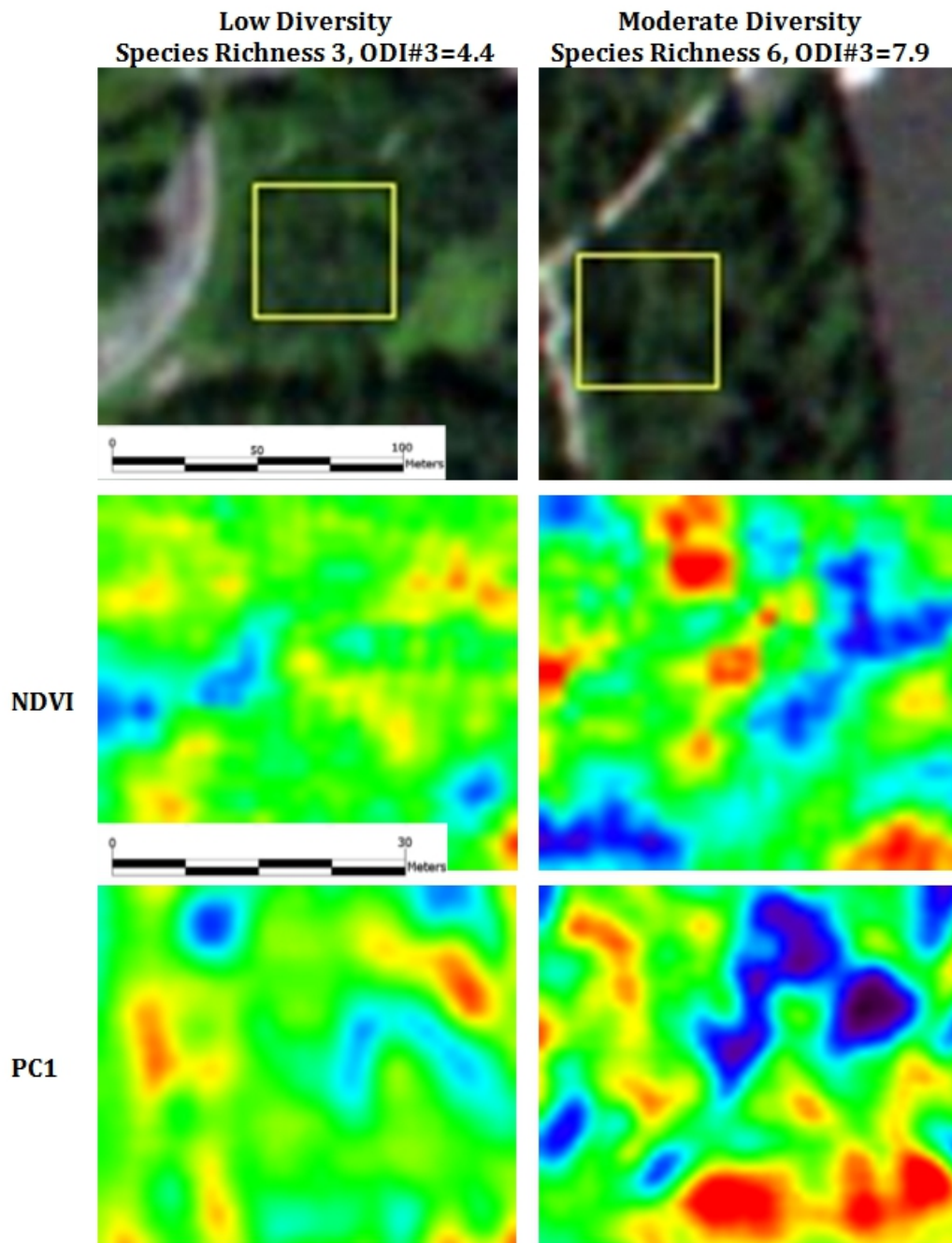


Figure 3-3: Two contrasting vegetation plots in the Fort Edmonton park area (the top image is a 100x100m image with the 30x30m plot outlined in yellow while the rest of the images are 30x30m plots). The left panel is plot#8 (see Figure 3-1) and has a species richness of 3 while the right panel is plot 10 (see Figure 3-1) and has a species richness of 6. The middle panel is NDVI and the bottom panel is the first principal component of variation (red values represent high PC1/NDVI values and blue represents low PC1/NDVI values).

The standard deviation of NDVI, and PRI each had a positive linear relation with species richness, Simpson Index, and Shannon Index. Shannon Index showed the strongest correlation with both NDVI (0.74) and PRI (0.553) (Figures 3-4 and 3-5). Results of ODI tests are listed in Table 3-2. When PRI and NDVI were combined in a linear model and correlated against Shannon Index (ODI#4, see Equation 3-5) the R<sup>2</sup> value increased to 0.75 (Figure 3-6).

The principal components method showed similar positive correlations with field-based assessment of diversity. Both PC1 and PC2 showed positive linear relationships with Simpson Index, Shannon Index and species richness. When PC1 and 2 were combined (ODI #2, equation 3-6 and Figure 3-7) the correlation with species richness increased to an R<sup>2</sup> of 0.80. Finally, when the principal component method was put in combination with NDVI (ODI #3), the R<sup>2</sup> value rose to 0.86 (equation 3-7 and Figure 3-8).

Table 3-2: Optical Diversity Indices (ODIs) and their associated species diversity indices, spectral variables (used to correlate against diversity indices), R<sup>2</sup> value, p-value and RMSE value. Equations for ODIs #1-3 are provided below (Eq. 2.5-2.7).

<b>ODI#</b>	<b>Diversity index</b>	<b>Spectral variables</b>	<b>R<sup>2</sup> value</b>	<b>p-value</b>	<b>RMSE</b>
<b>4</b>	<b>Shannon</b>	<b>NDVI<sub>sd</sub> + PRI<sub>sd</sub></b>	<b>0.75</b>	<b>0.007</b>	<b>0.461</b>
<b>5</b>	<b>Species Richness</b>	<b>PC1<sub>sd</sub> + PC2<sub>sd</sub></b>	<b>0.80</b>	<b>0.0036</b>	<b>1.60</b>
<b>6</b>	<b>Species Richness</b>	<b>NDVI<sub>sd</sub> + PC1<sub>sd</sub> + PC2<sub>sd</sub></b>	<b>0.86</b>	<b>0.005</b>	<b>1.32</b>
7	Species Richness	NDVI <sub>sd</sub> + PRI <sub>sd</sub>	0.56	0.055	1.88
8	Simpson	NDVI <sub>sd</sub> + PRI <sub>sd</sub>	0.59	0.014	1.46
9	Simpson	PC1 <sub>sd</sub> + PC2 <sub>sd</sub>	0.66	0.025	1.33
10	Shannon	NDVI <sub>sd</sub> + PC1 <sub>sd</sub> + PC2 <sub>sd</sub>	0.81	0.014	0.408

$$\text{ODI\#4} = 44.063\text{NDVI}_{\text{sd}} + 14.18\text{PRI}_{\text{sd}} - 1.339 \quad (3-5)$$

$$\text{ODI\#5} = 0.08572\text{PC1}_{\text{sd}} + 1.06073\text{PC2}_{\text{sd}} - 8.378 \quad (3-6)$$

$$\text{ODI\#6} = 95.95\text{NDVI}_{\text{sd}} + 0.0330\text{PC1}_{\text{sd}} + 0.733\text{PC2}_{\text{sd}} - 8.01 \quad (3-7)$$

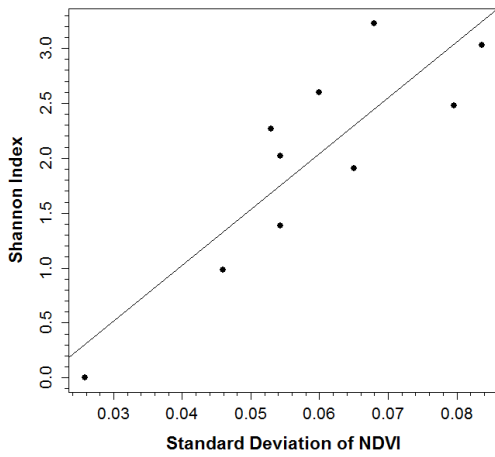


Figure 3-4: The relationship between the standard deviation of NDVI and Shannon Index for ten 30x30m forested plots sampled ( $R^2=0.74$ ,  $RMSE=0.468$ ,  $p\text{-value}=0.0013$ ).

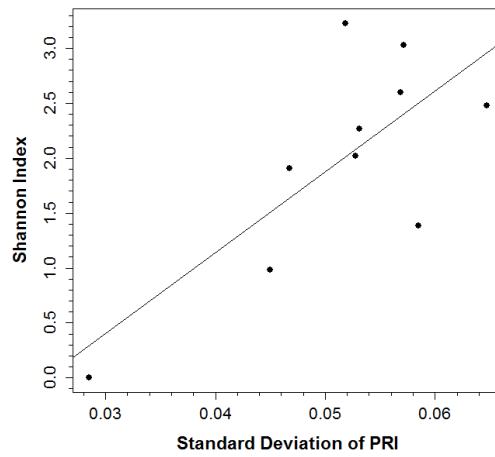


Figure 3-5: The relationship between the standard deviation of PRI and Shannon Index for ten 30x30m forested plots sampled ( $R^2=0.553$ ,  $RMSE=0.622$ ,  $p\text{-value}=0.013$ ).

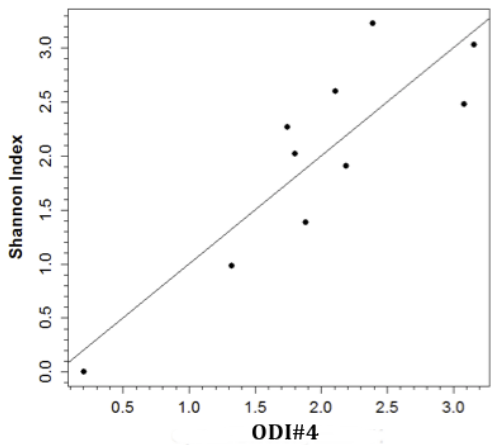


Figure 3-6: The relationship between Optical Diversity Index #4 (a linear combination of NDVI and PRI, equation 3-5) and Shannon Index for the ten 30x30m forested plots sampled ( $R^2=0.75$ ,  $RMSE=0.461$ ,  $p\text{-value}=0.0074$ ).

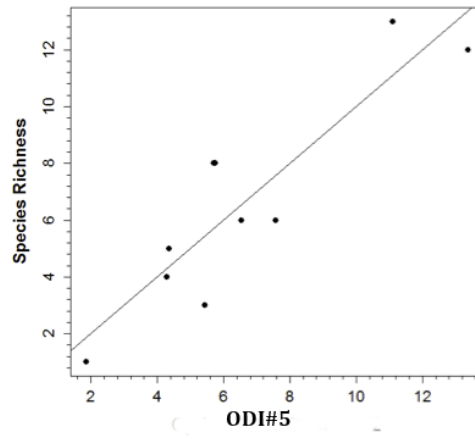


Figure 3-7: The relationship between Optical Diversity Index #5 (a linear combination of PC 1 and 2, equation 3-6) and species richness for ten 30x30m forested plots sampled ( $R^2=0.80$ ,  $RMSE=1.60$ ,  $p\text{-value}=0.0036$ ).

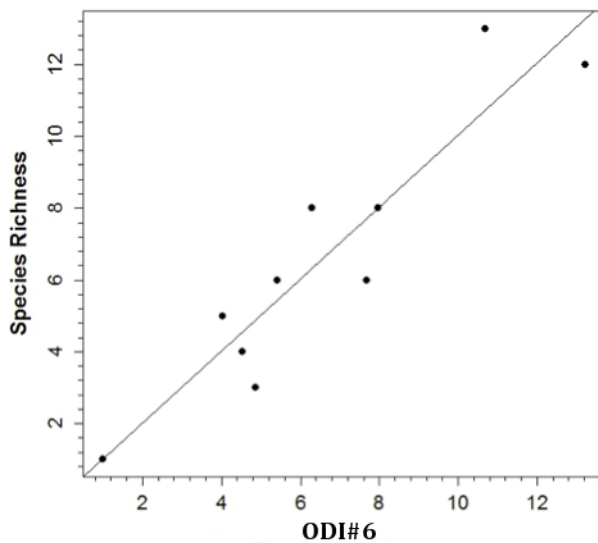


Figure 3-8: The relationship between Optical Diversity Index #3 (a combination of NDVI, PC1, and PC2, equation 3-7) and Species richness for ten 30x30m forested plots sampled ( $R^2=0.86$ ,  $RMSE=1.32$ ,  $p\text{-value}=0.005$ ).

To understand the weightings assigned to individual wavelength by the principal components transformation, I plotted the correlations ( $R^2$ ) of each principal component (1-3) against wavelength (Figure 3-9).

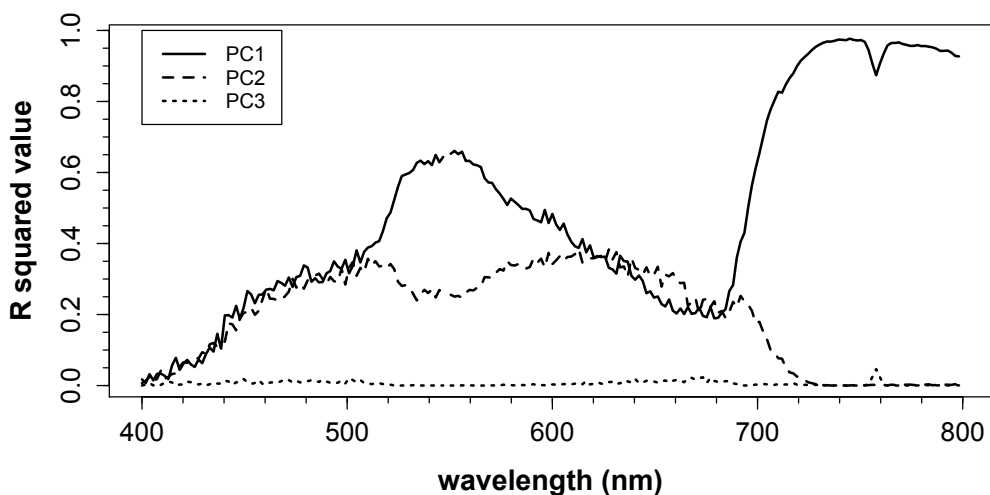


Figure 3-9: Correlation between reflectance value and PC value ( $R^2$  value) as a function of wavelength (400-800nm) for of PCs 1-3.

The correlation of PC1 with wavelength resembles a green vegetation reflectance spectrum, and is particularly high in the green and NIR regions. PC2 appears to be most strongly related to the two chlorophyll absorption areas in the blue and red region. PC3 was relatively flat, and did not show a strong correlation with wavelength or vegetation indices.

## **Discussion**

### *Optical diversity, species diversity correlation*

As expected from similar work in other ecosystems (Carlson *et al.* 2007, Zutta 2003, Rocchini *et al.* 2007, Oldeland *et al.* 2010), and Chapter 2, vegetation diversity was correlated with several metrics of optical diversity for these boreal forest plots. Notably, all optical diversity indices were sensitive to the green and NIR spectral regions (see equations 3-5, 3-6, 3-7, and Figure 3-9), suggesting these regions largely drive the correlations between spectral reflectance and species diversity for my results. These spectral regions include two of the more important areas of vegetation spectra for assessing pigment levels, potential photosynthetic activity and total biomass. The NDVI (NIR & red) region tells us about the potential photosynthetic activity and green canopy structure of the plant (Gamon *et al.* 1995, Gitelson & Merzlyak 1997). Similarly, the PRI (green) region used in ODIs #1-3 yields information on the relative chlorophyll:carotenoid levels of the plant (Sims & Gamon 2002, Stylinski *et al.* 2002, Filella *et al.* 2009, Garrity *et al.* 2011). The ODIs are most likely responding to differences in photosynthetic pigment content or activity and canopy structure between species, as expressed in their leaf and canopy spectra. It is also possible that the ODIs are responding to variation in biomass within the plot, which is expressed through variation in NDVI and PC1. My ODIs (4

and 5) also show a high degree of convergence in that they utilize similar spectral regions and yield very similar results, despite their different methods (index versus PC).

### *Study comparisons*

The concept of directly linking the variation in optical signals to biodiversity is relatively new and the results presented here are consistent with several recent studies in other ecosystems that indicate a strong potential for airborne and satellite remote sensing assessment of biodiversity. The indices (NDVI, PRI, ODI#4, ODI#5, and ODI#6) offered here suggest there may be many alternate ways to link optical properties to other metrics of biodiversity. Methods using single variable (NDVI and PRI) regression in this study (Figures 3-4 and 3-5) showed similar results to methods used in other studies (Gould 2000, Oindo and Skidmore 2002, Gillespie 2005, Lassau *et al.* 2005, Levin *et al.* 2007). My ODI #4 is consistent with the findings of Zutta (2003) in chaparral ecosystems and shows that a similar ODI derived from the vegetation indices NDVI and PRI using airborne imagery can also indicate tree species diversity in a boreal ecosystem.

The use of the standard deviation of PCA bands (ODI#5) showed a higher correlation than Oldeland *et al.* (2010) who used distance from a spectral centroid of PCA bands. Carlson *et al.* (2007) showed an almost identical correlation to my ODI #6 by using the spectral variation (range) of reflectance-derivative spectra. ODI#5 provides an new method of estimating vegetation diversity from airborne data by using the standard deviation of principal component bands. This method is comparable to the work of Rocchini *et al.* (2007) and Oldeland *et al.* (2010) who use similar PCA methods on multispectral and hyperspectral data sets but used the

distance from centroid rather than the standard deviation. ODI#6 combines both index and PCA methods and yielded the highest correlation (0.86), comparable to similar correlations reported for other ecosystems (Carlson et al. 2007, Zutta 2003).

#### *Factors behind optical diversity – species diversity correlation*

This research shows that optical diversity correlates to vegetation diversity but it is not known precisely why it does, but several possibilities have been reported. The results of Chapter 2 demonstrate that variation in leaf properties is the primary reason for the OD species diversity correlation (in a controlled setting). In a real world setting it is likely that both variation in leaf traits and variation in canopy structure or biomass are controlling the correlation.

Based on a review of other literature, Asner (1998) states that, in forest ecosystems, spectral variability is caused by differing leaf area and leaf angle with a lesser effect of leaf optical properties. Variation in leaf properties becomes more significant in specific spectral regions. Ustin & Gamon (2010) proposed that optical diversity is a function of leaf traits (e.g. leaf structure and chemical composition), canopy structure, and phenology. The results of this study suggest that photosynthetic pigment levels, or their expression via canopy structure (which affects the visible and NIR regions) are dominant drivers of the OD-biodiversity correlations for boreal forests, at least for the spectral range covered by the sensor. An additional theory could be that the variation in biomass, seen through variation in NDVI and PC1, is the driving force behind the OD-species diversity correlation. This would mean variation in leaf traits do not play a role in the correlation. The data from Chapter 2 suggests there is a correlation between OD and species diversity at the leaf level, but it is not known if airborne data can pick up on this.

Studies such as Asner & Martin (2008) and Carlson *et al.* (2007) have argued that variation from leaf chemical properties can be observed from airborne data when canopies are optically thick (tropical ecosystems). It is not known if the canopies of this Chapter were of suitable optical thickness to detect variation in leaf traits.

Besides canopy chemistry, and canopy structure, non-species factors could alter the spectral signal as well, including physiological or ontogenetic and phenological influences. Stressed plants can cause optical variation due to their reduced NDVI (Jones and Vaughan, 2010) and PRI (Gamon *et al.*, 1997) relative to their healthier counterpart. Leaf or tree age also affects the optical properties. Older, taller trees will lead to rougher canopy surface with complex multiple scattering and BRDF effects (Jones and Vaughan, 2010). The effect of tree height (canopy roughness) was shown to increase optical diversity in Chapter 2. It is likely that this increase in OD actually helped the OD-species diversity correlation in this chapter since rough canopies will usually correlate high species diversity because different trees tend to grow at different rates.

The scatter of my ODIs may be partly due to confounding, non-species based factors, but it could also be due to the fact that traditional diversity indices based on field measurements are also not perfect measures of biodiversity. Diversity is defined by the index used to measure it (Hulbert 1971, Peet 1974, Izak & Papp 2000), and different diversity metrics yield different results (Figures 3-4 to 3-8, Tables 3-1 and 3-2). I propose that optical diversity can capture different aspects of vegetation diversity than more traditional field methods based on species. For example, optical diversity may be explicitly capturing *functionally significant* variation in leaf traits, canopy structure, and their seasonal expression, as proposed in Ustin & Gamon (2010), and may be secondarily related to species diversity *per se*.

### *Surrogacy*

Through relationships between canopy structure and functional processes such as biogeochemical cycles (Asner *et al.*, 1998) optical diversity could also yield information on the diversity of other community levels such as understory plant diversity, soil microbe diversity, insect diversity, and bird diversity. This link between different levels or definitions of diversity has been called surrogacy (Pharo & Beattie 2001, Negi & Gadgil 2002, Williams *et al.* 2006, Gamon 2008), and deserves further study.

### *Future research needs*

To truly understand optical diversity, comparative experimental approaches are needed to examine the causes behind optical diversity. In particular, experiments are needed to investigate the effect of the three variables (canopy structure, physiology/chemistry, and phenology) of the optical diversity hypothesis (Ustin and Gamon, 2010). A challenge could be the difficulty and high costs of large-scale experiments using remote sensing, which often does not easily lend itself to manipulative experiments. Also, remote sensing may have an inherent problem capturing full community diversity due to fact that airborne methods are heavily weighted towards visible or dominant tree species. On the other hand, the diversity of dominant vegetation can also correlate to the diversity of many other taxa due to the principal of surrogacy (Pharo & Beattie 2001, Negi & Gadgil 2002, Williams *et al.* 2006 Gamon 2008).

### *Study Limitations*

One limitation of this study appears to be the number of data points (10) in the ODI correlations. While this low number of data points can lead to less significant correlations, all ODIs were still found to have significant correlation to  $p < 0.01$ . More data points could certainly help fill some gaps in the data such as the lack of points between SR 9-11, but the data points provided in this study still give a good representation for the OD species diversity relationship.

The spectral range and the noise of the data in this study appear to be limitations, but there may be several reasons why the noise is a minor factor. PCs 1 and 2 recombine information from many bands in the VIS and NIR and therefore reduce the effect of noise in the spectra. PCAs have been used to deal with noise in hyperspectral data in many studies (Bajcsy & Groves, 2004) and have also been used in biodiversity studies (Oldeland *et al.*, 2010). PRI is in the least noisy area of the spectrum and should be minimally affected by noise. Similarly, the large contrast in reflectance values at the red edge tend to minimize the noise limitations for this spectral region (NDVI). However, it is possible that improvements in signal-to-noise could yield improved results with the methods shown here.

It could be beneficial to add spectral range (e.g. to include the water band at 970nm used by Zutta (2003), and additional absorption features in the SWIR reported in Asner *et al.* (2007)), but the cost increase may not necessarily be worth the added benefit of increased range. Chapter 2 suggests that extending the spectral range to 1600nm slightly increases the correlation between optical diversity and species diversity, but at a substantial increase in cost and computational complexity. Lucas *et al.* (2008) found similar results in that most tree species could be identified from VIS-NIR data and the inclusion of SWIR slightly improved classification results.

Further studies are clearly needed to evaluate the relative cost and benefit of different spectral regions for biodiversity assessment. The identification of the “best” spectral regions for biodiversity assessment could help clarify if full-range spectrometers are needed for biodiversity work.

The more important factor in instrument capabilities may be spatial resolution. Low spatial resolution limits the spectral heterogeneity (Rocchini *et al.*, 2010) and can reduce the information content needed for assessing spectral variance. This study shows that high spatial resolution (~1m), equal to or smaller than the tree canopies in question, can be successful in measuring spectral heterogeneity of a forest landscape, but leaves open the question of defining the ideal resolution, which may vary with ecosystem depending upon canopy size and scale of heterogeneity (another area where more work is needed).

## **Conclusion & Recommendations**

These results indicate that optical diversity provides an alternate and complementary measure of vegetation diversity that scales well with several established field methods (species richness, Shannon Index or Simpson Index) and readily samples the diversity of dominant plant species of an area. Each method, from single variable indices to combined ODIs, correlated with species diversity, indicating many possible methods of sampling optical diversity. Index- and PCA-based methods also converged on similar spectral regions, which gives insight into the best spectral regions for biodiversity assessment in the VIS/NIR region. Even lacking full-range, high quality spectral data, the results reported here for boreal forests are comparable to other findings with other sensors from other ecosystems.

Remote sensing of biodiversity could provide advantages over traditional methods, particularly for large-scale surveying of diversity, and may provide a novel way of looking at biodiversity via optical diversity. Further experimental work is needed to understand the relative contributions of leaf properties, canopy structure and phenology to optical diversity. Also, more work is needed to clarify the ideal or necessary spatial resolution for assessing biodiversity with remote sensing.

Disadvantages of estimating vegetation diversity via imaging spectrometry include the cost of airborne data collection and the complexity of data processing. However, with the trend of increasing computing power and decreasing cost, digital data acquisition and processing will likely get easier. Similarly, the advent of automated aircraft (UAVs) provides new opportunities for low-cost image collection for biodiversity mapping. My results suggest that further development of the PCA method may be a promising approach. Once questions of the ideal spatial and spectral resolution are resolved, optical diversity sampling methods could be used with high altitude aircraft or satellite, and large areas of forests could be sampled regularly to track the changes of biodiversity. This could be particularly beneficial for vast and relatively inaccessible regions like the boreal forest ecosystems.

## Literature Cited

- Asner, G.P. (1998). Biophysical and biochemical sources of variability in canopy reflectance. *Remote Sensing of Environment*, 64(3), 234-253.
- Asner, G.P., Wessman, C.A., & Schimel, D.S. (1998). Heterogeneity of savanna canopy structure and function from imaging spectrometry and inverse modeling. *Ecological Applications*, 8, 1022-1036.
- Asner, G.P., Knapp, D.E., Kennedy-Bowdoin, T., Jones, M.O., Martin, R.E., Boardman, J., & Field, C.B. (2007). Carnegie Airborne Observatory: inflight fusion of hyperspectral imaging and waveform light detection and ranging (wLiDAR) for three-dimensional studies of ecosystems. *Journal of Applied Remote Sensing*, 1, 2-21.
- Asner, G.P., & Martin, R.E. (2008). Airborne spectranomics: mapping canopy chemical and taxonomic diversity in tropical forests. *Frontiers in Ecology and the Environment*, 7, 269-276.
- Bajcsy, P., & Groves, P. (2004). Methodology for hyperspectral band selection. *Photogrammetric Engineering and Remote Sensing*. 70, 793-802.
- Bergeron, Y., & Dubuc, M. (1989). Succession in the southern part of the Canadian boreal forest. *Vegetatio*, 79, 51-63.
- Buermann, W., Saatchi S., Smith T.B., Chaves B.R., Mila B., & Graham, C.H. (2008). Predicting species distributions across the Amazonian and Andean regions using remote sensing data. *Journal of Biogeography*, 35(7), 1160-1176.
- Carlson, K.M., Asner, G.P., Hughes, R.F., Ostertag, R., & Martin, R.E. (2007). Hyperspectral remote sensing of canopy biodiversity in Hawaiian lowland rainforest. *Ecosystems*, 10(4), 536-549.
- Chaves, J.A., Smith, T.B., Pollinger, J.P., & LeBuhn, G. (2007). The role of geography

- and ecology in shaping the phylogeography of the speckled humming bird in Ecuador. *Molecular Phylogenetics and Evolution*, 43, 795-807.
- City of Edmonton. Edmonton Parks and Recreation. (1992). *River Valley and Ravine System Master Plan*. Edmonton, Alberta.
- Clark, M.L. & Roberts, D.A. (2012). Species-level differences in hyperspectral metrics among tropical rainforest trees as determined by a tree based classifier. *Remote Sensing*, 4, 1820-1855.
- Colgan, M.S., Baldeck, C.A., Féret, J.B., & Asner, G.P. (2012). Mapping savanna tree species at ecosystem scales using support vector machine classification and BRDF correlation on airborne hyperspectral and LiDAR data. *Remote Sensing*, 4-11, 3462-3480.
- Dyer, S., Grant, J., Lesack, T., & Weber, M. (2008). *Catching up: Conservation and Biodiversity offsets in Alberta's boreal forest*. Canadian Boreal Initiative, Ottawa, Canada.
- Elith, J., Graham, C.H., Anderson, R.P., Dudik, M., Ferrier, S., Guisan, A., Hijmans, R.J., Huettmann, F., Leathwick, J.R., Lehmann, A., Li, J., Lohmann, L.G., Loizelle, B.A., Manion, G., Moritz, C., Nakamura, M., Nakazawa, Y., Overton, J., Townsend Peterson, A., Phillips, S.J., Richardson, K., Scachetti-Pereira, R., Schapire, R.E., Soberon, J., Williams, S., Wisz, M.S. & Zimmermann, N.E. (2006). Novel methods improve prediction of species' distributions from occurrence data. *Ecography* 29, 129-51.
- Fairbanks, D.H.K. & McGwire, K.C. (2004). Patterns of floristic richness in vegetation communities of California: regional scale analysis with multi-temporal NDVI. *Global Ecology and Biogeography*, 13, 221-235.
- Féret, J.B. & Asner, G.P. (2012). Semi-supervised methods to identify individual

- crowns of lowland tropical canopy species using imaging spectroscopy and LiDAR. *Remote Sensing*, 4, 2457-2476.
- Filella, I., Peñuelas, J., Llorens, L., & Estiarte, M. (2004). Reflectance assessment of seasonal and annual changes in biomass and CO<sub>2</sub> uptake of a Mediterranean shrubland submitted to experimental warming and drought. *Remote Sensing of Environment*, 90, 308–318.
- Filella, I., Porcar-Castell, A., Munné- Bosch, S., Bäck, J., Garbulsky, M., & Peñuelas, J. (2009). PRI assessment of long-term changes in carotenoids/chlorophyll ratio and short-term changes in de-epoxidation state of the xanthophyll cycle. *International Journal of Remote Sensing*, 30, 4443-4455.
- Gamon, J.A., Peñuelas, J., & Field, C.B. (1992) A narrow-waveband spectral index that tracks diurnal changes in photosynthetic efficiency. *Remote Sensing of Environment*. 41, 35-44.
- Gamon, J.A., Filella, I., & Peñuelas, J. (1993). The dynamic 531-nanometer  $\Delta$  reflectance signal: a survey of twenty angiosperm species. In: H.Y. Yamamoto, C.M. Smith (Eds). *Photosynthetic Responses to the Environment* (pp. 172-177). American Society of Plant Physiologists, Rockville.
- Gamon J.A., Field C.B., Goulden M., Griffin K., Hartley A., Joel G., Peñuelas J., & Valentini, R. (1995). Relationships between NDVI, canopy structure, and photosynthetic activity in three Californian vegetation types. *Ecological Applications*. 5(1), 28-41.
- Gamon J.A., Serrano, L., & Surfus, J.S. (1997). The Photochemical reflectance index: an optical indicator of photosynthetic radiation use efficiency across species, functional types, and nutrient levels. *Oecologia*, 112, 492-501.
- Gamon, J.A. (2008). Tropical Remote Sensing – Opportunities and Challenges. In: G.

- Kalacska, & A. Sanchez-Azofeifa. *Hyperspectral Remote Sensing of Tropical and Subtropical Forests* (pp.297-304). Taylor & Francis Group, Boca Raton, FL, USA.
- Garrity, S.R., Eitel, J.U.H., & Vierling, L.A. (2011). Disentangling the relationships between plant pigments and the photochemical reflectance index reveals a new approach for remote estimation of carotenoid content. *Remote Sensing of Environment*, 115(2), 628-635.
- Gillespie, T.W. (2005). Predicting woody-plant species richness in tropical dry forests: a case study from South Florida, USA, *Ecological Applications*, 15, 27-37.
- Gitelson, A.A., & Merzlyak, M.N. (1997). Remote estimation of chlorophyll content in higher plant leaves. *International Journal of Remote Sensing*, 18(12), 2691-2697.
- Goodman, D. 1975. The theory of diversity-stability relation in ecology. *Quarterly Review of Biology*, 50, 237-266.
- Gould, W. (2000). Remote sensing of vegetation, plant species richness, and regional biodiversity hotspots. *Ecological Applications*, 10(6), 1861-1870.
- Hamilton, A.J. (2005). Species diversity or biodiversity. *Journal of Environmental Management*, 75, 89-92.
- Huggett, R.J. (2004). *Fundamentals of Biogeography (second edition)*. Routledge, New York, NY, USA.
- Hulbert, S.H. (1971). The nonconcept of species diversity: a critique and alternative parameters. *Ecology*, 52, 577-586.
- Izsak, J., & Papp, L. (2000). A Link between ecological diversity indices and measures of biodiversity. *Ecological Modeling*, 130, 151-156.

- Itten, K.I., Dell'Endice, F., Hueni, A., Kneubler, M., Schlapfer D., Odermatt, D., Seidel, F., Huber, S., Schopfer, J., Kellenberg, T., Buhler, Y., D'Odorico P., Nieke, J., Alberti, E., & Meuleman, K. (2008). APEX- the hyperspectral ESA airborne PRISM experiment. *Sensors*, 8, 6235-6259.
- Jones, H.G., & Vaughan, R.A. (2010). *Remote Sensing of Vegetation*. Oxford University Press, Oxford, UK.
- Jones, T.G., Coops, N., & Sharma, T. (2010). Assessing the utility of airborne hyperspectral and LiDAR data for species distribution mapping in the costal Pacific Northwest, Canada. *Remote Sensing of Environment*, 114, 2841-2852.
- Kampe, T.U., Johnson, B.R., Kuester, M., & Keller, M. (2010). NEON: the first continental-scale ecological observatory with airborne remote sensing of vegetation canopy biochemistry and structure. *Journal of Applied Remote Sensing*, 4(1), 1-24.
- Lassau, S.A., Cassis, G., Flemons, P.K.J., Willkie, & L. Hochuli, D.F. (2005). Using high-resolution multi-spectral imagery to estimate habitat complexity in open-canopy forests: can we predict ant community patterns? *Ecography*, 28, 495-504.
- Lee, J.S. (1980). Digital image enhancement and noise filtering by use of local statistics. *IEEE Transactions Analysis and Machine Intelligence*, 2(2), 165-168.
- Leutner, B.F., Reineking B., Muller, J., Bachmann, M., Beierkuhnlein, C., Dech, S., & Wegmann. (2012). Modelling forest  $\alpha$ -diversity and floristic composition-on the added value of LiDAR plus hyperspectral remote sensing. *Remote Sensing*, 4, 2818-2845.
- Levin, N. Shmida, A. Levanoni, Q., Tomari, H., & Kark, S. (2007). Predicting mountain plant richness and rarity from space using satellite-derived vegetation

- indices. *Diversity and Distribution*, 13, 692-703.
- Lucas, L.K., & Carter, G.A. (2008). The use of hyperspectral remote sensing to assess vascular plant species richness on Horn Island, Mississippi. *Remote Sensing of Environment*, 112, 3908-3915.
- Lucas, R., Bunting, P., Paterson M., Chisholm, L. (2008). Classification of Australian forest communities using aerial photography CASI and HyMap data. *Remote Sensing of Environment*, 112, 2088-2103.
- Martin, M.E., & Aber, J.D. (1997). High spectral resolution remote sensing of forest canopy lignin, nitrogen, and ecosystem processes. *Ecological Applications*, 7(2), 431-443.
- Nagendra, H., Rocchini, D., Ghate, R., Sharma, B., & Pareeth, S. (2010). Assessing plant diversity in a dry tropical forest: comparing the utility of Landsat and IKONOS satellite imagers. *Remote Sensing*, 2, 478-496.
- Negi, H.R., & Gadgil M. (2002). Cross-taxon surrogacy of biodiversity on the Indian Garhwal Himalaya. *Biological Conservation*, 105(2), 143-155.
- Oindo, B.O., & Skidmore, A.K. (2002). Interannual variability of NDVI and species richness in Kenya. *International Journal of Remote Sensing*. 23, 285-298.
- Oldeland, J., Wesuls, D., Rocchini, D., Schmidt, M., & Jurgens, N. (2010). Does using species abundance data improve estimates of species diversity from remotely sensed spectral heterogeneity? *Ecological Indicators*, 10, 390-396.
- Palmer, M.W., Wohlgemuth, T., Earls, P., Arevalo, J.R., & Thompson, S.D. (2000). Opportunities for long-term ecological research at the tallgrass prairie preserve, Oklahoma. *Proceedings of ILTER regional workshop, Budapest, Hungary, 22-25 June, 1999 (2000)*, 123-128.
- Palmer, M.W., Earls, P.G., Hoagland, B.W., White, P.S., & Wohlgemuth, T. (2002).

- Quantitative tools for perfecting species lists. *Environmetrics*, 13, 121-137.
- Parvianine, M., Luoto, M., & Heikkinen, R.K. (2009). The role of local and landscape level measure of greenness in modeling boreal plant species richness. *Ecological Modeling*, 220, 2690-2701.
- Pearson, R.G., Raxworthy, C.J., Nakamura, M., & Peterson, A. (2007). Predicting species distributions from small numbers of occurrence records: a test case using cryptic geckos in Madagascar. *Journal of Biogeography* 34, 102–17.
- Peet, P.K. (1974). The measurement of species diversity. *Annual Review of Ecology and Systematics*, 5, 285-307.
- Peñuelas, J., Filella, I., Biel, C., Serrano, L., & Save, R. (1993). The reflectance at the 950-970 nm region as an indicator of plant water stress. *International Journal of Remote Sensing*, 24, 1799-1810.
- Peñuelas, J., Gamon, J.A., Fredeen, A.L., Merino, J., & Field, C.B. (1994) Reflectance indices associated with physiological changes in nitrogen- and water-limited sunflower leaves. *Remote Sensing of Environment*, 48, 135-146.
- Peñuelas, J., Filella, I., & Gamon, J.A. (1995) Assessment of photosynthetic radiation-use efficiency with spectral reflectance. *New Phytologist*, 131, 291-296.
- Pharo, E.J. & Beattie, A.J. (2001). Management forest types as a surrogate for vascular plant, bryophyte and lichen diversity. *Australian Journal of Botany*, 49(1), 23-30.
- Richards, J.A. (2013). *Remote Sensing Digital Image Analysis (fifth edition)*. Springer Heidelberg, New York, N.Y., USA.
- Roberts, D.A., Yamaguchi, Y., & Lyon, R.J.P. (1985). Calibration of Airborne Imaging Spectrometer data to percent reflectance using field spectral measurements. *Proc. 19<sup>th</sup> Int. Symp. On Remote Sensing Environment*, Ann Arbor, Michigan,

679-688.

- Roberts, D.A., Yamaguchi, Y., & Lyon, R. (1986). Comparison of various techniques for calibration of AIS data in Proceedings of the 2<sup>nd</sup> Airborne Imaging Spectrometer Data Analysis Workshop (G. Vane and A.F.H. Goetz, Eds.), *JPL Publication 86-35*, Jet Propulsion Lab, Pasadena, CA. pp. 21-30.
- Roberts, D.A., Ustin, S.L., Ogunjemiyo, S., Greenburg, J., Dobrowski, S.Z., Chen, Jiquan, & Hinckley, T.M. (2004). Spectral and structural measures of northwest forest vegetation at leaf to landscape scales. *Ecosystems*, 7(5), 545-562.
- Rocchini, D., Chiarucci, A., & Loiselle, S.A. (2004). Testing the spectral variation hypothesis by using satellite multispectral images. *Acta Oecologica*, 26, 117-120.
- Rocchini, D. (2007). Effects of spatial and spectral resolution in estimating ecosystem-diversity by satellite imagery. *Remote Sensing of Environment*, 111, 423-434.
- Rocchini, D., Ricotta, C., & Chiarucci, A. (2007). Using satellite imagery to assess plant species richness: the role of multispectral systems. *Applied Vegetation Sciences*, 10, 325-331.
- Rocchini, D., Balkenhol, N., Carter, G.A., Foody, G.M., Gillespie, T.W., He, K.S., Kark, S., Levin, N., Lucas, K., Luoto, M., Nagendra, H., Oldeland, J., Ricotta, C., Southworth, J., & Neteler, M. (2010). Remotely sensed spectral heterogeneity as a proxy of species diversity: Recent advances and open challenges. *Ecological Informatics*, 5(5), 318-329.
- Rocchini, D., Foody, G.M., Nagendra, H., Rocotta, C., Anand, M., He, K.S., Amici, V., Kleinschmit, B., Forster, M., Schmidlein, S., Feilhauer, H., Ghisla, A., Metz, M., & Neteler, M. (2013). Uncertainty in ecosystem mapping by remote sensing.

*Computers & Geosciences*, 50, 128-135.

Rouse, J.W., Haas, R.H., Schell, J.A. & Deering, D.W. (1973). *Monitoring vegetation systems in the Great Plains with ERTS. In 3rd ERTS Symposium, NASA SP-351 I*, pp. 309–317.

Saatchi, S., Buerman, W., Mori, S., ter Steege, H., & Smith, T. (2008). Modeling distribution of Amazonian tree species and diversity using remote sensing measurements. *Remote Sensing of Environment*, 112(5), 2000-2017.

Schindler, D.W., & Lee, P.G. (2010). Comprehensive conservation planning to protect biodiversity and ecosystem services in Canadian boreal regions under a warming climate and increasing exploitation. *Biological Conservation*, 143, 1571–1586.

Schowengerdt, R.A. (2007). *Remote Sensing: models and methods for image processing*. Academic Press, Burlington, MA, USA.

Simpson, E. H. (1949). Measurement of diversity. *Nature*, 163, 688.

Sims, D.A., & Gamon, J.A. (2002). Relationships between leaf pigment content and spectral reflectance across a wide range of species, leaf structures and developmental stages. *Remote Sensing of Environment*. 81, 337-354.

Sims, D.A., & Gamon, J.A. (2003) Estimation of vegetation water content and photosynthetic tissue area from spectral reflectance: a comparison of indices based on liquid water and chlorophyll absorption. *Remote Sensing of Environment*, 84, 526-537.

Shannon, C. E. (1948). A mathematical theory of communication. *The Bell System Technical Journal*, 27, 379-423 and 623-656.

Stickler, C.M., & Southworth, J. (2008). Application of a multi-scale spatial and spectral analysis to predict primate occurrence and habitat associations in

- Kibale National Park, Uganda. *Remote Sensing of Environment*, 112, 2170-2186.
- Stylinski, C.D., Gamon, J.A., & Oechel, W.C. (2002). Seasonal patterns of reflectance indices, carotenoid pigments and photosynthesis of evergreen chaparral species. *Oecologia*, 131, 366-374.
- Teillet, P.M., Staenz, K., & Williams D.J. (1997). Effects of spectral, spatial and radiometric characteristics on remote sensing vegetation indices of forested regions. *Remote Sensing of Environment*, 61,139-149.
- Thenkabail, P.S., Enclona, E.A., Ashton, M.S., & Van Der Meer, B. (2004). Accuracy assessments of hyperspectral waveband performance for vegetation analysis applications. *Remote Sensing of Environment*, 91, 354-376.
- Turner, W., Spector, S., Gardiner, N., Fladeland, M., Streling, E., & Steininger M. (2003). Remote sensing for biodiversity science and conservation. *Trends in Ecology and Evolution*, 18(6), 306-314.
- Ustin S.L., Roberts, D.A., Gamon, J.A., Asner, G.P., & Green, R.O. (2004). Using imaging spectroscopy to study ecosystem processes and properties. *BioScience*, 54, 523-534.
- Ustin, S.L., & Gamon, J.A . (2010). Remote sensing of plant functional types. *New Phytologist*, 186, 795-816.
- Whittaker, R.H., (1960). Vegetation of the Siskiyou Mountains, Oregon, and California. *Ecological Monographs*, 30, 279-338.
- Williams, G.L., Faith, D., Manne, L., Sechrest, W., & Preston, C. (2006). Complementarity analysis: Mapping the performance of surrogates for biodiversity. *Biological Conservation*, 128, 253-264.
- Williams, C.B. (1964). *Patterns in the balance of nature*. Academic. London, U.K.

Zutta, B. (2003). Assessing Vegetation Functional Type and Biodiversity in Southern California Using Spectral Reflectance. *Masters Thesis*. California State University, Los Angeles.

## **Chapter 4 – Synthesis, Conclusions, and Future Research**

### **Synthesis of Rooftop and airborne data**

#### **Synthesis**

This study has outlined many methods with which biodiversity can be sampled using spectral information. The end goal of the remote sensing of biodiversity (using optical diversity) should be an operational method, which works for many data sets, in many locations. While Chapters 2 and 3 have shown ODIs that correlate to species diversity, the methods and variables in the ODIs have not been consistent. Therefore, in this chapter I will demonstrate a standardized method to build an ODI and attempt to use this method on both the airborne and rooftop data sets.

Figure 4-1 outlines this method and shows how it can be repeated. Spectral variables are selected for an ODI based upon their  $R^2$  value and significance of correlation to the diversity of the tree plots. If this method is used for the rooftop and airborne data, three common spectral variables are output ( $NDVI_{sd}$ ,  $PC1_{sd}$ , and  $PC2/3_{sd}$ ). PC 2 is used for airborne while PC3 is used for rooftop because they utilize similar spectral regions.

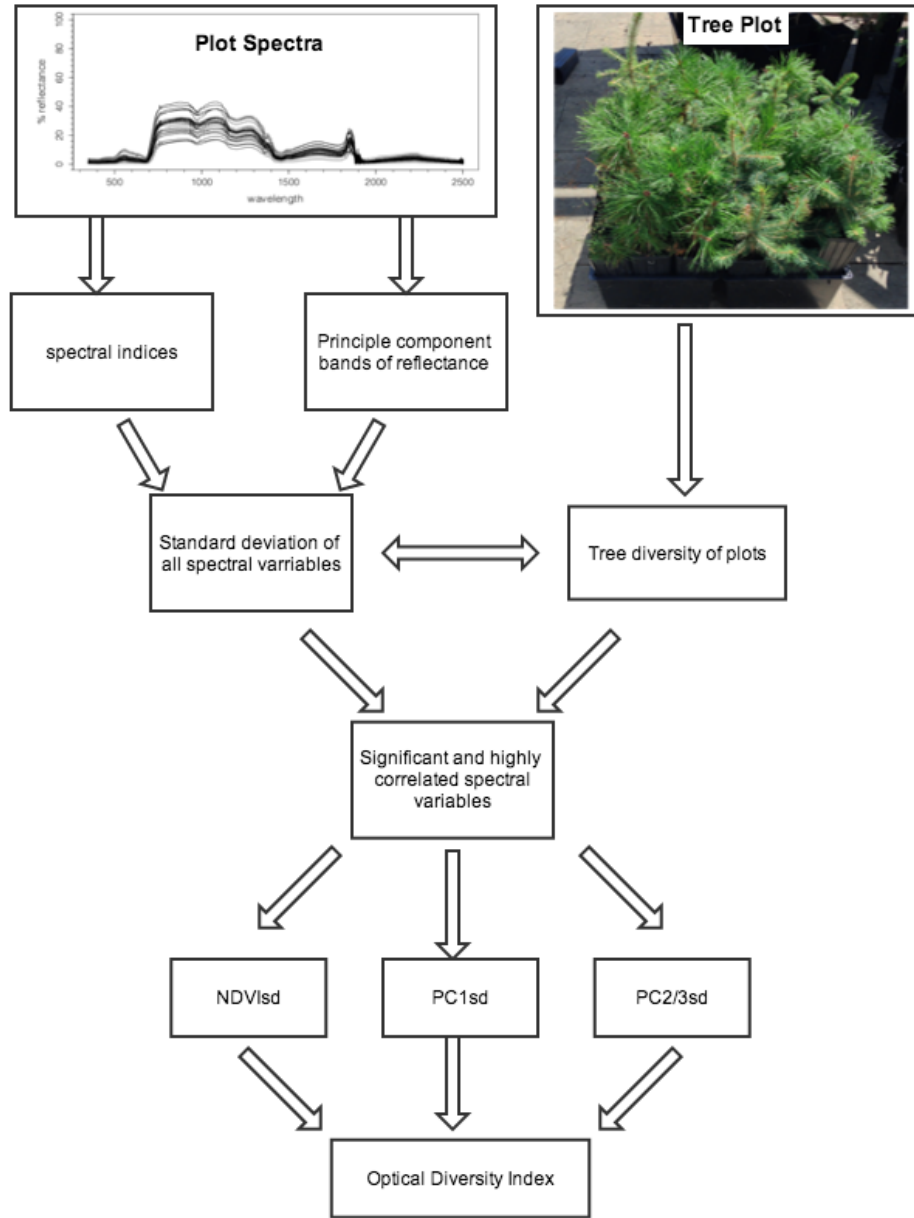


Figure 4-1: Flow diagram working from original spectral data to an optical diversity index.

If the methods from Figure 4-1 are used I get a similar, significant correlation for both data sets (The airborne data may show a higher correlation due to the larger spread of diversity values) (Figure 4-2). I propose this ODI as a possible operational index for estimating the Simpson Index of 900m<sup>2</sup> forest plots (equation 4-1).

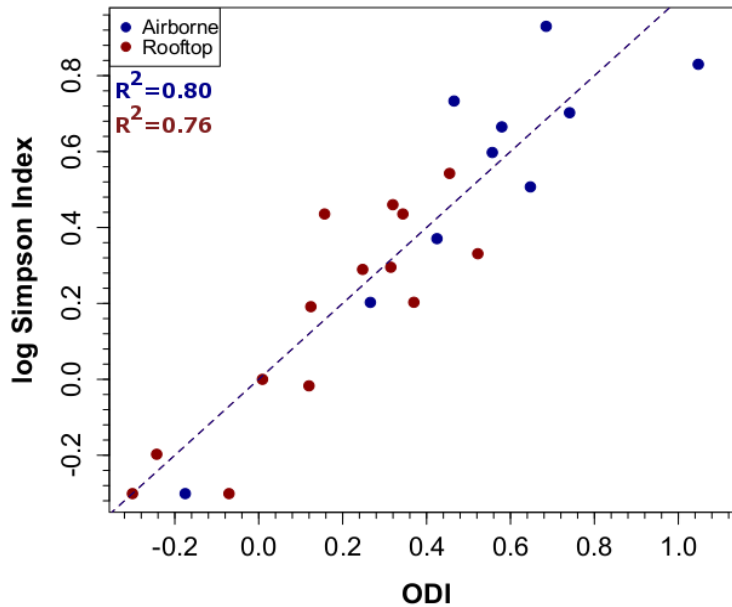


Figure 4-2: An ODI (linear combination of NDVI, PC1, and PC2 or PC3 for rooftop) correlated against log of Simpsons Index. Airborne data shown with blue (10 points) and rooftop data shown with red (14 points). Airborne (p-value = 0.016, RMSE = 0.15) rooftop (p-value = 0.0020, RMSE = 0.14). PC2 used for airborne while PC3 used for rooftop due to similar wavelength weightings.

$$Simpson\ Index = 10^{(12NDVI_{sd}+0.008PC1_{sd}+0.02PC2_{sd}-0.82)} \quad (4-1)$$

Where PC1 weightings are based upon NIR brightness, PC2/3 weightings are based upon green region brightness, and sd represents the standard deviation of all pixels contained in the 900m<sup>2</sup> plot of variable x.

Given higher quality spectral data and a larger spectral range (limited by the data of Chapter 3), other variables may be preferable to the ones seen in equation 4-1. For example, Chapter 2 has shown that slope analysis at 525nm may be preferable to PC2/3 even though they utilize similar regions. Chapter 2 has also shown that the inclusion of WBI can improve ODI-species diversity correlations. Therefore, less noisy data along with a larger spectral range will likely lead to a different ODI with slightly better results (see ODI#3).

## Conclusions

The main goal of this research was to investigate if optical diversity could accurately predict species diversity of tree species. In the end, optical diversity showed significant correlation to species diversity at several spatial scales, using airborne (1m pixel), canopy (10cm pixel), and leaf (<1mm pixel) measurements. Additionally, it was found that optical diversity can be measured in many ways and the majority of these methods significantly correlate to species diversity. These measures include: the standard deviation of vegetation indices, standard deviation of principal components of reflectance and derivative spectra, and the standard deviation and range in slope analysis. Optical diversity was found to have the strongest relationship to species diversity when three to five variables were combined into an optical diversity index. This yielded  $R^2$  values of 0.90 for ODI#3 and 0.86 for ODI#6.

Chapter 2 investigated the factors behind the OD-species diversity relationship. In the conditions of this controlled experiment, the OD-species diversity relationship was primarily based upon variation in leaf properties (or its expression via canopy structure). In the real world conditions as shown in Chapter 3 the correlation is likely based upon variation in leaf properties, canopy structure, and biomass. Another important factor affecting OD was found to be plot level canopy roughness. Chapter 2 found that increased canopy roughness leads to an increase in optical diversity. I predict that this may help the airborne correlation in Chapter 3 because varying canopy height tends to correlate to a higher diversity canopy. Finally, Chapter 2 found that an increased spectral range (up to 400-1600nm) improves the OD-species diversity correlation but not to a large degree ( $\Delta R^2 < 0.1$ ).

## Future Research

Standardized ODIs may prove to be very useful for biodiversity monitoring but much more work is still needed to fully understand the many factors, which affect optical diversity and its correlation to species diversity. Experimental work, similar to this study, at a larger scale (i.e. fully grown trees) could see if the results of Chapter 2 scale up to real world scenarios (as partially explored by Clark & Roberts 2012). These experiments could also include tests addressing phenology, ideal spectral resolution, and ideal instrumentation. The effect of phenology could be addressed by collecting data every month and testing if the OD-species diversity correlation changes across seasons. Spatial resolution could be addressed by using a high spatial resolution airborne instrument (<1m) and incrementally increasing the pixel size. The ideal pixel size for biodiversity studies could then be identified by the pixel size that yields the highest correlation to species diversity.

Another crucial issue is which measure of variability to use. The relationship between OD and species diversity is clearly evident, but we do not know if the various measures of variance (standard deviation (Chapters 2 and 3, Zutta 2003, Gould 2000), range (Carlson *et al.* 2007), and distance from centroid (Rocchini *et al.* 2007, Oldeland *et al.* 2010)) are accurately interpreting this variance. Developing a new way to measure the variation in information content, such as maximum entropy (McCallum *et al.*, 2000), may be the way to move forward or experimental methods could test to see which measure of variance best relates to species diversity.

Using optical diversity to survey biodiversity can provide research, or conservation groups with an alternative to traditional biodiversity sampling methods. Remote sensing techniques are particularly beneficial for extensive

forests because many square kilometers of forests can be sampled in a single day. Additionally, remote sensing provides unbiased data. This is often a problem with field diversity measurements. This study moves towards a standardized method where vegetation diversity can be sampled with remote sensing data, as seen in Figures 4-1 and 4-2. This is important because optical diversity values from around the world should be able to be compared. This study also provided important spectral indices for use in ODI equations. In the end, this study is a necessary step for working towards a standardized method of remotely sensed biodiversity. A fully functioning method of airborne or satellite biodiversity sampling would be vital to conservation efforts during a time of rapid biodiversity decline.

## Literature Cited

- Carlson, K.M., Asner, G.P., Hughes, R.F., Ostertag, R., & Martin, R.E. (2007). Hyperspectral remote sensing of canopy biodiversity in Hawaiian lowland rainforest. *Ecosystems*, 10(4), 536-549.
- Clark, M.L. & Roberts, D.A. (2012). Species-level differences in hyperspectral metrics among tropical rainforest trees as determined by a tree based classifier. *Remote Sensing*, 4, 1820-1855.
- McCallum, A., Freitag, D., & Pereira, F. (2000) Maximum Entropy Markov Models for Information Extraction and Segmentation. *Proc 17<sup>th</sup> International Conf. on Machine Learning*, 591-598.
- Oldeland, J., Wesuls, D., Rocchini, D., Schmidt, M., & Jurgens, N. (2010). Does using species abundance data improve estimates of species diversity from remotely sensed spectral heterogeneity? *Ecological Indicators*, 10, 390-396.
- Rocchini, D., Balkenhol, N., Carter, G.A., Foody, G.M., Gillespie, T.W., He, K.S., Kark, S., Levin, N., Lucas, K., Luoto, M., Nagendra, H., Oldeland, J., Ricotta, C., Southworth, J., & Neteler, M. (2010). Remotely sensed spectral heterogeneity as a proxy of species diversity: Recent advances and open challenges. *Ecological Informatics*, 5(5), 318-329.
- Zutta, B. (2003). Assessing Vegetation Functional Type and Biodiversity in Southern California Using Spectral Reflectance. *Masters Thesis*. California State University, Los Angeles.

## Appendix A – Index and PCA calculation for rooftop data

### Index calculation

The following code takes reflectance data from rooftop plots and calculates the standard deviation of all vegetation indices and slope variables. A csv file of reflectance data is read into `r` as a matrix. Using the row number corresponding to the proper wavelength, the indices are calculated for each column. This results in 25 index values per plot. The standard deviation of that index is then calculated using the `sd` function in R.

```
setwd("C:\\Users\\Evan DeLancey\\Desktop\\summer_2013_analysis\\specev\\22082013\\SR2")
#folder name notifies you of the species richness of the plot

data=read.csv("full.csv")
#read data set

ref=as.matrix(data)
git.ci=ref[223,]/ref[184,]
#number in brackets represents the waveband which corresponds to the proper wavelength
needed for the index calculation

sd(git.ci)
#Takes the standard deviation of the 25 values of the spectral variable

NDVI=(ref[263,]-ref[165,])/(ref[263,]+ref[165,])
sd(NDVI)
WBI=ref[427,]/ref[353,]
sd(WBI)
PRI=(ref[62,]-ref[89,])/(ref[62,]+ref[89,])
sd(PRI)
SIP1=(ref[263,]-ref[4,])/(ref[263,]-ref[169,])
sd(SIP1)
RWC=ref[488,]/ref[576,]
sd(RWC)
d=read.csv("wave.csv")
wave=d$wave
wave.d=diff(wave)
deriv=diff(ref)/wave.d
#Calculates the derivate spectra

green=deriv[72,]
sd(green)
red=deriv[154,]
sd(red)
green1=deriv[57,]
sd(green1)
rg=range(green1)
rg[2]-rg[1]
red1=deriv[197,]
sd(red1)
rr=range(red1)
rr[2]-rr[1]
water1=deriv[501,]
sd(water1)
rw=range(water1)
rw[2]-rw[1]
```

## PCA Analysis

The following code performs a PCA on the highest diversity tree plot. It then applies these weightings to every other plot and calculates the standard deviation of principal components 1-4 for each plot.

```
setwd("C:\\Users\\Evan DeLancey\\Desktop\\deriv_pca")
d6=read.csv("SR7_20.csv")
d4=read.csv("SR7_21.csv")
d2=read.csv("SR2_22.csv")
data6=as.matrix(d6)
data4=as.matrix(d4)
data2=as.matrix(d2)
prc=prcomp(data6,center=T,scale=T)

#Uses SR7 plot as base for weightings in the PCA

varimax1=varimax(prc$rotation)
#Saves the weightings of the SR7 PCA so they can be applied to other plots

new6=data6*%*%varimax1$loadings
sd(new6[,1])
sd(new6[,2])
sd(new6[,3])
sd(new6[,4])
sd(new2[,1])
new2=data2*%*%varimax1$loadings
new4=data4*%*%varimax1$loadings
sd(new2[,1])
sd(new2[,2])
sd(new2[,3])
sd(new2[,4])
sd(new4[,1])
sd(new4[,2])
sd(new4[,3])
sd(new4[,4])

#outputs the standard deviation of PCs 1-4
```

## Appendix B - Calculating an Optical Diversity index (ODI) from raw airborne data

### I. Georeferencing

Credit of rectification process goes to David Stonehouse (Verimap Plus, Calgary, Alberta, Canada). To alter the code, open with notepad. See Instructions below to convert raw data to a TIFF georeferenced image.

#### Dave's batch file

The first executable is PPOcorrect. Below is the syntax and an example batch call that I have used successfully on the 0430 data.

Some parameters are the same, some are different and some are new so please read carefully.

Example:

```
ppocorrect 0.0 0.0 0.0 777 "I:\0430\Session 04-30-002\NavData\ppo0430.001" 0 6000 2000  
I:\0430\RA_1000_img\ I:\0430\RA_1000_img\dems\50cm_1_00000.bt  
I:\0430\RA_1000_img\camcfg.txt I:\0430\RA_1000_img\filename-00000-0-meta.txt  
I:\0430\RA_1000_img\filename-00000.cube I:\0430\RA_1000_img\outcube2.tif
```

## 1. PPO Correct

Syntax - There are new parameters, namely configuration files.

```
ppocorrect <Pitch_Offset> <Roll_Offset> <Yaw_Offset> <start_line>
```

```
<PPOFileName> <PPO_position> <start_line> <num_lines> <output_directory>
```

```
<BT_DTM_file> <camcfg.txt> <meta_filename> <cube_config>
```

Pitch\_Offset Roll\_Offset Yaw\_Offset are to correct geometry

start\_line - correlation between the IMU file and the image GPS time stamp

Ideally this should be zero but may need to be tuned to get

rid of line wobble due to time offsets between data sets

PPOFileName - input file containing aircraft attitude - no flipping necessary

PPO\_Position - integer number containing shortcut into PPO

file (0 if not known)

start\_line - Line within the BLOCK to start rectification. You can get this from the trajectory files on the I: drive

num\_lines - the number of lines to rectify

output\_directory - rectified output directory

BT\_DTM\_file - input Binary Terrain DTM to rectify to. \*File size should be less than 5,000 KB when using all bands. If needed crop .bt file in global mapper.

camcfg.txt - text file containing FL and IC for camera

meta\_filename - filename containing the necessary meta data for the line

cube\_config - configuration file for the hyperspectral cube

out\_name - name of the output file (tif)

## 2. camcfg.txt format:

focal\_len=17

width=1000

height=1004

pitch=7.4

img\_center=500

focal\_len is the focal length of the lens used

width is the width of the sensor

height is the height of the sensor

pitch is the pitch of the sensor

img\_center is where the center of the lens hits the center of the diffraction grating (half the width is ideal)

### 3. cube\_config (filename-00000.cube)

session\_number=0

prefix=filename

frames\_per\_block=200

blocks\_in\_session=271

number\_of\_bands\_to\_process=4

nm\_bands=800 670 550 490

pixel\_disp=1.862

pixel0\_wave=-192.9385145

image\_folder=I:\0430\RA\_1000\_img

session\_number is the number of the session and can be retrieved from the file names. Example (filename-00023-0.raw is session 23).

prefix is the starting part of the file name, established by the capture software (example: test\_flight-00000-0.raw has a prefix "test\_flight")

frames\_per\_block is established during the capture and is usually 200

blocks\_in\_session is how many blocks were captured in a given flight line. This number will be the number of saved files for a given session. The files are numbered so just look at the last file to be captured and add one.

number\_of\_bands\_to\_process is how many bands to process. Right now I just have the "QuickLooks" version, so you specify how many bands to do. In the not too distant future I will be adding a "-1" option to do all the bands. This should be a good start.

nm\_bands is nanometer bands to process. Specify one wavelength for each of the number of bands to process.

pixel\_disp is the number of wavelengths represented by each pixel. Leave this at 1.862.

pixel0\_wave is the y-intercept of the linear equation of the wavelength vs. pixel position. Leave this at -192.9385145

image\_folder is where the raw input images are stored

Once the image is rectified, it will produce a multiband TIFF image. The first three bands listed in nm\_bands become the R, G, and B components, respectively. If there is 2 bands to be rectified, a multiband grey image will be produced. If a single band is rectified, a single band grey image will be produced.

#### 4. GenerateLinePositions

The second executable is GenerateLinePositions (add ".exe" extension). Example:

```
GenerateLinePositions 100 770 "I:\0430\Session 04-30-002\NavData\PP00430.001" 200  
271 I:\0430\RA_1000_img\filename-00000-0-meta.txt I:\0430\RA_1000_img\linepos.csv
```

GenerateLinePositions <line interval> <offset> <ppofile>

<frames\_per\_block> <blocks\_in\_session>

<meta\_file> <output\_file>

line\_interval is the number of scanlines between the position

reporting

offset is the GPS/UTC Offset represented in scanlines

(15 sec. offset = 15/0.01949 = 770)

ppofile is the navigation file

frames\_per\_block is the number of frames captured in a single

image block (ex. 200)

blocks\_in\_session is the number of blocks saved for this session

meta\_file is the meta file associated with this session

output\_file is name of the comma separated values file that will be output

#### General changes (line by line changes to executable file)

```
1. ppocorrect 0.0 0.0 0.0 777 "I:\0430\Session 04-30-002\NavData\ppo0430.001" 0 6000 2000  
I:\0430\RA_1000_img\ I:\0430\RA_1000_img\dems\50cm_1_00000.bt  
I:\0430\RA_1000_img\camcfg.txt I:\0430\RA_1000_img\filename-00000-0-meta.txt  
I:\0430\RA_1000_img\filename-00000.cube I:\0430\RA_1000_img\outcube2.tif  
- experiment with till you get the desired result. Or if using the 2011 summer data  
use -1.8 6.2 0.5 785
```

```
2. ppocorrect 0.0 0.0 0.0 777 "I:\0430\Session 04-30-002\NavData\ppo0430.001" 0 6000 2000  
I:\0430\RA_1000_img\ I:\0430\RA_1000_img\dems\50cm_1_00000.bt  
I:\0430\RA_1000_img\camcfg.txt I:\0430\RA_1000_img\filename-00000-0-meta.txt  
I:\0430\RA_1000_img\filename-00000.cube I:\0430\RA_1000_img\outcube2.tif  
-insert location of ppo file for flight
```

```
3. ppocorrect 0.0 0.0 0.0 777 "I:\0430\Session 04-30-002\NavData\ppo0430.001" 0 6000 2000  
I:\0430\RA_1000_img\ I:\0430\RA_1000_img\dems\50cm_1_00000.bt  
I:\0430\RA_1000_img\camcfg.txt I:\0430\RA_1000_img\filename-00000-0-meta.txt  
I:\0430\RA_1000_img\filename-00000.cube I:\0430\RA_1000_img\outcube2.tif
```

- Keep the first number 0, second should be start line (get from google earth trajectory images of your needed session), third number the number of lines needed (last line – start line)

4. ppocorrect 0.0 0.0 0.0 777 "I:\0430\Session 04-30-002\NavData\ppo0430.001" 0 6000 2000  
I:\0430\RA\_1000\_img\ I:\0430\RA\_1000\_img\dems\50cm\_1\_00000.bt  
I:\0430\RA\_1000\_img\camcfg.txt I:\0430\RA\_1000\_img\filename-00000-0-meta.txt  
I:\0430\RA\_1000\_img\filename-00000.cube I:\0430\RA\_1000\_img\outcube2.tif  
-insert location where you want TIFF saved

5. ppocorrect 0.0 0.0 0.0 777 "I:\0430\Session 04-30-002\NavData\ppo0430.001" 0 6000 2000  
I:\0430\RA\_1000\_img\ I:\0430\RA\_1000\_img\dems\50cm\_1\_00000.bt  
I:\0430\RA\_1000\_img\camcfg.txt I:\0430\RA\_1000\_img\filename-00000-0-meta.txt  
I:\0430\RA\_1000\_img\filename-00000.cube I:\0430\RA\_1000\_img\outcube2.tif  
-insert location of .bt DEM file for the area where your image is located

6. ppocorrect 0.0 0.0 0.0 777 "I:\0430\Session 04-30-002\NavData\ppo0430.001" 0 6000 2000  
I:\0430\RA\_1000\_img\ I:\0430\RA\_1000\_img\dems\50cm\_1\_00000.bt  
I:\0430\RA\_1000\_img\camcfg.txt I:\0430\RA\_1000\_img\filename-00000-0-meta.txt  
I:\0430\RA\_1000\_img\filename-00000.cube I:\0430\RA\_1000\_img\outcube2.tif  
-insert location of .txt file for your session

7. ppocorrect 0.0 0.0 0.0 777 "I:\0430\Session 04-30-002\NavData\ppo0430.001" 0 6000 2000  
I:\0430\RA\_1000\_img\ I:\0430\RA\_1000\_img\dems\50cm\_1\_00000.bt  
I:\0430\RA\_1000\_img\camcfg.txt I:\0430\RA\_1000\_img\filename-00000-0-meta.txt  
I:\0430\RA\_1000\_img\filename-00000.cube I:\0430\RA\_1000\_img\outcube2.tif  
-insert .cube file found on I: drive adjust according to instructions above

8. ppocorrect 0.0 0.0 0.0 777 "I:\0430\Session 04-30-002\NavData\ppo0430.001" 0 6000 2000  
I:\0430\RA\_1000\_img\ I:\0430\RA\_1000\_img\dems\50cm\_1\_00000.bt  
I:\0430\RA\_1000\_img\camcfg.txt I:\0430\RA\_1000\_img\filename-00000-0-meta.txt  
I:\0430\RA\_1000\_img\filename-00000.cube I:\0430\RA\_1000\_img\outcube2.tif  
-name of your file

## II. Flat field correction (FFC)

Using Li Haitao's IDL code available on the lab computer of Dr. John Gamon's lab in the folder "I:\tutorial\_calibration\_2011\code" filename: aircraft\_ffc.

## III. Oxygen Band Correction

Using Li Haitao's IDL code available on the Lab computer of Dr. John Gamon's lab in the folder "I:\tutorial\_calibration\_2011\code" filename: headwall\_fraunhofer.

Alternatively open TIFF image in ENVI.

- Find wavelength where oxygen band A occurs
- Count the number of bands between the real oxygen band and the one in the image in the .hdr file

- Subtract or add the corresponding number of bands so the oxygen band lines up with the proper wavelength
  - o Delete the first x number 0.000nm bands if subtracting and add on x number 0.000nm if adding

#### IV. Empirical Line Correction

Credit goes to Li Haitao for the code and the work. Code can be found below and on the computer in Dr. John Gamon's lab in the folder

"I:\tutorial\_calibration\_2011\code" filename: elc.

Keep all code the same except the parts highlighted below

**PRO ELC**

```

factorpath='I:\tutorial_calibration_2011\'

imgpath='I:\Evan_airborne\ELC'
imgfile=file_search(imgpath, '*.tiff', count=num_file)
imgn=N_ELEMENTS(imgfile)-1

outputpath='I:\Evan_airborne\plots_reflectance'

dspa=1000
drad=991
dtem=200

print, imgfile
;read factors, ascii
fct=READ_ASCII(factorpath+'ELC_00011_26.cff',RECORD_START=5,TEMPLA
TE = sTemplate)
factors=fct.field1[0:3,*]
solar_irr=factors[1,*]
path_rad=factors[2,*]
;-----

envi, /restore_base_save_files
envi_batch_init, log_file='batch.txt'
;
; Open the input file
;

FOR imgi=0,1 DO BEGIN

envi_open_data_file, imgfile[imgi], r_fid=fid
if (fid eq -1) then return
envi_file_query, fid, dims=dims, nb=nb

```

```

if (fid eq -1) then begin
  envi_batch_exit
  return
endif

envi_file_query, fid, ns=ns, nl=nl, nb=nb
dims = [-1, 0, ns-1, 0, nl-1]
pos = lindgen(nb)

bgpos=strpos(imgfile[imgi], 'cube_WOO')
enpos=strpos(imgfile[imgi], '.tif')
out_name=strmid(imgfile[imgi], bgpos, enpos-bgpos)
out_name=outpath+'ELC_'+out_name+'.img'

print, out_name
envi_doit, 'eline_cal_doit', $
  fid=fid, pos=pos, dims=dims, $
  path_rad=path_rad, $
  solar_irr=solar_irr, $
  out_name=out_name, r_fid=r_fid
;
; Exit ENVI
;

ENDFOR

; envi_batch_exit
print, '-----END-----'

```

Highlight 1: Location of .tif files

Highlight 2: Output location

Highlight 3: Number of bands (may have changed from 1004 if you deleted or added bands with oxygen band correction)

\*Note 1: If values for reflectance go between 0 and 20 (ie. white roofs are a flat line at a value of 20) use band math to divide by 20.

- Enter "float(b1)/20" into band math select b1 to be all the bands in the reflectance image

\*Note 2: Subset number of bands as needed. For Summer 2011 data take 400nm-900nm (reduces processing time in next steps).

## V. Georeferencing (ENVI)

1. Open reflectance image in ENVI
2. Open .bt files used in generating .TIFF in global mapper and save as JPEG.

3. Open JPEG terrain file in ENVI
4. Under Map→registration “select GCPs: image to image “
  - a. Base image (JPEG), warp image (TIF)
5. Add four points to GCPs the corners of the maps should match up exactly
  - a. Make sure both maps are in the same projection and coordinate system
6. Save GCPs and warp with map→registration “warp image: image to image”
7. You have a reflectance image with corresponding lat/long values for each pixel
8. Add plots to map with ROI tool and pixel locator and save ROIs

## VI. Image smoothing (ENVI)

Used to smooth the spectra and reduce noise.

1. Under filter→adaptive select “Lee”
2. Select the reflectance image (subset bands to 400-900nm if not already done)
3. Filter size of 3x3 or 4x4, noise model “Multiplicative”, set Multiplicative Noise mean to 0.25.

## VII. NDVI, PRI, green/red index and Masking (ENVI)

Calculating NDVI, PRI, green/red index and eliminating all non-vegetation for the image.

1. Basic tools→band math
2. Calculate NDVI and PRI: Enter expression “(float(b1)-float(b2))/(float(b1)+float(b2))”
  - a. NDVI: Enter wavelength closest to 750nm for b1 and closest to 705nm for b2
  - b. PRI: Enter wavelength closest to 531nm for b1 and closest to 570nm for b2
  - c. Green/red index: Enter wavelength closest to 550nm for b1 and closest to 675nm for b2
  - d. If spectra is noisy use average value of 3 or 4 bands around 750nm and 705nm  

$$\frac{((\text{float}(b1)+\text{float}(b2)+\text{float}(b3)+\text{float}(b4))/4)/((\text{float}(b5)+\text{float}(b6)+\text{float}(b7)+\text{float}(b8))/4)}$$
3. Load NDVI image to display
4. Basic tools → masking → build mask
  - a. Select the NDVI display
  - b. Options→import data range
  - c. Data min value=0.3 or 0.4
  - d. Save mask

### **VIII. Principal Component Analysis ENVI**

1. Take largest section of continuous forest as an ROI
2. Run PCA from menu
  - a. Transform → Principal Components → Forward PC rotation → Compute new statistics and rotate
  - b. Save PCA file
3. Perform PCA on whole image where plots are located
  - a. Transform → Principal Components → Forward PC rotation → PC rotation from existing statistics
4. Each band will be a PC band
  - a. Take the standard deviation of your plots for PC1, 2, and 3

### **IX. Optical Diversity Index (ENVI)**

1. Load any index to display
2. Basic tools → masking → apply mask
  - a. Select index file and select NDVI 0.3 mask from previous step for “select mask band”
  - b. Set mask values to NaN
3. Load masked image to display
4. Load ROIs to display
5. Go to band math and enter equation “float(b1)”
  - a. Select masked file
  - b. Select spatial subset → ROI/EVF → select one of the plots
  - c. Select quick stats from display of ROI and record the standard deviation, mean, and max of the plot
  - d. Repeat for all plots in image
6. Repeat for all other indices
7. Alternatively from masked image window select tools → ROIs → export ROIs to ASCII
  - a. Export each ROI and analyses in R
8. Build linear model on combinations of the 3 indices relating to species richness or Simpsons index